

R-2401-AF
April 1980

Military Weather Calculations for the NATO Theater: Weather and Warplanes VIII

R. E. Huschke, R. R. Rapp, C. Schutz

A Project AIR FORCE report
prepared for the
United States Air Force

Rand
SANTA MONICA, CA. 90406

The research reported here was sponsored by the Directorate of Operational Requirements, Deputy Chief of Staff/Research, Development, and Acquisition, Hq USAF, under Contract F49620-77-C-0023. The United States Government is authorized to reproduce and distribute reprints for governmental purposes notwithstanding any copyright notation hereon.

Library of Congress Cataloging in Publication Data

Huschke, Ralph E
Military weather calculations for the NATO theater.

([Report] - The Rand Corporation ; R-2401-AF)
Bibliography: p.
1. Meteorology, Military. 2. Europe--
Climate. I. Rapp, R. Robert, joint
author. II. Schutz, Charles, 1921- joint
author. III. United States. Air Force. IV. Title. V. Series: Rand Corporation. Rand
report ; R-2401-AF.
AS36.R3 R-2401 [UG467] 018s [355.4'23]
ISBN 0-8330-0245-7 80-36722

The Rand Publications Series: The Report is the principal publication documenting and transmitting Rand's major research findings and final research results. The Rand Note reports other outputs of sponsored research for general distribution. Publications of The Rand Corporation do not necessarily reflect the opinions or policies of the sponsors of Rand research.

R-2401-AF
April 1980

Military Weather Calculations for the NATO Theater: Weather and Warplanes VIII

R. E. Huschke, R. R. Rapp, C. Schutz

A Project AIR FORCE report
prepared for the
United States Air Force



PREFACE

The study project, Weather Effects on Air Force Missions, is part of Project AIR FORCE, which encompasses the broad scope of research conducted by The Rand Corporation on behalf of the U.S. Air Force. Among the responsibilities of the "Weather Effects" project personnel is the provision of meteorological consulting services to support a variety of Project AIR FORCE activities. Many of these internal consulting efforts have required that weather information be processed and presented in ways not previously available in any published sources of weather data. Some of the results of these special studies, usually in abbreviated form, are contained in various Rand reports; many were unpublished until this time.

This report collects some previously unpublished statistical weather information that was generated over the past ten or more years for use in Rand's research on Air Force problems. It is a potpourri of information, no single portion of which represents a "comprehensive study" of a major weather problem. However, there is a sufficient variety and depth of information to constitute a useful reference volume for the Air Force community. The contents address both the traditional "ceiling and visibility" problems of air operations and the newer problems of atmospheric effects on electro-optical sensors and guidance systems as well.

Weather and Warplanes VIII, as this report is subtitled, is the most recent of a family of reports dealing with the effects of weather and weather information on military systems and operations. Four of the previous seven reports are unclassified:

R-740-PR, *Use of Weather Information in Determining Cost/ Performance and Force-Mix Tradeoffs: Weather and Warplanes I*, R. E. Huschke, June 1971.

R-742-PR, *Ten Guidelines for the Simulation of Weather Sensitive Military Operations: Weather and Warplanes II*, R. E. Huschke, June 1971.

R-774-PR, *A Simple Model to Elucidate the Utility of Weather Forecasting in Military Operations: Weather and Warplanes III*, R. R. Rapp, August 1971.

R-2016-PR, *Atmospheric Visual and Infrared Transmission Deduced from Surface Weather Observations: Weather and Warplanes VI*, R. E. Huschke, October 1976.

This work should be useful to Air Force and other DoD agencies concerned with assessing the effects of NATO-area weather conditions on aircraft operations in general and on visual and 8-12 μm infrared sensor systems.

SUMMARY

Rand Corporation research for the Air Force and other defense agencies frequently requires consideration of weather effects on systems and operations. Many of these military studies have remained unpublished, have been published in abbreviated form, or were published in fairly inaccessible documents. This report contains a collection of such analyses thought to be of value in assessing military weather problems in the NATO theater.

The report is divided into three sections. Section I is a general introduction and a guide to the data sources used in the various analyses. Section II consists of statistical analyses of recorded weather data, "weather observables," mainly the cloud and visibility data that are important in aircraft operations. Ceiling and visibility joint frequencies are presented graphically and in tables for many locations along the entire NATO eastern perimeter, concentrated mainly in Germany. These and other analyses emphasize the interannual, annual, and diurnal variability of flying conditions. One section presents three different looks at the durations of adverse weather. Two studies examine cloud amount frequencies as a function of altitude, one covering a vast area of west-central Europe. Last, some thunderstorm and wind statistics are presented.

Section III pertains to the effect of the atmosphere on visual and infrared (electro-optical) sensor systems. A model of visible contrast and 8-12 μm atmospheric transmission is used to derive statistics of relevant weather effects from historical standard weather records. Visual target detection probabilities are calculated for the Fulda area; and a comparison is made of atmospheric effects on visual and imaging infrared target detection from northern to southern Germany. Cumulative frequencies of visible contrast transmission as a function of range are presented for a representative German location, for different seasons and times of day. The concluding analysis examines the occurrence frequencies of 8-12 μm extinction coefficient, monthly and annually at four German locations.

Sections II and III are each introduced by an "Introduction and Guide" that contains brief abstracts of all analyses in that section of the report.

There are two appendixes. The first presents graphs of visual target detection probability as a function of target size and contrast, range, magnification, and atmospheric contrast transmission. The second is a glossary of technical terms related to the subject matter of this report. It defines many terms pertaining to atmospheric electro-optical transmission and clarifies the meanings of some more common but often misunderstood terms, such as "ceiling" and "visibility."

ACKNOWLEDGMENTS

The basic weather data on which the contents of this report are based were furnished to The Rand Corporation by the U.S. Air Force Environmental Technical Applications Center (USAFETAC), a component of the Air Weather Service (MAC). The cooperation of USAFETAC personnel in supplying the large quantity of computerized data is sincerely appreciated.

Rand colleagues T. M. Parker and F. W. Murray provided thorough and helpful reviews of this report. Additionally, T. M. Parker is responsible for the weather persistence analysis at Bitburg and Heidelberg.

CONTENTS

PREFACE	iii
SUMMARY	v
ACKNOWLEDGMENTS	vii
TABLES	xi
FIGURES	xiii
I. GENERAL INTRODUCTION	1
II. WEATHER OBSERVABLES	4
1. Introduction and Guide	4
2. Interannual and Spatial Variability of Low Ceiling and Visibility	7
3. Diurnal-Annual Frequencies of Ceiling and Visibility Combinations at 17 Locations	9
4. Seasonal Ceiling and Visibility Joint Frequencies at Eight Locations	34
5. Hourly-Monthly Ceiling and Visibility Frequencies at Berlin	48
6. Durations of Adverse Ceiling and Visibility at Three German Locations	62
7. Monthly Visibility Frequencies at Fulda	69
8. Seasonal Cloud Amount Frequency Versus Altitude at Berlin	72
9. Monthly Cloud Amount Frequency Versus Altitude at 21 Locations in West and Central Europe	74
10. Thunderstorm Frequency in Northern Germany	80
11. Surface Winds at Three German Airfields	82
III. TARGET DETECTION AND ATMOSPHERIC TRANSMISSION MODEL CALCULATIONS	86
1. Introduction and Guide	86
2. Visual Ground-to-Ground Target Detection Probabilities in December and July at Leinefelde	90
3. Visual and IIR Target Detection Comparison in January and July at Four German Locations	95
4. Diurnal and Seasonal Visible Contrast Probabilities at Low Altitudes at Kitzingen	99
5. Intra-Annual 8-12 μm Extinction Coefficient Probabilities for the Surface Layer at Four German Locations	108

APPENDIXES

- A. Visual Target Detection Probabilities as a Function
of Range, Size, Contrast, and Transmission 115
- B. Glossary 121

REFERENCES 129

TABLES

1.	Weather Data Source and Station Information.....	3
2.	Frequency of Ceilings < 500 Ft or Visibility < 4 Mi in January...	8
3.	Index to Figures Depicting Diurnal-Annual Ceiling and Visibility Frequencies.....	10
4.	Index to Figures Depicting Seasonal Ceiling and Visibility Joint Frequencies.....	35
5.	Hourly-Monthly Ceiling Frequencies at Berlin	49
6.	Hourly-Monthly Visibility Frequencies at Berlin	55
7.	Monthly Visibility Quartiles At Fulda	70
8.	Monthly Cloud Amount Percent Frequencies for Selected Altitudes in West Central Europe: 21 Locations	74
9.	Percent Frequency of Surface Wind Speeds at Three Air Bases in Germany	82
10.	Near-Ground Visual Target Detection Probabilities at Leinefelde, December 1959.....	92
11.	Near-Ground Visual Target Detection Probabilities at Leinefelde, July 1953.....	93
12.	Comparison of Visual and IIR Target Seeker Utility in Germany: January 1965-1970; Detection at 7500 Feet	97
13.	Comparison of Visual and IIR Target Seeker Utility in Germany: July 1965-1970; Detection at 7500 Feet	98
14.	Cumulative Probability of Visible Contrast Transmission as a Function of Morning and Afternoon Solar Elevation Angle at Kitzingen; Summer (May-August); 5000 Ft Range.....	101

FIGURES

1.	Locations of Weather Data Sources Used for Analyses in this Report.....	2
2.	Distribution of Percent of Hours Having Ceiling < 500 Ft or Visibility < 4 Mi During 24 Januarys at Wiesbaden.....	8
3.	Hourly-Monthly Percent Frequencies of Concurrent Ceiling and Visibility at Berlin	11
4.	Hourly-Monthly Percent Frequencies of Concurrent Ceiling and Visibility at Bremerhaven	20
5.	Hourly-Monthly Percent Frequencies of Concurrent Ceiling and Visibility at Emden-Hafen	21
6.	Hourly-Monthly Percent Frequencies of Concurrent Ceiling and Visibility at Hamburg	22
7.	Hourly-Monthly Percent Frequencies of Concurrent Ceiling and Visibility at Hannover.....	23
8.	Hourly-Monthly Percent Frequencies of Concurrent Ceiling and Visibility at Hof.....	24
9.	Hourly-Monthly Percent Frequencies of Concurrent Ceiling and Visibility at Münster	25
10.	Hourly-Monthly Percent Frequencies of Concurrent Ceiling and Visibility at Neubiberg	26
11.	Hourly-Monthly Percent Frequencies of Concurrent Ceiling and Visibility at Bardufoss.....	28
12.	Hourly-Monthly Percent Frequencies of Concurrent Ceiling and Visibility at Kirkenes.....	29
13.	Hourly-Monthly Percent Frequencies of Concurrent Ceiling and Visibility at Tromsø	30
14.	Hourly-Monthly Percent Frequencies of Concurrent Ceiling and Visibility at Sodankyla	31
15.	Hourly-Monthly Percent Frequencies of Concurrent Ceiling and Visibility at Istanbul	32
16.	Hourly-Monthly Percent Frequencies of Concurrent Ceiling and Visibility at Four Locations in Yugoslavia	33
17.	Percent Frequency that Concurrent Ceiling and Visibility Values Are Equaled or Exceeded at Berlin.....	36
18.	Percent Frequency that Concurrent Ceiling and Visibility Values Are Equaled or Exceeded at Grafenwöhr	40
19.	Percent Frequency that Concurrent Ceiling and Visibility Values Are Equaled or Exceeded at Heidelberg	42
20.	Percent Frequency that Concurrent Ceiling and Visibility Values Are Equaled or Exceeded at Bardufoss	43
21.	Percent Frequency that Concurrent Ceiling and Visibility Values Are Equaled or Exceeded at Kirkenes.....	44

22.	Percent Frequency that Concurrent Ceiling and Visibility Values Are Equaled or Exceeded at Tromsø	45
23.	Percent Frequency that Concurrent Ceiling and Visibility Values Are Equaled or Exceeded at Sodankyla	46
24.	Percent Frequency that Concurrent Ceiling and Visibility Values Are Equaled or Exceeded at Istanbul	47
25.	Monthly Frequencies at Low Visibility (< 5 mi) at Two Times of Day at Berlin	61
26.	Monthly Frequencies of High and Low Visibilities at Berlin	61
27.	Monthly Frequencies of High and Low Ceilings at Berlin	61
28.	Weather State Duration Probabilities, Given Random Encounter with Weather State: Berlin, January 1946-1953	63
29.	Bad Weather Duration Probability, Number of Daylight Hours: Berlin, January 1954-1963	64
30.	Bad Weather Duration Probability, Number of Days: Berlin, January 1954-1963	65
31.	Frequency Distribution of Durations of Runs of Consecutive "Bad Weather Days": Berlin, January 1954-1963	66
32.	Weather State Duration Probabilities: Bitburg, 1963-1967	67
33.	Weather State Duration Probabilities: Heidelberg, 1963-1967	68
34.	Mid-Season Frequency Distributions of Visibility at Fulda	71
35.	Seasonal Frequencies of Cloud Amount as a Function of Altitude at Berlin	73
36.	Thunderstorm Days per Month in Northern Germany	81
37.	Hourly Probability of Thunderstorms within 20 km, June-August in Northern Germany	81
38.	Surface Wind Data for Bitburg	83
39.	Surface Wind Data for Ramstein	84
40.	Surface Wind Data for Spangdahlem	85
41.	Comparison of WETTA Predictions and OPAQUE Measurements of Total Atmospheric Extinction in the 8-13 μm Region	88
42.	Monthly Relative Frequencies of Ceiling < 500 ft or Visibility < 3 mi at Leinefelde	91
43.	Visual Target Detection Probabilities (6-power binoculars) Averaged over 500 m to 3000 m Range: Leinefelde, July 1953 and December 1959	94
44.	Monthly Median Values of 1-km Visible Contrast Transmission in Germany	100
45.	Curves of Cumulative Contrast Transmission Probability vs. Range at Kitzingen	102
46.	WETTA Calculations of 8-12 μm Extinction Coefficient Probabilities at Hamburg	109
47.	WETTA Calculations of 8-12 μm Extinction Coefficient Probabilities at Hannover	110
48.	WETTA Calculations of 8-12 μm Extinction Coefficient Probabilities at Kitzingen	111
49.	WETTA Calculations of 8-12 μm Extinction Coefficient Probabilities at Grafenwöhr	112

50.	Schematic of Monthly Extreme Cumulative Frequency Distributions of 8-12 μm Extinction Coefficient.....	113
A.1	Probability of Detecting a Target as a Function of Range, R (km or kft), Magnification Power, M, Characteristic Target Size, L (m or ft), Atmospheric Contrast Transmission, T_C , and Inherent Target-to-Background Contrast, C_0	117

I. GENERAL INTRODUCTION

Technology is just beginning to produce a limited capability to permit tactical and ground forces to operate in combat at night and in cloudy and poor visibility conditions. Operational target acquisition, which is largely dependent upon the human eye or TV and infrared (IR) sensors, and visual navigation may often be compromised by clouds, visibility, and other weather factors enroute and in the target vicinity. Therefore, decisionmakers must consider weather variables and the signal transmission parameters derived from them when assessing the capabilities of target acquisition and weapon delivery systems.

This report contains a collection of previously unpublished weather data and derivations from weather data primarily pertaining to air operations in the NATO theater. The data were generated over the past ten years in support of many Rand Corporation study projects. No specific attempt was made to make the contents more comprehensive or cohesive; and the mixture of English and metric units in which the results were originally expressed has been left unchanged.

The analyses are presented in three sections. Section II presents statistics on the weather observables themselves—mainly cloud amounts, cloud heights, and visibilities—most of which were calculated from digital files or archived surface weather observations. Section III presents statistics on atmospheric variables that are *derived* from the weather observables—for example, the atmospheric transmission of visual contrast and 8-12 μm IR radiation—based on the same historical data files. There is no adequate data base of these latter variables, so they are derived by means of “models” of their relationships to the commonly observed (and archived) meteorological quantities.

The data base of surface weather observations referred to above was developed, and grows, at The Rand Corporation strictly in response to the internal needs of Rand studies for the U.S. Air Force. All Rand Weather Data Bank (RAWDAB) data are obtained originally from the U.S. Air Force Environmental Technical Applications Center (USAFETAC). RAWDAB reformats the original data, with a few data transformations—e.g., ceiling heights inferred from cloud descriptions for data sets that do not contain explicit ceiling measurement. (Rodriguez and Huschke, 1974.)

The various analyses represented in Secs. II and III drew upon weather data from the locations mapped in Fig. 1 and listed in Table 1. The high concentration of analyses using weather stations in Germany reflects the preponderance of concern over the NATO Central Front as a potential war theater and equally great concern over the effect of Germany's weather on air operations and target acquisition.

Table 1 gives basic information about each station and a guide to the analyses that used its data as well.



Fig. 1—Locations of Weather Data Sources Used for Analyses in this Report

Table 1
WEATHER DATA SOURCE AND STATION INFORMATION

No. on Fig. 1 (Map)	WMO Station Number	Weather Station (Place Name)	N. Lat.	E. Long.	Station Elev. (m)	Period of Record	Location of Data in this report (Section No.)
NORTHERN FLANK							
Finland 1	02836	Sodankyla	67°22'	29°39'	180	1/52 - 12/63	II. 3,4
Norway 2	01023	Bardufoss	69°03'	18°33'	79	1/51 - 12/55	II. 3,4
3	01089	Kirkenes	69°44'	29°54'	91	1/51 - 12/55	II. 3,4
4	01030	Tromsø-Skattora	69°42'	19°01'	19	1/51 - 12/55	II. 3,4
CENTRAL AREA							
Austria 5	11035	Wien (Vienna)	48°15'	16°22'	209	pre-1939 (5yr)	II. 9
6	11231	Klagenfurt	46°39'	14°20'	452	pre-1939 (5yr)	II. 9
Czechoslovakia 7	11518	Praha (Prague)	50°06'	14°15'	369	pre-1939 (5yr)	II. 9
France 8	07028	Le Havre	49°31'	00°04'	103	pre-1939 (5yr)	II. 9
9	07180	Nancy	48°41'	06°13'	217	pre-1939 (5yr)	II. 9
10	07150	Paris-Le Bourget	48°58'	02°27'	65	pre-1939 (5yr)	II. 9
11	07240	Tours	47°27'	00°43'	112	pre-1939 (5yr)	II. 9
Germany (East and West) 12	10501	Aachen	50°47'	06°06'	205	pre-1939 (5yr)	II. 9
13	10384	Berlin-Tempelhof	52°28'	13°24'	49	pre-1939 (5yr) 3/46 - 12/63	II. 9 II. 2,3,4,5,6,8
14	10610	Bitburg	49°57'	06°34'	374	1/52 - 12/72	II. 2,6,11
15	10224	Bremen	53°03'	08°47'	13	pre-1939 (5yr)	II. 9
16	10129	Bremerhaven	53°32'	08°35'	11	1/49 - 11/71	II. 3
17	10488	Dresden	51°08'	13°46'	230	pre-1939 (5yr)	II. 9
18	10203	Emden-Hafen	53°20'	07°12'	12	4/60 - 11/71	II. 3
19	---	Erfurt	51°01'	11°02'	180	pre-1939 (5yr)	II. 9
20	10637	Frankfurt am Main	50°03'	08°35'	112	pre-1939 (5yr) 1/54 - 12/70	II. 9 II. 2
21	---	Fulda	50°33'	09°39'	308	9/60 - 12/70	II. 7
22	10687	Grafenwohr	49°42'	11°57'	415	6/62 - 12/70	II. 4; III. 3,4,5
23	10147	Hamburg	53°38'	09°59'	16	1/49 - 11/71	II. 3; III. 3,4,5
24	10338	Hannover	52°28'	09°42'	56	1/49 - 11/71	II. 3; III. 3,4,5
25	10734	Heidelberg	49°24'	08°39'	110	4/51 - 12/70	II. 2,4,6
26	10685	Hof	50°19'	11°53'	568	1/60 - 11/71	II. 3
27	10659	Kitzingen	49°45'	10°12'	210	7/63 - 12/70	III. 3,4,5
28	10449	Leinefelde	51°23'	10°19'	354	1/52 - 12/60	III. 2
30	10866	Munich (Munich)	48°08'	11°43'	529	pre-1939 (5yr)	II. 9
31	10313	Munster	51°58'	07°36'	66	8/59 - 11/71	II. 3
32	10864	Neubiberg	48°04'	11°38'	551	2/46 - 1/58	II. 3
33	10763	Nurnberg	49°30'	11°05'	312	pre-1939 (5yr)	II. 9
34	10614	Ramstein	49°26'	07°36'	238	1/52 - 12/70	II. 11
35	10607	Spangdahlem	49°59'	06°42'	365	1/54 - 12/72	II. 11
36	10738	Stuttgart	48°41'	09°12'	419	pre-1939 (5yr)	II. 9
37	10633	Weisbaden	50°03'	08°20'	140	1/47 - 1/70	II. 2
Netherlands 38	06310	Vlissingen (Flushing)	51°27'	03°36'	10	pre-1939 (5yr)	II. 9
Poland 39	12375	Warszawa (Warsaw)	52°09'	20°59'	107	pre-1939 (5yr)	II. 9
40	12566	Krakow	50°05'	19°48'	237	pre-1939 (5yr)	II. 9
41	12424	Wroclaw (Breslau)	51°06'	16°53'	121	pre-1939 (5yr)	II. 9
USSR 42	26702	Kaliningrad (Konigsberg)	54°42'	20°37'	27	pre-1939 (5yr)	II. 9
SOUTHERN FLANK							
Turkey 43	17060	Istanbul-Yesilkoy	40°58'	28°49'	27	12/49 - 12/54	II. 3,4
Yugoslavia 44	13272	Belgrade-International	44°49'	20°17'	99	1/71 - 12/75	II. 3
45	13209	Pula	44°54'	13°55'	63	1/71 - 12/75	II. 3
46	13586	Skopje	41°58'	21°39'	239	1/71 - 12/75	II. 3
47	13131	Zagreb-Pleso	45°44'	16°04'	107	1/71 - 12/75	II. 3

II. WEATHER OBSERVABLES

1. INTRODUCTION AND GUIDE

Clouds (or "ceilings") and visibilities are the weather variables traditionally invoked by pilots in describing the quality of flying conditions. Flying safety criteria—"weather minimums"—are expressed in terms of ceiling and visibility combinations. Although there are other weather hazards to aviation (runway crosswinds, icing conditions, turbulence) and refinements to the visibility criteria (runway visual range, reported runway visibility), estimates of the ceiling and the visibility remain the most widely used description of flying weather.

There are many complexities and subjectivities involved in reporting the "state of the sky" (sky cover and ceiling) and visibility; the details are clearly laid out in the *Federal Meteorological Handbook No. 1* (1979), and simple definitions are given in the Glossary, Appendix B. In general, a weather observation is a simplistic description of the state of the atmosphere at one point in time and space. It is a mixture of judgments and measurements of differing precision and accuracy, and it contains some biases and truncations. The time and space distributions of weather observations are not fine enough to capture some of the time and space variations in the weather that might be important in operational analyses. Nevertheless, the enormous archives of surface weather observations are "the best we have" for many military analytical uses, and accurate insights can be wrung from these data if they are approached with an understanding of their idiosyncrasies. Where appropriate throughout this report, specific caveats and warnings are stated regarding data quality and interpretation.

Cloud height is usually determined instrumentally by a ceilometer. Cloud amount (in eighths or tenths of the total sky) is the observer's subjective estimate. Fortunately, the sky tends to be either very cloudy or very clear, giving cloud amount a U- or J-shaped frequency distribution. Therefore, the observer is not often faced with a difficult decision as to whether the cloud cover constitutes a "ceiling."

Visibility values are the least objective of all meteorological data. The observer scans the horizon looking for known visibility checkpoints (buildings, towers, hills, lights, etc.) on which to base his estimate. Not only do observers vary in eyesight and judgment, but the unique topography of every location influences the distribution of reported visibilities. For obvious reasons, the lower visibilities are the more accurately estimated.

For problems involving oblique lines of sight through the atmosphere, there is no high confidence way to infer the vertical distribution of visibility from surface visibility observations. However, several series of airborne measurements (e.g., Duntley et al., 1972) indicate that the visible extinction coefficient, and hence the visibility, at the earth's surface is usually representative of the visibility through the atmospheric "mixed layer." The mixed layer extends from the surface to altitudes from about 0.5 km to 3 km, averaging about 1.5 km deep.

The foregoing paragraphs have explicitly pointed out some inherent shortcomings of the observations on which these summaries are based. There are two addi-

tional warnings to potential users of these data. The first concerns possible trends in the weather and the second concerns obtaining stable frequency (or probability) estimates in the face of the appreciable year-to-year variability found in many weather parameters.

The interpretation of past weather frequencies as future weather probabilities must be done with caution. Such an interpretation implies two assumptions: (1) Future weather will not be qualitatively different from past weather; and (2) the past weather used to calculate frequencies is a representative sample, with no biases toward "good" or "bad" years. In this report we made no attempt to test for long-term trends; extrapolation of trends into the future cannot be done with confidence. As for the adequacy of sample size, all calculations represented herein are based on at least five years of (mainly) post-WW II data. The goal was to use ten or more years of data in all calculations, but that was not always possible.

The first analysis in this report, Sec. II.2, emphasizes the year-to-year variability of weather. It is seen (Table 2) that over time periods ranging from 15 to 24 years, frequencies of bad weather in January range from near 20 percent to near 80 percent at each of five locations in Germany (bad weather defined as ceiling < 500 ft or visibility < 4 mi). In Sec. III.2, yearly data are presented for Leinefelde (with bad weather defined as ceiling < 500 ft or visibility < 3 mi) for December and July from 1952 through 1960 (see Fig. 42, which shows the same type of interannual variation as Table 2). Although the expected frequency of bad weather is higher in December than in July, individual summer months have worse weather than the expected winter weather, and individual winter months have almost as good weather as the expected summer weather.

The remainder of Sec. II contains the accumulated results of many "looks" at ceiling and visibility statistics along the NATO defense perimeter—mainly in Germany, but stretching from Turkey to northern Norway. The order of presentation and brief descriptions of these data are as follows:

Section	Title/Description
2.	<i>Interannual and Spatial Variability of Low Ceiling and Visibility.</i> For 5 locations in Germany, the occurrence frequencies of adverse weather (ceiling < 500 ft or visibility < 4 mi) are tabulated for all Januarys over time periods ranging from 15 to 24 years. An analysis of variance was done covering the 10-year period of concurrent data from all locations.
3.	<i>Diurnal-Annual Frequencies of Ceiling and Visibility Combinations at 17 Locations.</i> The frequencies at which given ceiling and visibility combinations are equaled or exceeded are plotted as frequency isopleths as a function of time of day and month of year.
4.	<i>Seasonal Ceiling and Visibility Joint Frequencies at Eight Locations.</i> The seasonal frequencies at which all combinations of ceiling and visibility meet certain criteria are plotted as frequency curves as a function of ceiling and visibility.
5.	<i>Hourly-Monthly Ceiling and Visibility Frequencies at Berlin.</i> Monthly tables give the 24 hourly frequencies of ceiling height (18 classes) and visibility (10 classes), plus the all-hours frequencies, at Berlin. Graphs illustrating the diurnal and annual variations of high and low ceiling and visibility frequencies are included.

6. *Durations of Adverse Ceiling and Visibility at Three German Locations.* Three questions concerning low ceiling and visibility durations are answered, the first two for Berlin and the third for Bitburg and Heidelberg. First: If a ceiling < 1000 ft or visibility < 1 mi were encountered on entering an hourly weather series at random, what is the probability that either or both of those conditions would continue for H hours in each of three seasons? The duration probabilities of < 4000 ft or < 4 mi are also determined. Second: If "good" weather turns to "bad" in the month of January, what is the probability that bad weather would continue for H hours or D days, considering only daylight hours? Third: If good weather turns to bad, what is the probability that bad weather would continue for H hours (all hours, day and night, included)?
7. *Monthly Visibility Frequencies at Fulda.* Month-to-month visibility frequencies are presented in quartile format. Visibility frequency distributions for four months, representing the seasons, are also shown.
8. *Seasonal Cloud Amount Frequency Versus Altitude at Berlin.* The frequencies of cloud amounts (overcast, broken, scattered, and clear) between ground level and any altitude up to 16,000 ft are calculated for the four seasons.
9. *Monthly Cloud Amount Frequency Versus Altitude at 21 Locations in West and Central Europe.* Tables give the monthly frequency of cloud amounts less than 0.2 and greater than 0.5 below 1000, 5000, 8000, 12,000, and 35,000 ft at 21 locations. These data are calculated for each month from observations at 0700, 1300, and 1900 hr local standard time.
10. *Thunderstorm Frequency in Northern Germany.* A distribution of "thunderstorm days" is given for each month, along with the hourly summer probability of thunderstorms occurring within a 20 km radius.
11. *Surface Winds at Three German Airfields.* Surface wind roses are presented from hourly observations during the mid-season months of January, April, July, and October, along with the peak wind observed for each of these months during the period analyzed.

2. INTERANNUAL AND SPATIAL VARIABILITY OF LOW CEILING AND VISIBILITY

Although most weather analyses of the types in this report deal with conditions aggregated over many years, it is well known that in any given season at any location weather conditions can vary markedly from the average for that season and location. To gain some perspective on the nature and magnitude of such variation, we computed the frequency of ceilings below 500 ft or visibility less than 4 mi for individual Januarys for many years of record for five locations in Germany. Table 2 presents the frequencies for 24 years at Wiesbaden, 17 years at Berlin, 17 years at Frankfurt, 19 years at Heidelberg, and 15 years at Bitburg. Berlin is on the plains in the northeast of Germany, and the other four stations are in river valleys that wind through the low mountains of southwest Germany.

The means and standard deviations, σ , at the bottom of each column and the two right-hand columns suggest that there is little variation between the stations, but there is a fairly large interannual variation. To test this assumption, we performed an analysis of variance for the ten-year period from 1954 through 1963—a period with data for all locations. This distribution of frequencies is not truly normal; but if the normal assumption is accepted, the analysis indicates a highly significant interannual variation and an insignificant interstation variation (one that is well within the random fluctuation.) A year with an above-average frequency of bad weather at one station is likely to be a year with above-average frequency of bad weather at all stations, and vice versa. In the ten-year period from 1954 to 1963, 1955 was the worst year, with 7 percent to 17 percent higher-than-average frequency at all stations. In year 1962, however, all stations had between 12 percent and 25 percent less bad weather than the average.

Although Table 2 shows the variation only for five locations during January, it does suggest two points that should be borne in mind when data are averaged over many years: (1) there may be marked differences in frequency of bad weather from one year to another; and (2) above or below normal frequencies of bad weather at one location are likely to be accompanied by similar anomalies at other locations within the same geographical region.

An example of the frequency distribution of the given weather state is shown in Fig. 2, along with the log-normal fit to the distribution.

Table 2

FREQUENCY OF CEILINGS < 500 FT OR VISIBILITY < 4 MI IN JANUARY

Year	Weisbaden	Berlin	Frankfurt	Heidelberg	Bitburg	Mean	σ
1947	0.44	0.36					
1948	0.37	0.40					
1949	0.40	0.41					
1950	0.32	0.39					
1951	0.53	0.43					
1952	0.37	0.43		0.34			
1953	0.54	0.72		0.70	0.85		
1954	0.27	0.46	0.43	0.28	0.31	0.35	0.09
1955	0.61	0.62	0.62	0.49	0.59	0.58	0.06
1956	0.41	0.41	0.39	0.24	0.35	0.36	0.07
1957	0.59	0.61	0.61	0.44	0.46	0.54	0.08
1958	0.37	0.52	0.37	0.42	0.38	0.41	0.06
1959	0.37	0.38	0.40	0.30	0.25	0.35	0.06
1960	0.44	0.48	0.45	0.45	0.38	0.44	0.04
1961	0.51	0.48	0.44	0.45	0.45	0.47	0.03
1962	0.32	0.24	0.22	0.27	0.21	0.25	0.04
1963	0.47	0.57	0.52	0.55	0.52	0.53	0.04
1964	0.76		0.80	0.78	0.67		
1965	0.42		0.41	0.48	0.41		
1966	0.45		0.43	0.33	0.45		
1967	0.45		0.39	0.41	0.36		
1968	0.32		0.41	0.18			
1969	0.46		0.46	0.34			
1970	0.62		0.71	0.46			
Mean	0.44	0.46	0.47	0.42	0.44		
σ	0.12	0.12	0.12	0.15	0.16		

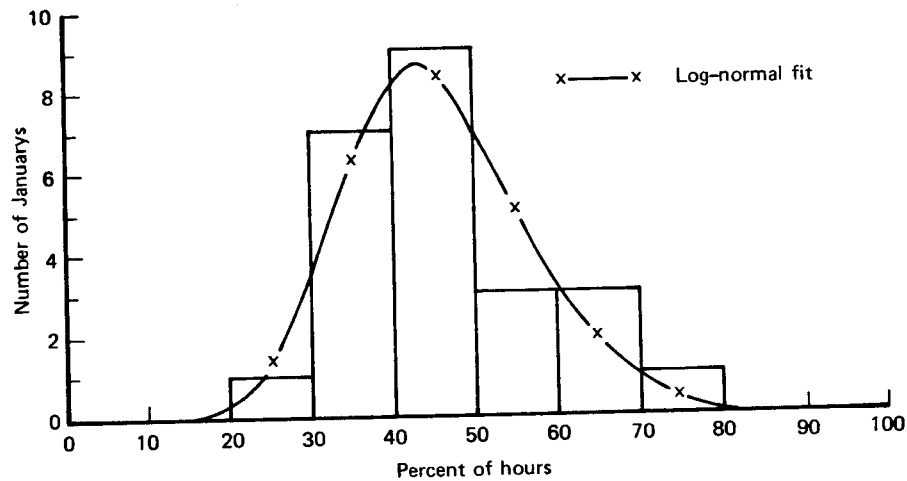


Fig. 2—Distribution of Percent of Hours Having Ceiling < 500 Ft or Visibility < 4 Mi During 24 Januarys at Wiesbaden

3. DIURNAL-ANNUAL FREQUENCIES OF CEILING AND VISIBILITY COMBINATIONS AT 17 LOCATIONS

The percent frequencies at which ceiling and visibility combinations meet given criteria are presented for 17 locations as a function of time of day and month of the year. Table 3, an index to Figs. 3-19, shows the locations (weather stations) and ceiling and visibility combinations for which these frequency statistics were calculated.

In Figs. 3-19, the hour (vertical) scale is the 24 hr clock in Local Standard Meridian Time (LSMT). LSMT would be the same as local time *if* all time zones were precisely defined by $\pm 7.5^\circ$ longitude from a standard meridian. The standard meridians are every 15° longitude counting from the 0° (Greenwich) meridian. On each of these graphs, the times of astronomical sunrise and sunset are shown, providing a ready means for separating day and night conditions.

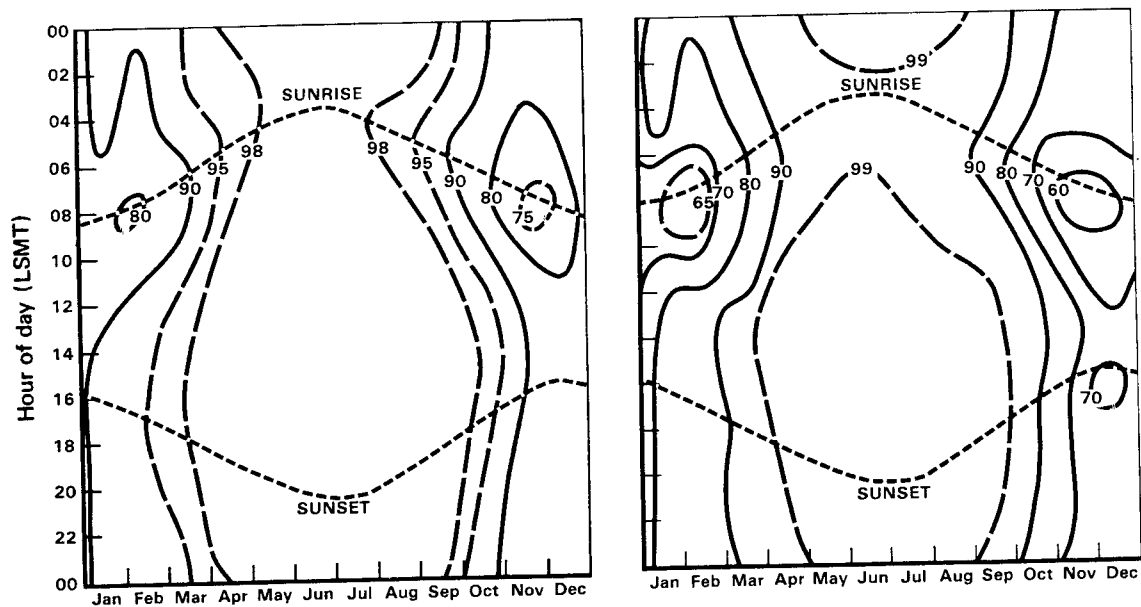
The frequency isopleths are based upon frequency calculations for every observational hour (at 1 hr or 3 hr intervals, depending on the station) and for every calendar month over the entire period of record (see Table 1) for each station. The longer periods of record produce the more representative and internally consistent frequency data. For example, there were only five years of data available for the three Norwegian stations. The rather chaotic appearance of their frequency isopleths (Figs. 11-13) is due to a combination of the absence of strong diurnal and annual cycles, and a too small sample size. Subjectively, confidence limits for the frequencies in Figs. 11-13 are estimated at from ± 5 to 10 percent; for most of the other locations, the limits are more like ± 2 to 3 percent.

These figures are simply interpreted in the same way as the following example: In Fig. 3(a), at 0800 LSMT in March, the ceiling equals or exceeds 500 ft *and* the visibility equals or exceeds 1 mi 90 percent of the time (i.e., with a 90 percent probability).

Table 3
 INDEX TO FIGURES DEPICTING DIURNAL-ANNUAL CEILING AND
 VISIBILITY FREQUENCIES

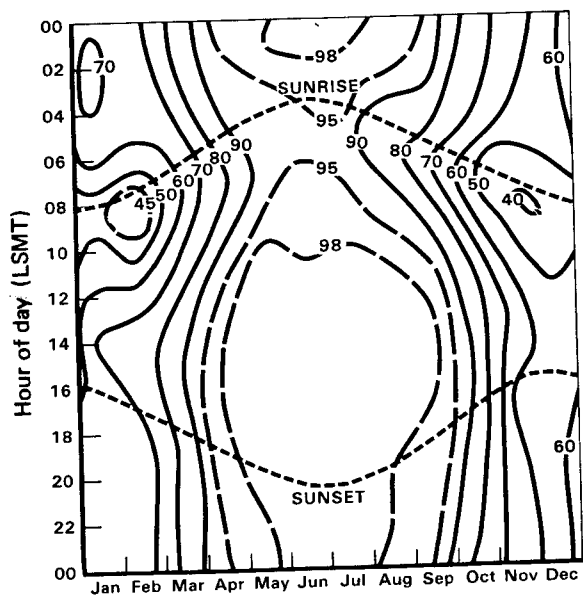
Location ^a	Ceiling (ft)/ Vis (mi)	Figure/Page	Location	Ceiling (ft)/ Vis (mi)	Figure/Page	
Berlin	500/1	3a/11	Hof	1500/3	8 /24	
	500/2	3b/11	Münster	1000/4	9a/25	
	500/3	3c/11		2000/3	9b/25	
	1000/1	3d/12	Neubiberg	500/2	10a/26	
	1000/3	3e/12		1000/3	10b/26	
	1000/4	3f/12		1000/4	10c/26	
	1000/5	3g/13		3500/5	10d/27	
	1000/6	3h/13		10000/7	10e/27	
	1500/3	3i/13		Bardufoss	500/3	11a/28
	2000/1	3j/14	3000/4		11b/28	
	2000/3	3k/14	10000/5		11c/28	
	2000/4	3l/14	Kirkenes		500/3	12a/29
	2000/5	3m/14			3000/4	12b/29
	2000/6	3n/15		10000/5	12c/29	
	2000/7	3o/15	Tromsø	500/3	13a/30	
	2000/10	3p/15		3000/4	13b/30	
	3000/4	3q/16		10000/5	13c/30	
	3500/5	3r/16		Sodankyla	500/3	14a/31
	5000/1	3s/17			3000/4	14b/31
	5000/3	3t/17	10000/5		14c/31	
	5000/7	3u/17	Istanbul	500/3	15a/32	
	5000/10	3v/17		3000/4	15b/32	
	10000/4	3w/18		10000/5	15c/32	
	10000/5	3x/18		Belgrade	1500/3	16a/33
	10000/7	3y/18			Pula	1500/3
	11000/1	3z/19	Skopje	1500/3		16c/33
11000/7	3aa/19	Zagreb		1500/3	16d/33	
11000/10	3bb/19		Bremerhaven	1000/4	4a/20	
12000/5	3cc/19	2000/3		4b/20		
Bremerhaven	1000/4	4a/20	Emden-Hafen	1000/4	5a/21	
	2000/3	4b/20		2000/3	5b/21	
Emden-Hafen	1000/4	5a/21	Hamburg	1000/4	6a/22	
	2000/3	5b/21		2000/3	6b/22	
Hamburg	1000/4	6a/22	Hannover	1000/4	7a/23	
	2000/3	6b/22		2000/3	7b/23	

^aSee Table 1 and Fig. 1 for location information.



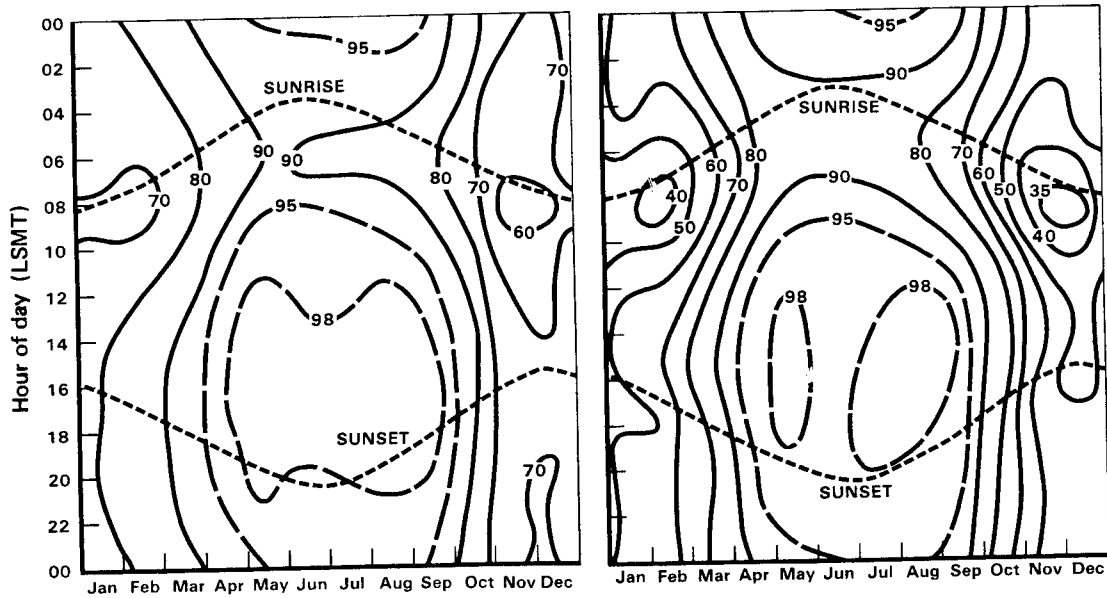
(a) Ceiling \geq 500 ft, and
Visibility \geq 1 st mi

(b) Ceiling \geq 500 ft, and
Visibility \geq 2 st mi



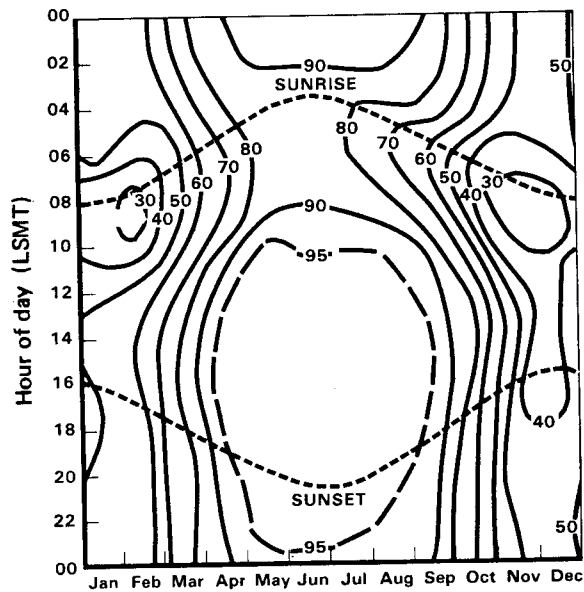
(c) Ceiling \geq 500 ft, and
Visibility \geq 3 st mi

Fig. 3—Hourly-Monthly Percent Frequencies of Concurrent Ceiling and Visibility at Berlin



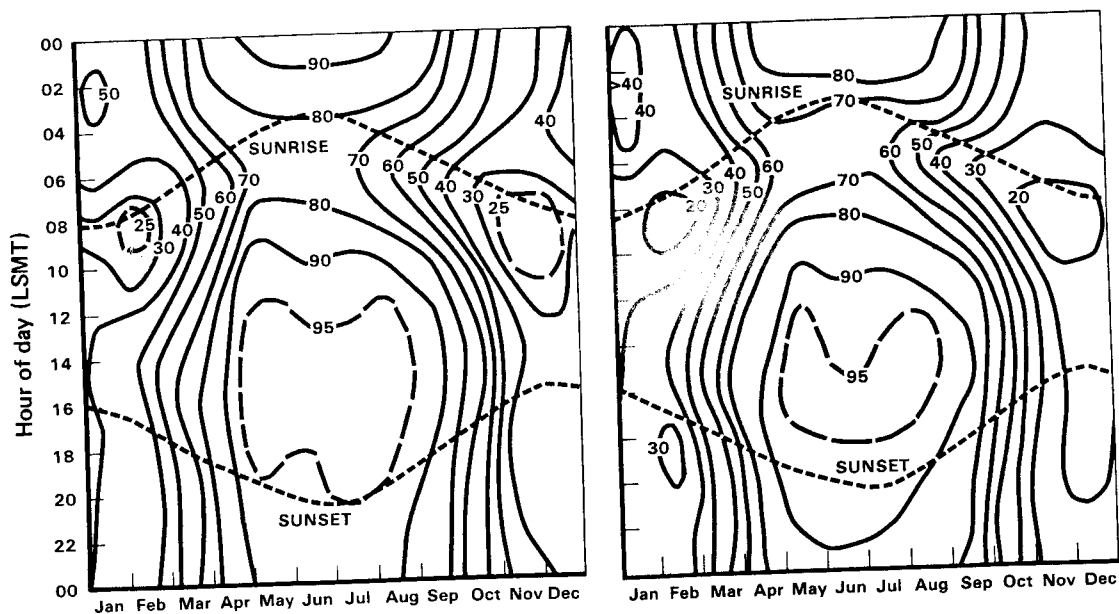
(d) Ceiling ≥ 1000 ft, and
Visibility ≥ 1 st mi

(e) Ceiling ≥ 1000 ft, and
Visibility ≥ 3 st mi



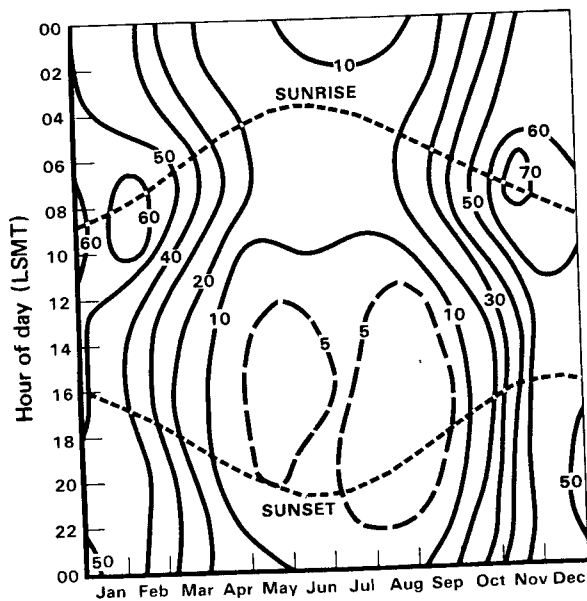
(f) Ceiling ≥ 1000 ft, and
Visibility ≥ 4 st mi

Fig. 3—Hourly-Monthly Percent Frequencies of Concurrent
Ceiling and Visibility at Berlin



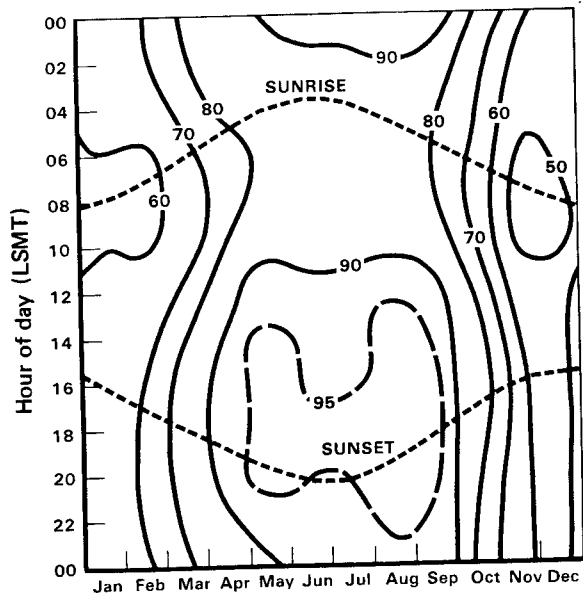
(g) Ceiling \geq 1000 ft, and
 Visibility \geq 5 st mi

(h) Ceiling \geq 1000 ft, and
 Visibility \geq 6 st mi

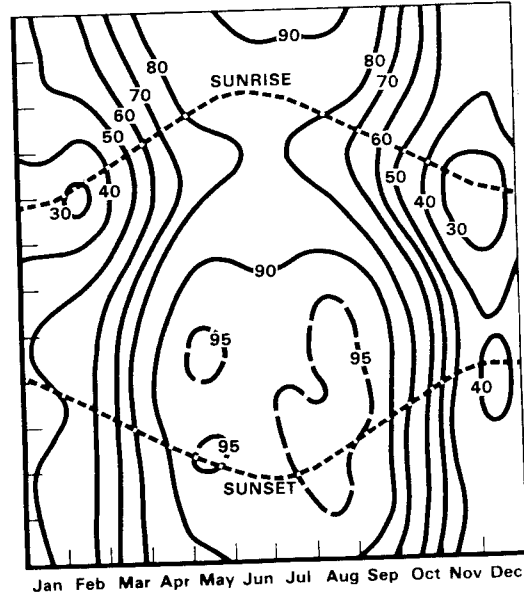


(i) Ceiling \leq 1500 ft, and
 Visibility \leq 3 st mi

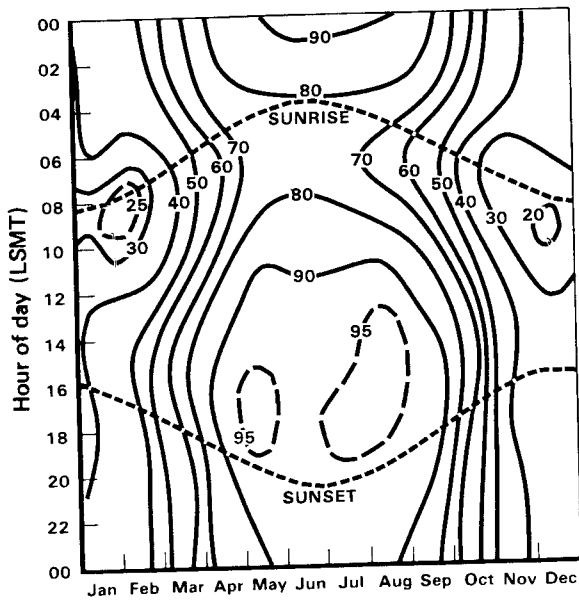
Fig. 3—Hourly-Monthly Percent Frequencies of Concurrent
 Ceiling and Visibility at Berlin



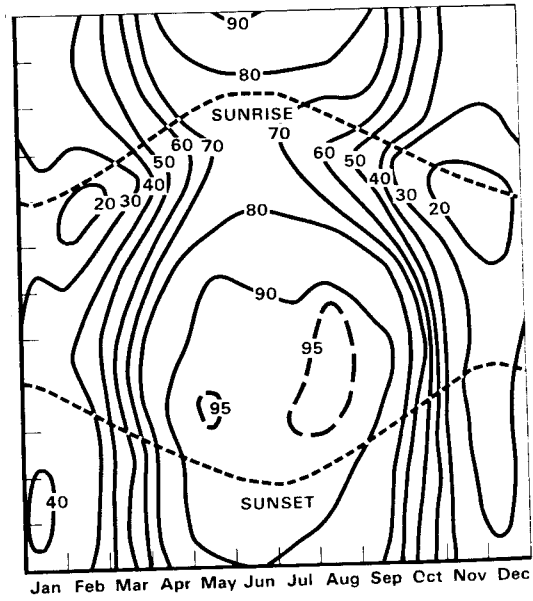
(j) Ceiling \geq 2000 ft, and
Visibility \geq 1 st mi



(k) Ceiling \geq 2000 ft, and
Visibility \geq 3 st mi

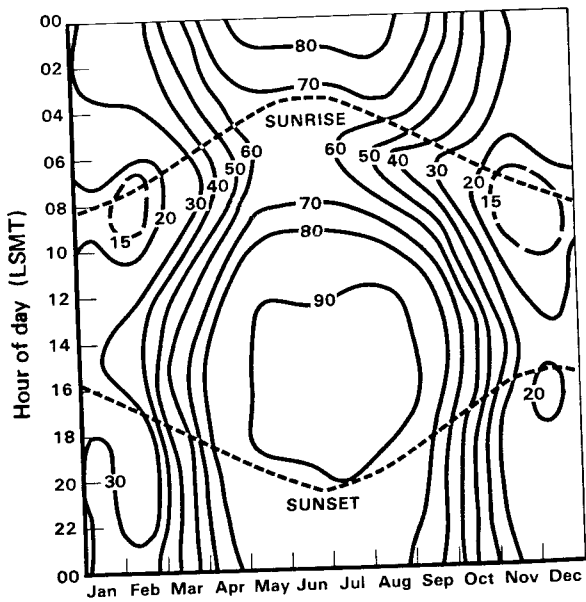


(l) Ceiling \geq 2000 ft, and
Visibility \geq 4 st mi

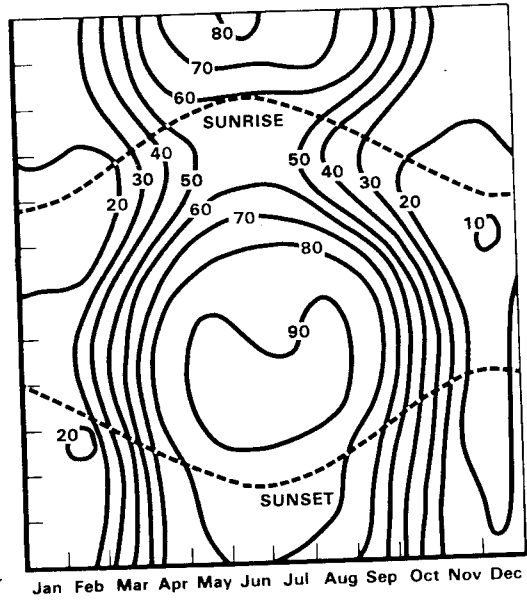


(m) Ceiling \geq 2000 ft, and
Visibility \geq 5 st mi

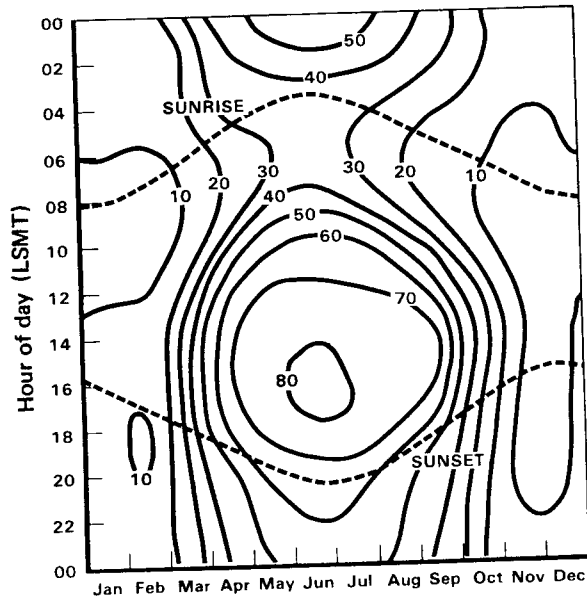
Fig. 3—Hourly-Monthly Percent Frequencies of Concurrent
Ceiling and Visibility at Berlin



(n) Ceiling \geq 2000 ft, and
Visibility \geq 6 st mi

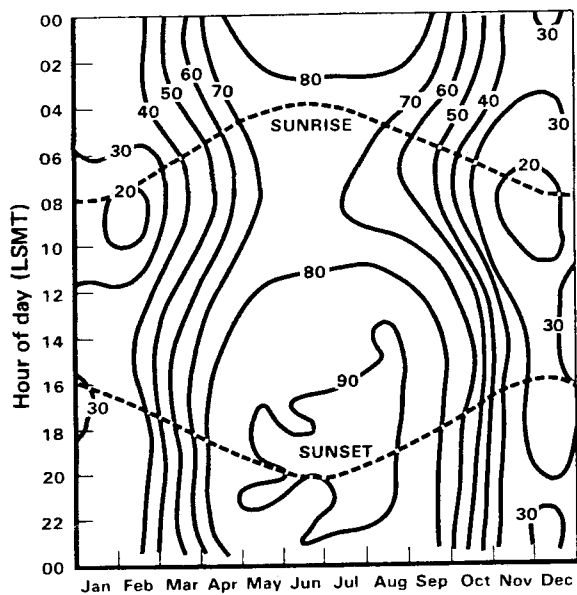


(o) Ceiling \geq 2000 ft, and
Visibility \geq 7 st mi

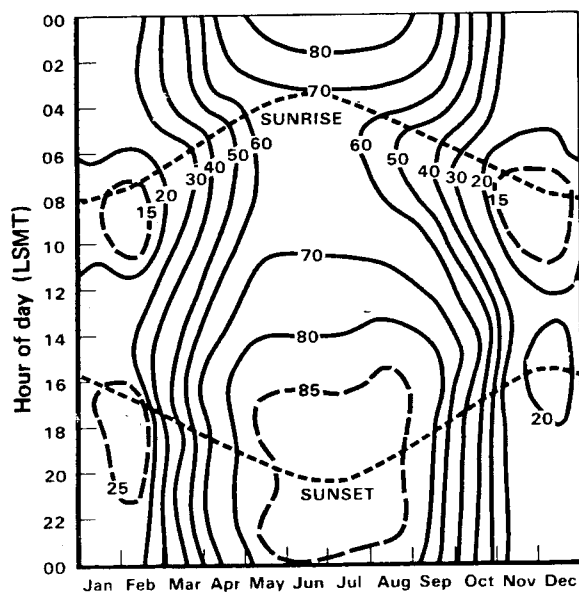


(p) Ceiling \geq 2000 ft, and
Visibility \geq 10 st mi

Fig. 3—Hourly-Monthly Percent Frequencies of Concurrent Ceiling and Visibility at Berlin

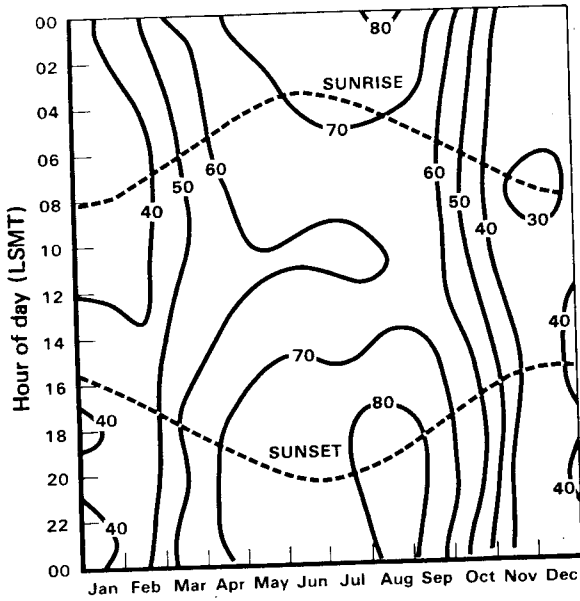


(q) Ceiling \geq 3000 ft, and
Visibility \geq 4 st mi

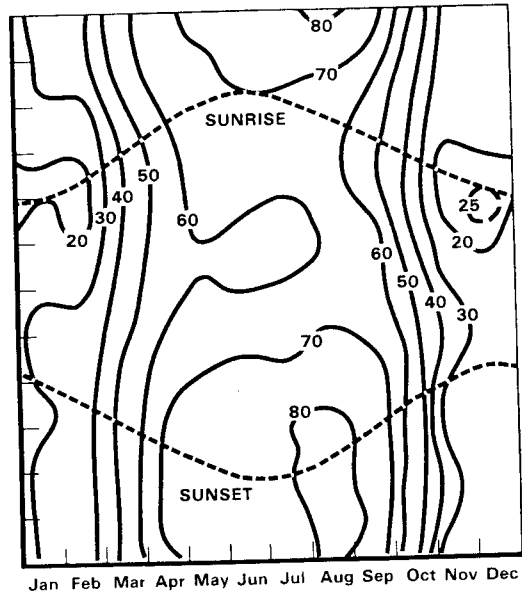


(r) Ceiling \geq 3500 ft, and
Visibility \geq 5 st mi

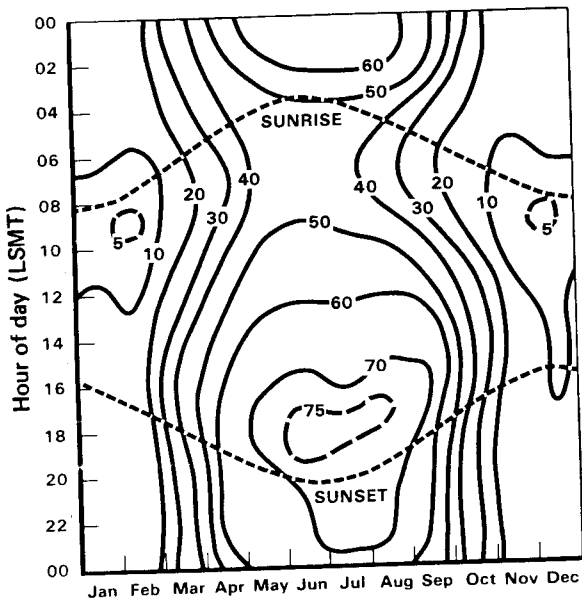
Fig. 3—Hourly-Monthly Percent Frequencies of Concurrent Ceiling and Visibility at Berlin



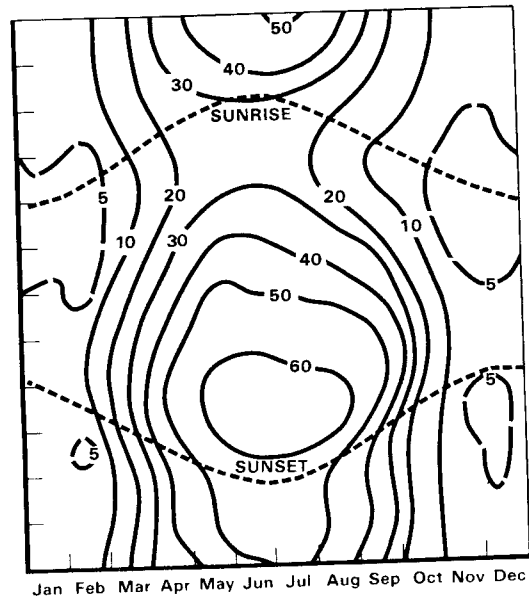
(s) Ceiling \geq 5000 ft, and
Visibility \geq 1 st mi



(t) Ceiling \geq 5000 ft, and
Visibility \geq 3 st mi

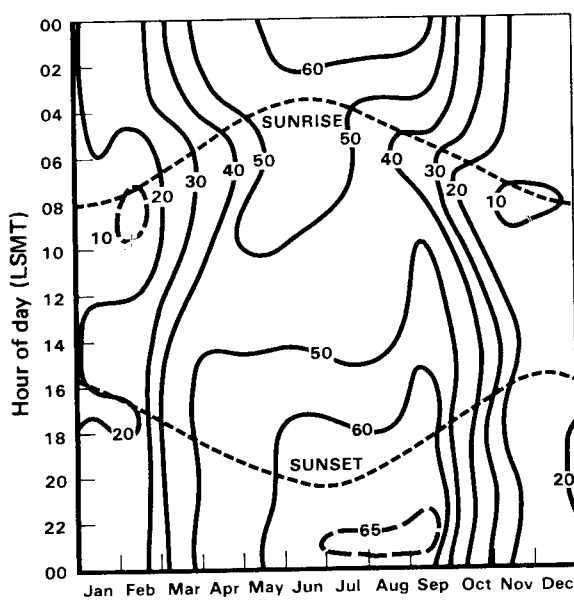


(u) Ceiling \geq 5000 ft, and
Visibility \geq 7 st mi

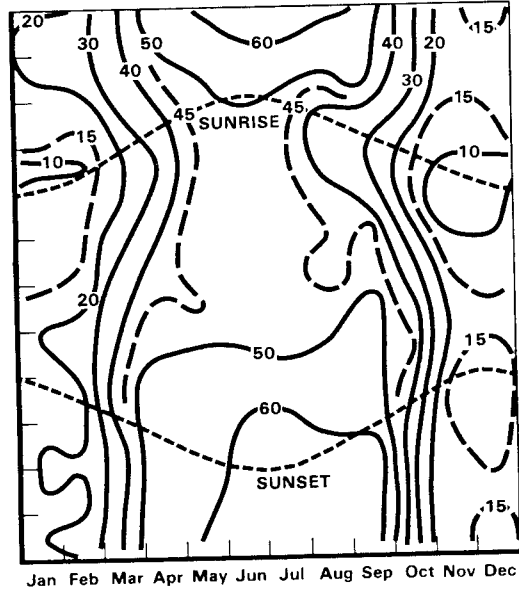


(v) Ceiling \geq 5000 ft, and
Visibility \geq 10 st mi

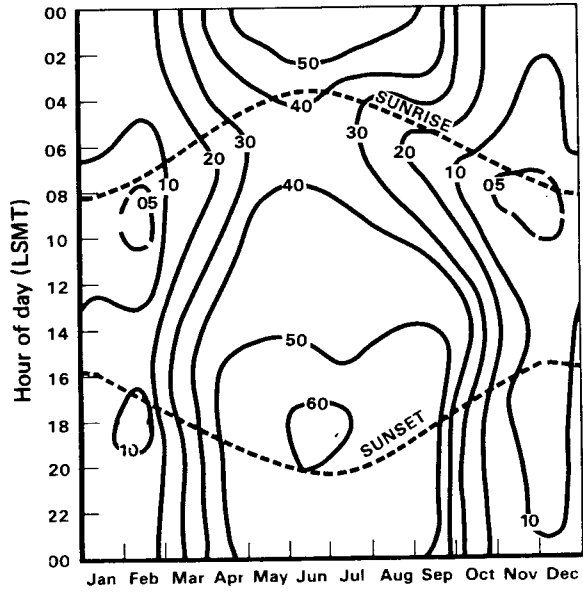
Fig. 3—Hourly-Monthly Percent Frequencies of Concurrent
Ceiling and Visibility at Berlin



(w) Ceiling \geq 10,000 ft, and
Visibility \geq 4 st mi

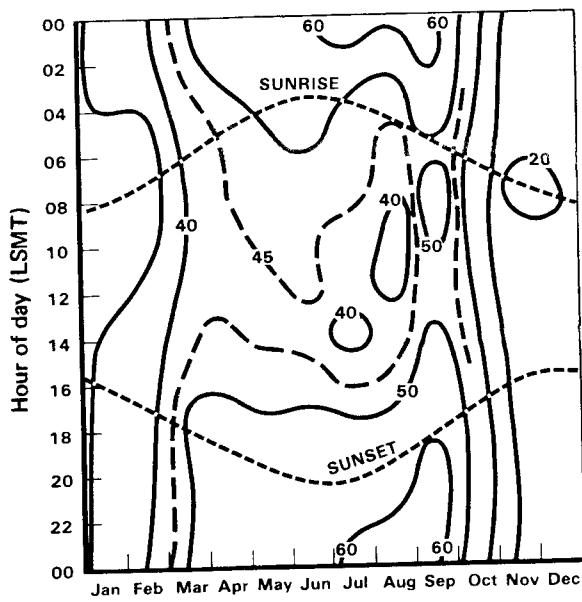


(x) Ceiling \geq 10,000 ft, and
Visibility \geq 5 st mi

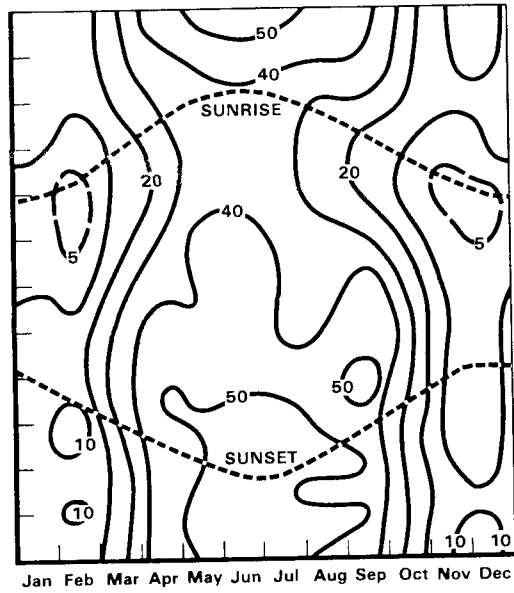


(y) Ceiling \geq 10,000 ft, and
Visibility \geq 7 st mi

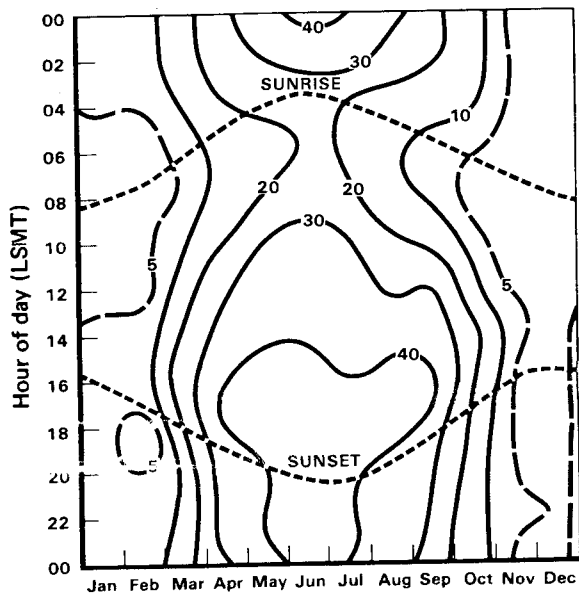
Fig. 3—Hourly-Monthly Percent Frequencies of Concurrent Ceiling and Visibility at Berlin



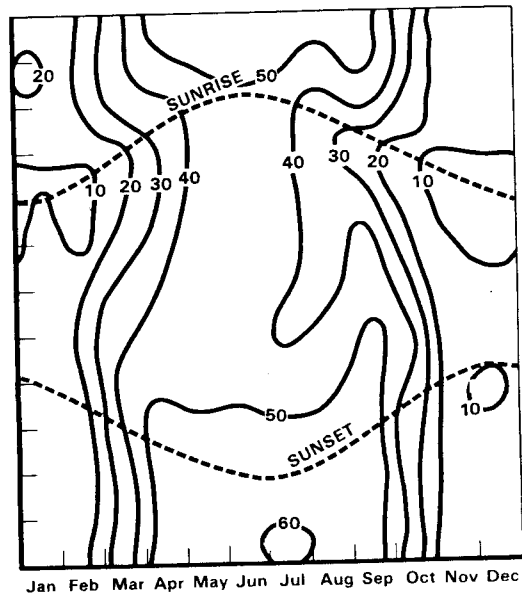
(z) Ceiling \geq 11,000 ft, and
Visibility \geq 1 st mi



(aa) Ceiling \geq 11,000 ft, and
Visibility \geq 7 st mi

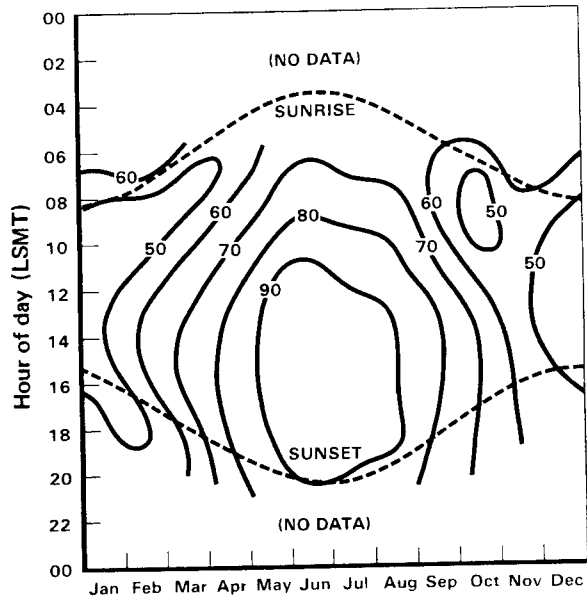


(bb) Ceiling \geq 11,000 ft, and
Visibility \geq 10 st mi

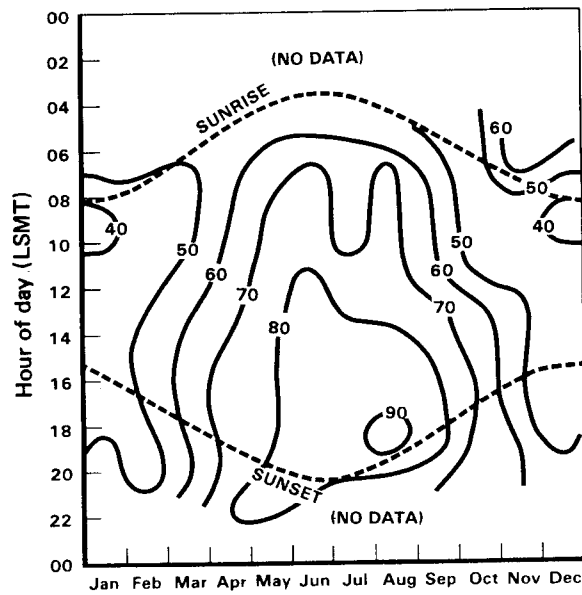


(cc) Ceiling \geq 12,000 ft, and
Visibility \geq 5 st mi

Fig. 3—Hourly-Monthly Percent Frequencies of Concurrent Ceiling and Visibility at Berlin

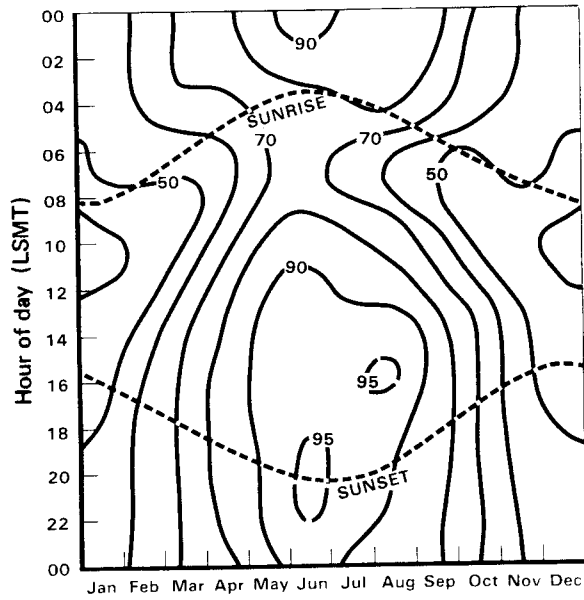


(a) Ceiling ≥ 1000 ft, and
Visibility ≥ 4 st mi

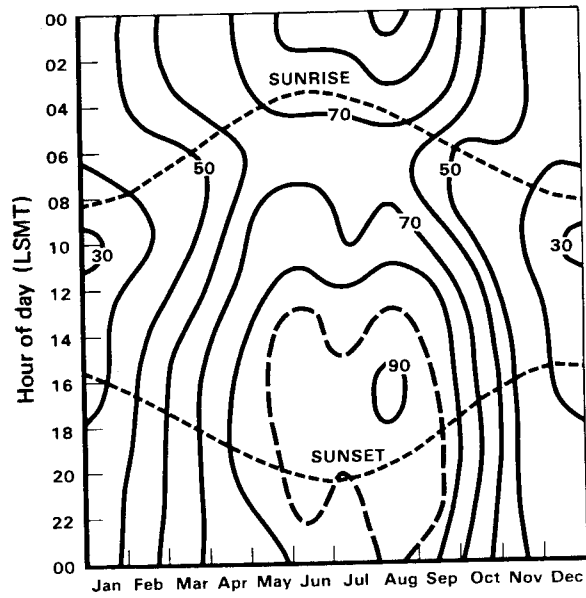


(b) Ceiling ≥ 2000 ft, and
Visibility ≥ 3 st mi

Fig. 4—Hourly-Monthly Percent Frequencies of Concurrent Ceiling and Visibility at Bremerhaven

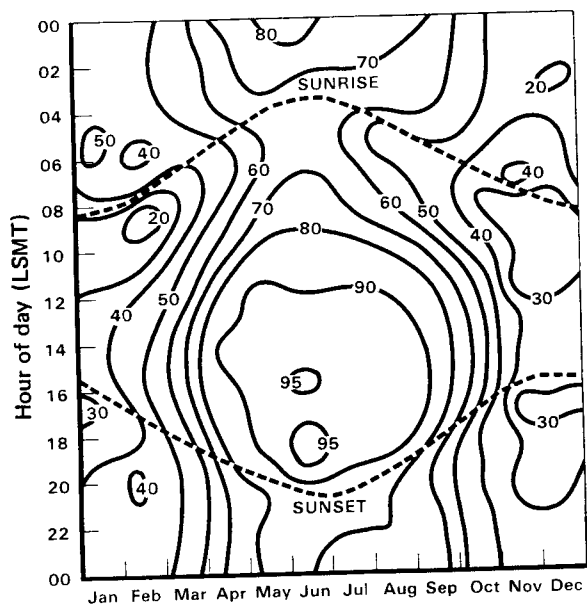


(a) Ceiling \geq 1000 ft, and
Visibility \geq 4 st mi

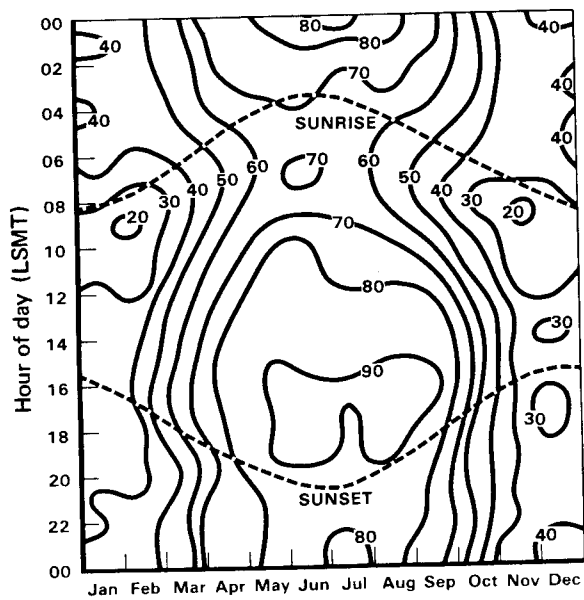


(b) Ceiling \geq 2000 ft, and
Visibility \geq 3 st mi

Fig. 5—Hourly-Monthly Percent Frequencies of Concurrent Ceiling and Visibility at Emden-Hafen

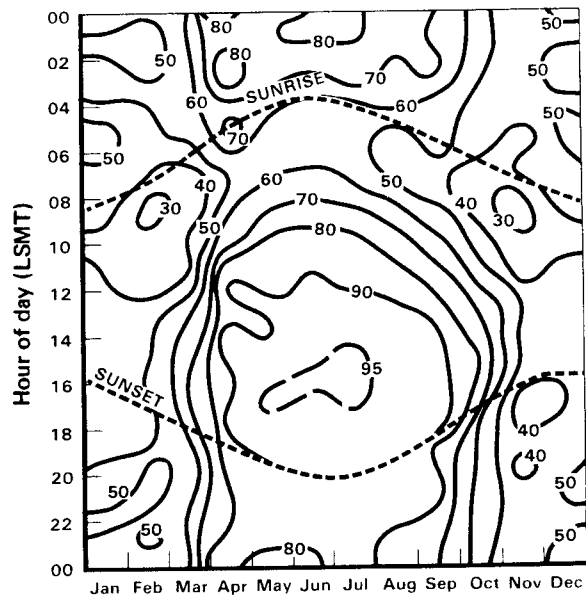


(a) Ceiling \geq 1000 ft, and
Visibility \geq 4 st mi

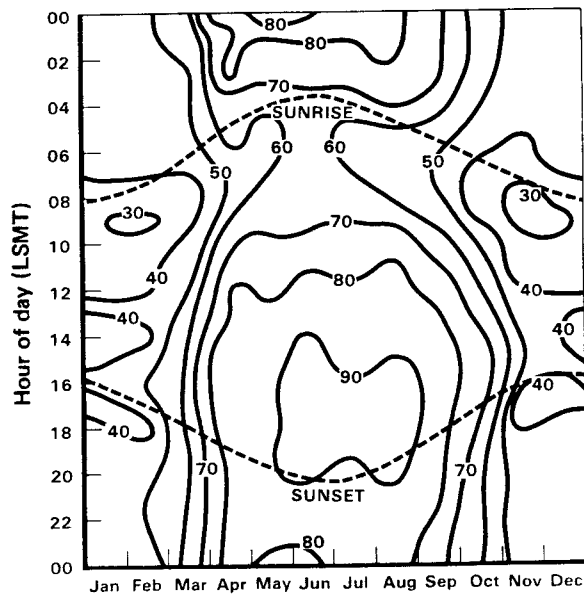


(b) Ceiling \geq 2000 ft, and
Visibility \geq 3 st mi

Fig. 6—Hourly-Monthly Percent Frequencies of Concurrent Ceiling and Visibility at Hamburg



(a) Ceiling \geq 1000 ft, and
Visibility \geq 4 st mi



(b) Ceiling \geq 2000 ft, and
Visibility \geq 3 st mi

Fig. 7—Hourly-Monthly Percent Frequencies of Concurrent Ceiling and Visibility at Hannover

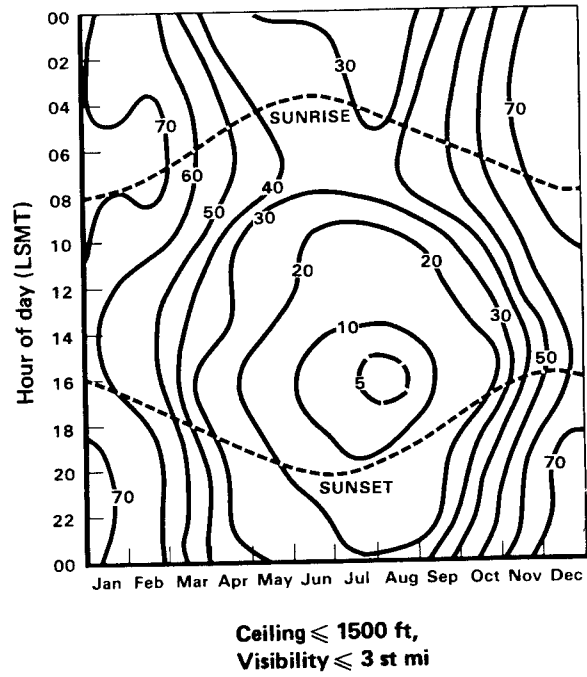
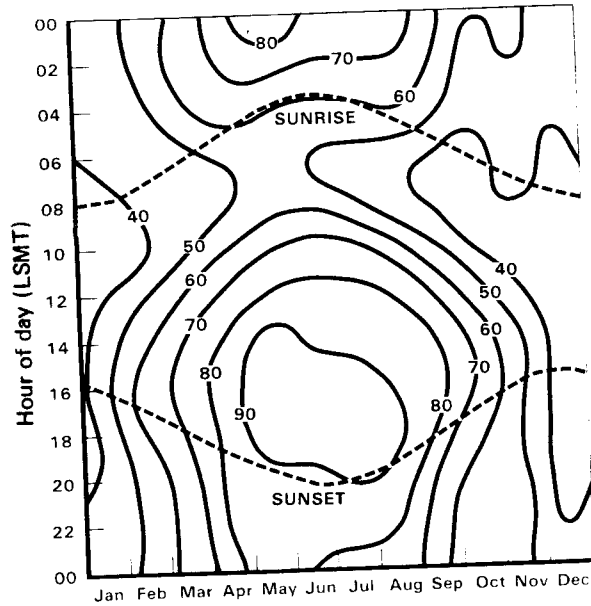
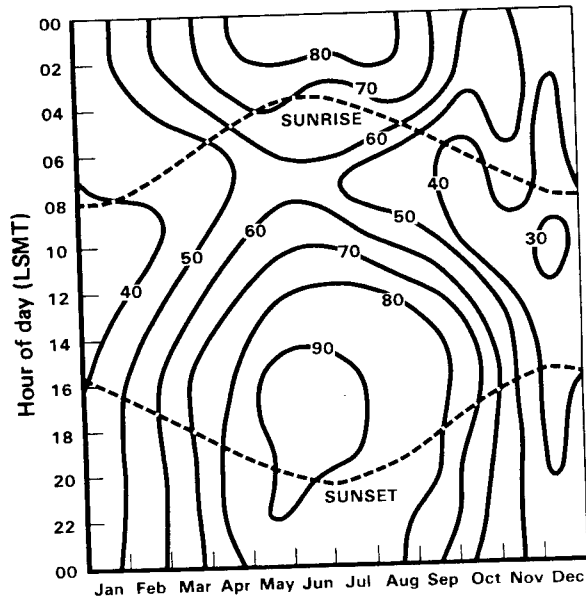


Fig. 8—Hourly-Monthly Percent Frequencies of Concurrent Ceiling and Visibility at Hof

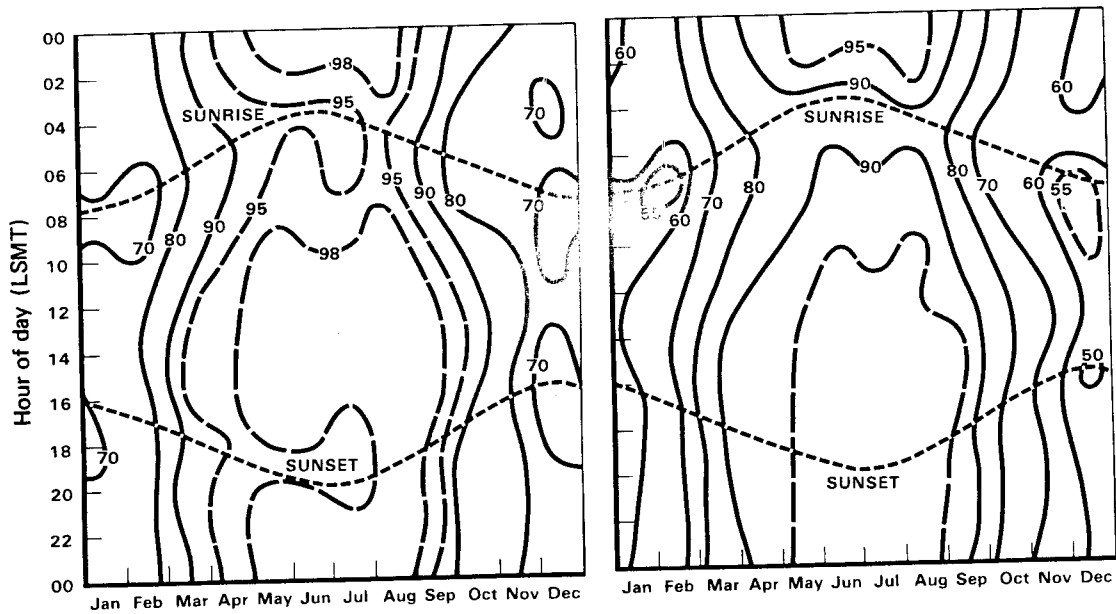


(a) Ceiling \geq 1000 ft, and
Visibility \geq 4 st mi



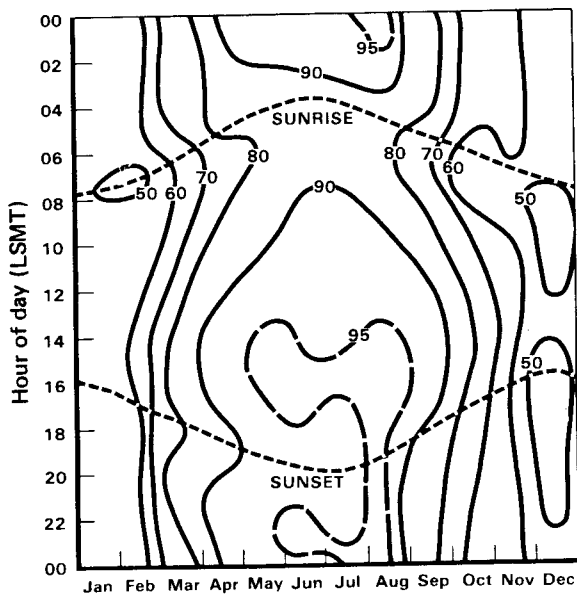
(b) Ceiling \geq 2000 ft, and
Visibility \geq 3 st mi

Fig. 9—Hourly-Monthly Percent Frequencies of Concurrent Ceiling and Visibility at Münster



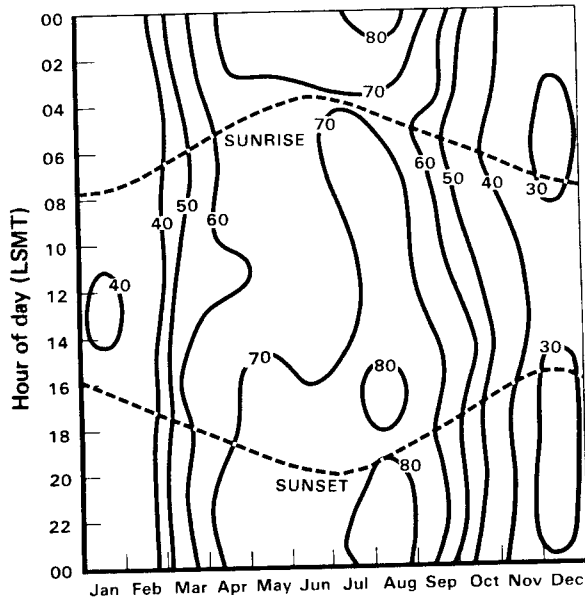
(a) Ceiling \geq 500 ft, and
Visibility \geq 2 st mi

(b) Ceiling \geq 1000 ft, and
Visibility \geq 3 st mi

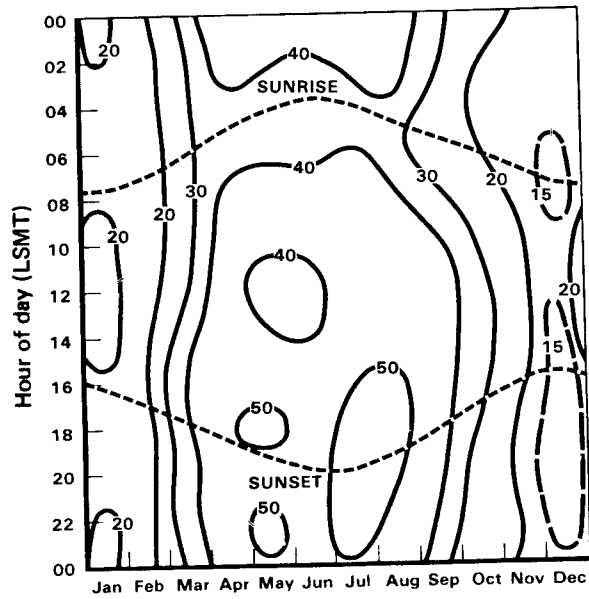


(c) Ceiling \geq 1000 ft, and
Visibility \geq 4 st mi

Fig. 10—Hourly-Monthly Percent Frequencies of Concurrent Ceiling and Visibility at Neubiberg

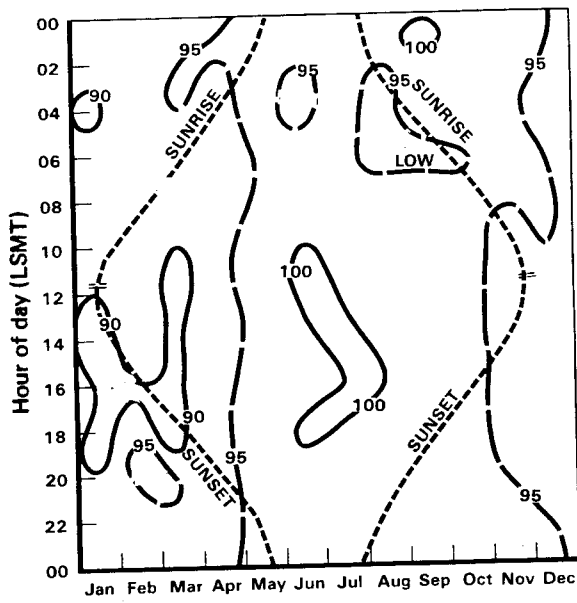


(d) Ceiling \geq 3500 ft, and
 Visibility \geq 5 st mi

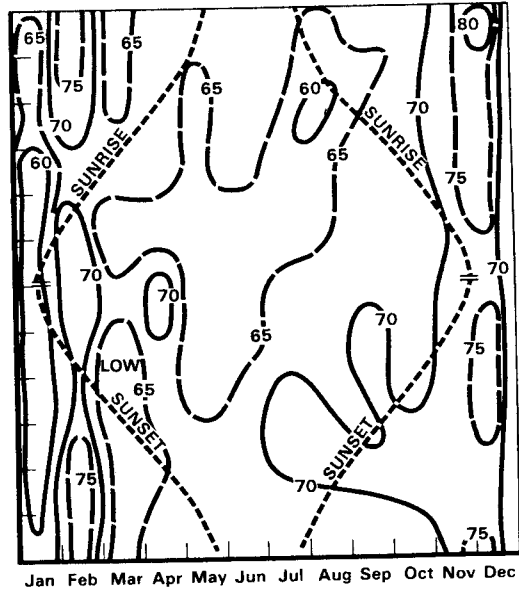


(e) Ceiling \geq 10,000 ft, and
 Visibility \geq 7 st mi

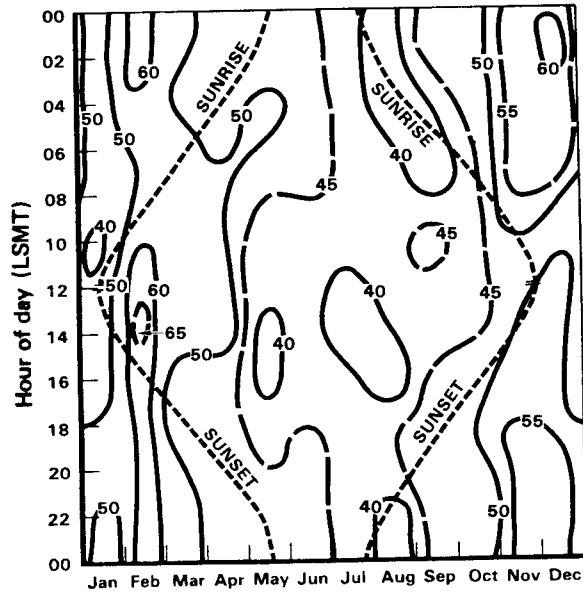
Fig. 10—Hourly-Monthly Percent Frequencies of Concurrent
 Ceiling and Visibility at Neubiberg



(a) Ceiling \geq 500 ft, and
Visibility \geq 3 st mi

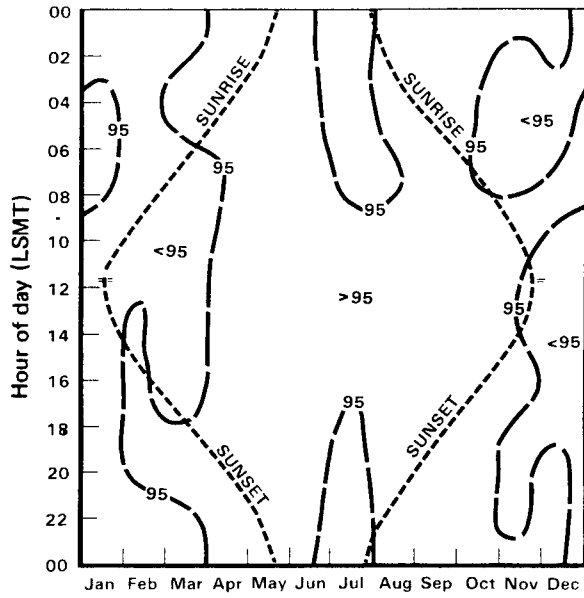


(b) Ceiling \geq 3000 ft, and
Visibility \geq 4 st mi

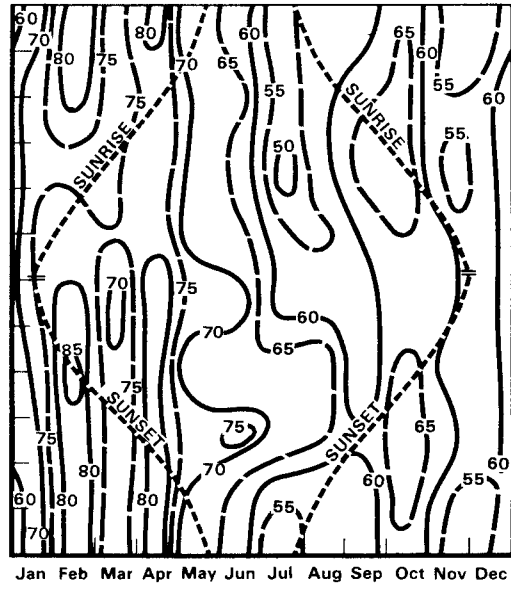


(c) Ceiling \geq 10,000 ft, and
Visibility \geq 5 st mi

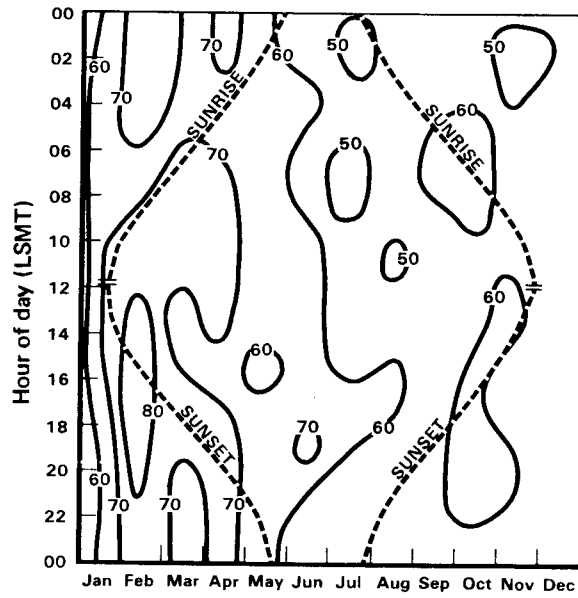
Fig. 11—Hourly-Monthly Percent Frequencies of Concurrent Ceiling and Visibility at Bardufoss



(a) Ceiling \geq 500 ft, and
Visibility \geq 3 st mi

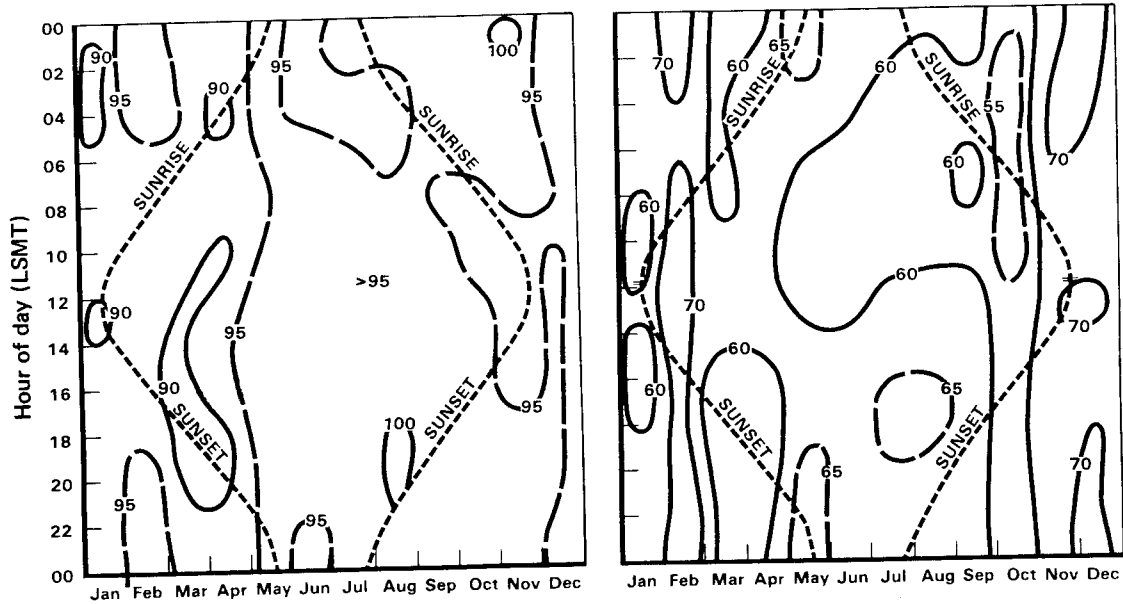


(b) Ceiling \geq 3000 ft, and
Visibility \geq 4 st mi



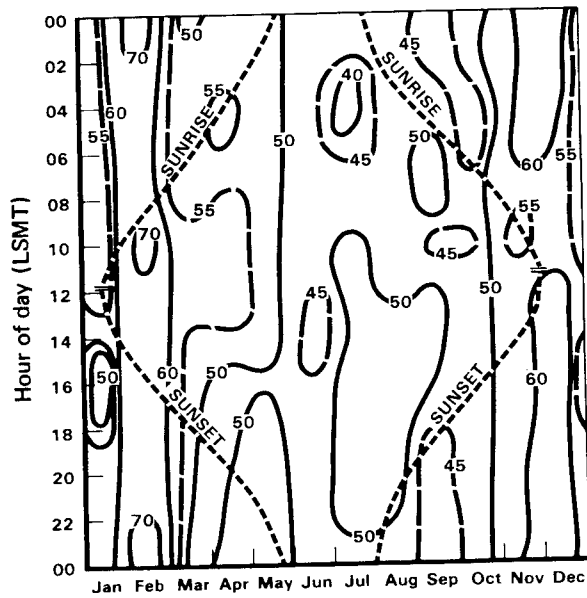
(c) Ceiling \geq 10,000 ft, and
Visibility \geq 5 st mi

Fig. 12—Hourly-Monthly Percent Frequencies of Concurrent Ceiling and Visibility at Kirkenes



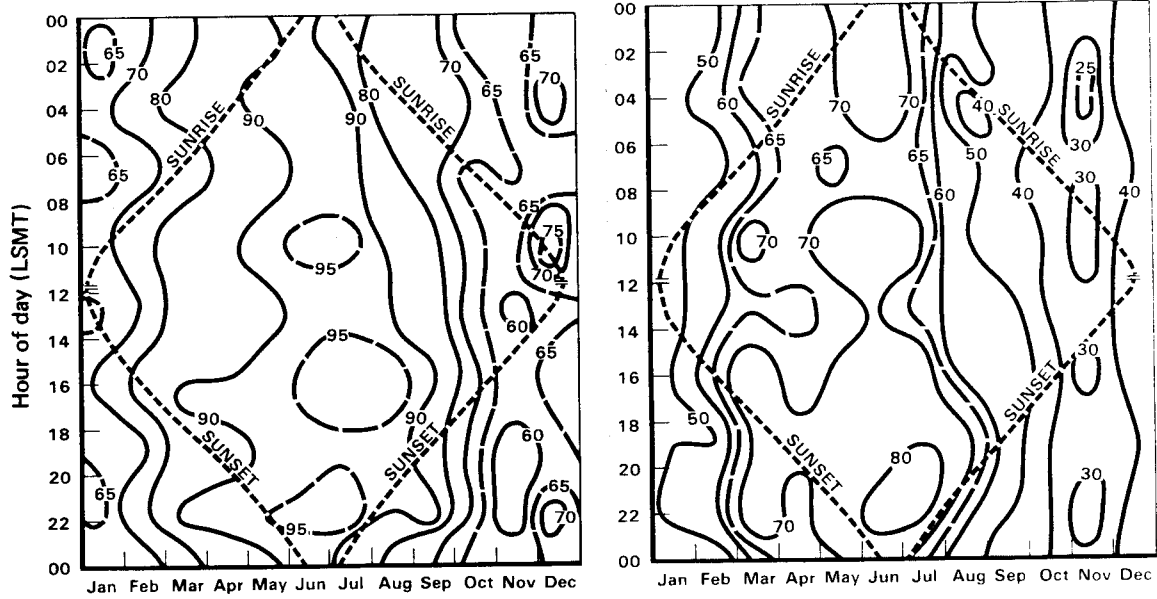
(a) Ceiling \geq 500 ft, and
Visibility \geq 3 st mi

(b) Ceiling \geq 3000 ft, and
Visibility \geq 4 st mi



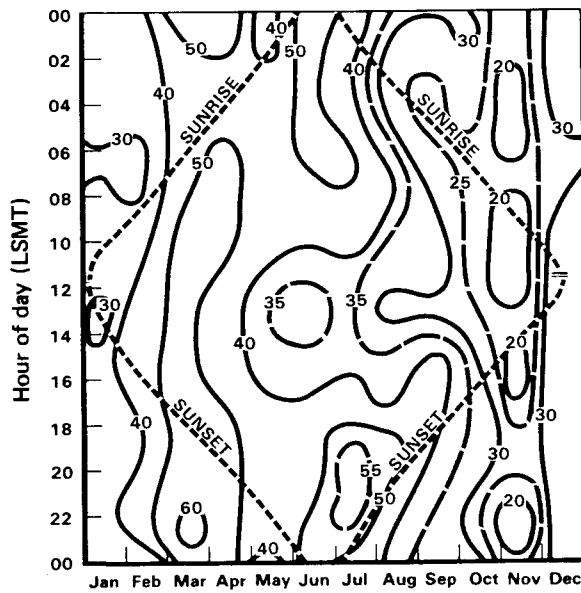
(c) Ceiling \geq 10,000 ft, and
Visibility \geq 5 st mi

Fig. 13—Hourly-Monthly Percent Frequencies of Concurrent Ceiling and Visibility at Tromsø



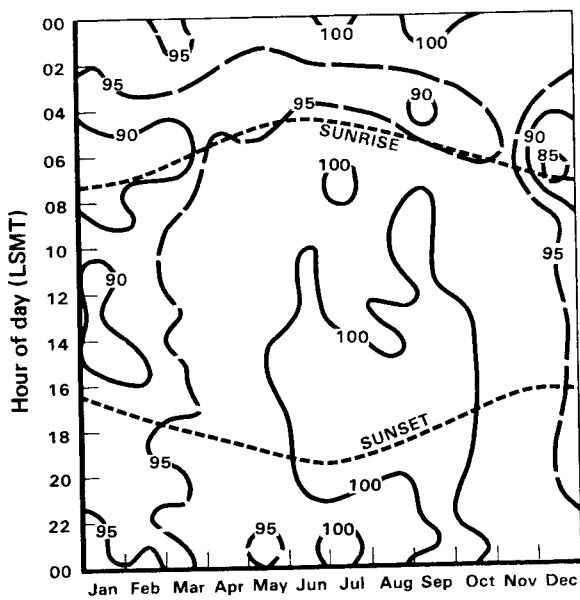
(a) Ceiling ≥ 500 ft, and
Visibility ≥ 3 st mi

(b) Ceiling ≥ 3000 ft, and
Visibility ≥ 4 st mi

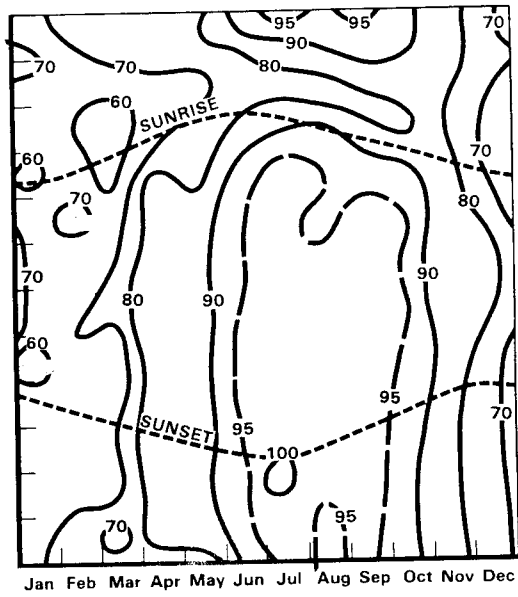


(c) Ceiling $\geq 10,000$ ft, and
Visibility ≥ 5 st mi

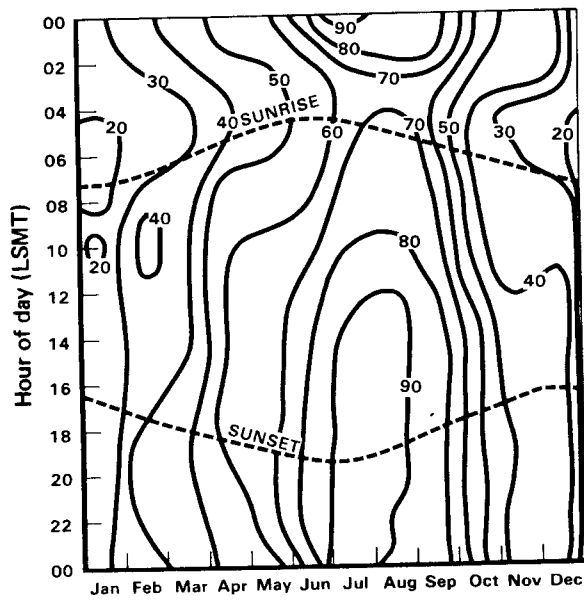
Fig. 14—Hourly-Monthly Percent Frequencies of Concurrent Ceiling and Visibility at Sodankyla



(a) Ceiling \geq 500 ft, and
Visibility \geq 3 st mi



(b) Ceiling \geq 3000 ft, and
Visibility \geq 4 st mi



(c) Ceiling \geq 10,000 ft, and
Visibility \geq 5 st mi

Fig. 15—Hourly-Monthly Percent Frequencies of Concurrent Ceiling and Visibility at Istanbul

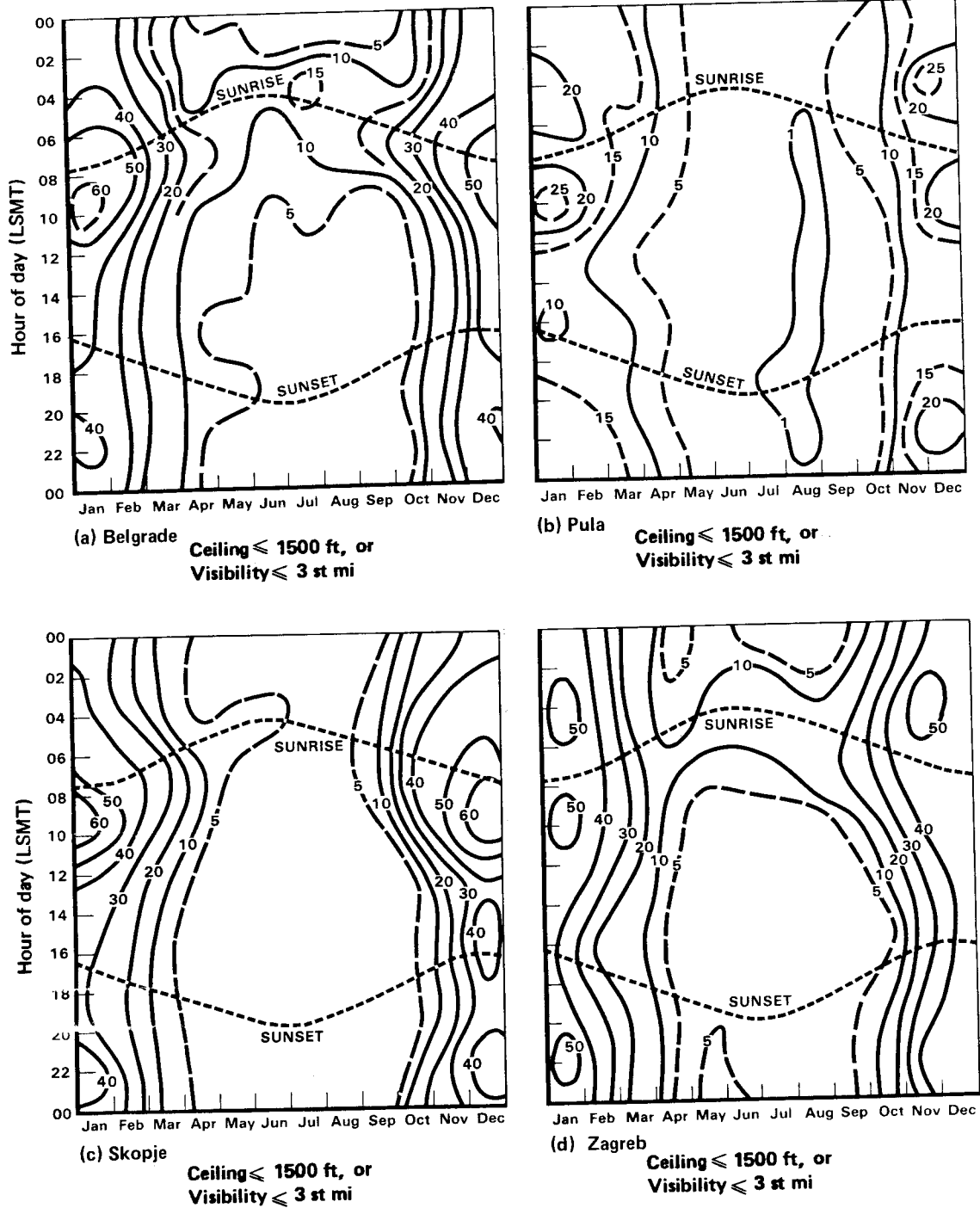


Fig. 16—Hourly-Monthly Percent Frequencies of Concurrent Ceiling and Visibility at Four Locations in Yugoslavia

4. SEASONAL CEILING AND VISIBILITY JOINT FREQUENCIES AT EIGHT LOCATIONS

The frequencies that any concurrent combinations of ceiling and visibility are equaled or exceeded are given here for eight locations. Table 4 shows the locations and time periods (seasons and times of day) for which these calculations are presented.

In Figs. 17-24, the independent frequencies of equaling or exceeding any ceiling or visibility values are read at the ordinate and abscissa. For example, in Fig. 17(a), for Berlin during November through February, the frequency of visibility equal to or greater than 3 mi is about 55 percent, and the frequency of a ceiling equal to or greater than 1000 ft is about 76 percent. The joint frequency that both 3 mi and 1000 ft will be equaled or exceeded, however, is found within the chart to be about 50 percent, or slightly higher than what would be expected if ceiling and visibility states were independent (or uncorrelated).¹

The joint frequency curves, except as noted below, are based on tabulations of the joint frequencies of 23 ceiling classes and 18 visibility classes, a total of 414 joint classes. Some minor smoothing was required to iron out observational idiosyncrasies (in the Berlin data, for example, two apparently permissible visibility classes were never reported). All of the curves, however, reflect the data to within 1 or 2 percent.

In Figs. 17(d)-(g), 17(k)-(n), and 18(a)-(j) the frequencies are based on a much coarser tabulation, seven ceiling and six visibility classes. The lowest ceiling class interval is "less than 1000 ft," so the segments of the frequency curves that lie below the 1000 ft ceiling value are estimates.

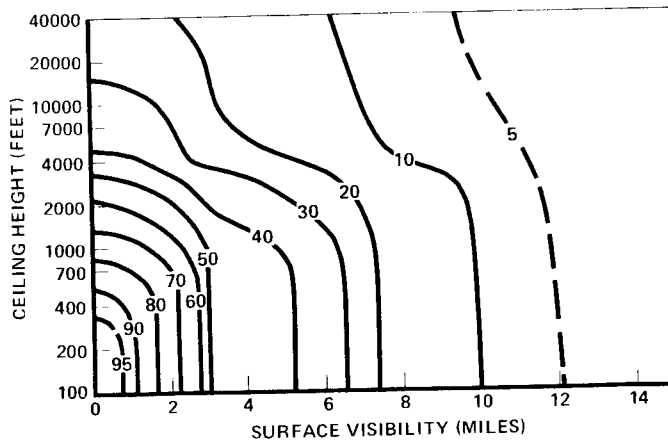
¹ If the ceiling and visibility were mutually independent, their joint frequency would be the product of their individual frequencies (42 percent in the example given).

Table 4

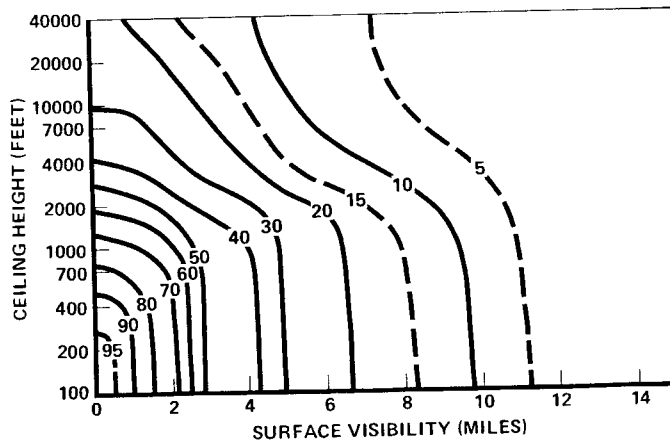
INDEX TO FIGURES DEPICTING SEASONAL CEILING AND VISIBILITY JOINT FREQUENCIES

Location ^a	Season, Months, Time of Day	Figure/Page	
Berlin	Winter, November-February, all hours	17a/36	
	Mid-winter, December-January, day	17b/36	
	Mid-winter, December-January, night	17c/36	
	Winter, November-February, day	17d/37	
	Winter, November-February, night	17e/37	
	Winter, November-February, forenoon	17f/37	
	Winter, November-February, afternoon	17g/37	
	Summer, May-August, all hours	17h/38	
	Mid-summer, June-July, day	17i/38	
	Mid-summer, June-July, night	17j/38	
	Summer, May-August, day	17k/39	
	Summer, May-August, night	17l/39	
	Summer, May-August, forenoon	17m/39	
	Summer, May-August, afternoon	17n/39	
	Grafenwöhr	Winter, November-February, all hours	18a/40
		Winter, November-February, day	18b/40
Winter, November-February, night		18c/40	
Winter, November-February, forenoon		18d/40	
Winter, November-February, afternoon		18e/40	
Summer, May-August, all hours		18f/41	
Summer, May-August, day		18g/41	
Summer, May-August, night		18h/41	
Summer, May-August, forenoon		18i/41	
Summer, May-August, afternoon		18j/41	
Heidelberg		Mid-winter, December-January, day	19a/42
	Mid-winter, December-January, night	19b/42	
	Mid-summer, June-July, day	19c/42	
	Mid-summer, June-July, night	19d/42	
Bardufoss	Winter, November-February, all hours	20a/43	
	Summer, May-August, all hours	20b/43	
Kirkenes	Winter, November-February, all hours	21a/44	
	Summer, May-August, all hours	21b/44	
Tromsø	Winter, November-February, all hours	22a/45	
	Summer, May-August, all hours	22b/45	
Sodankylä	Winter, November-February, all hours	23a/46	
	Summer, May-August, all hours	23b/46	
Istanbul	Winter, November-February, all hours	24a/47	
	Summer, May-August, all hours	24b/47	

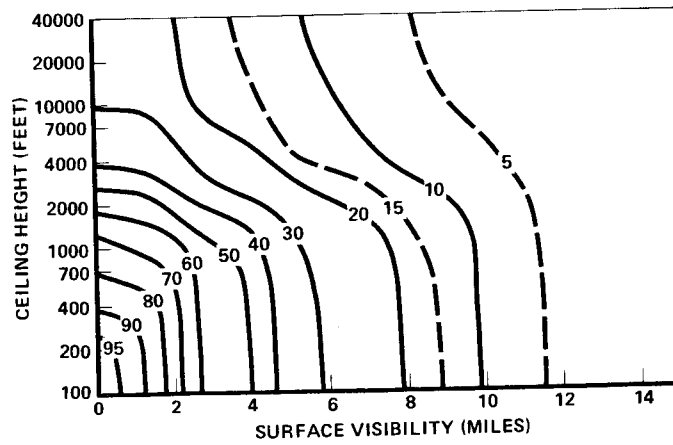
^aSee Table 1 and Fig. 1 for location information.



(a) Winter, November-February, all hours

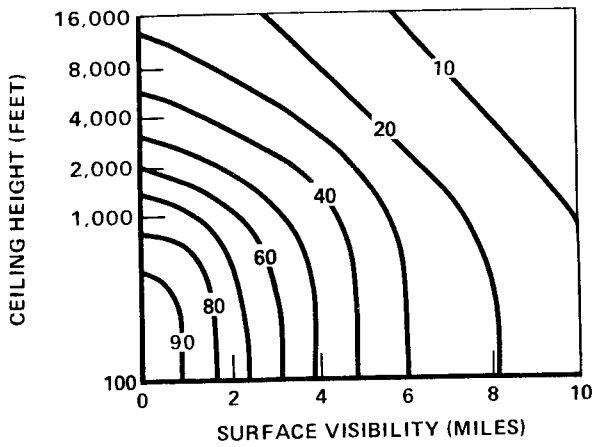


(b) Mid-winter, December-January, day

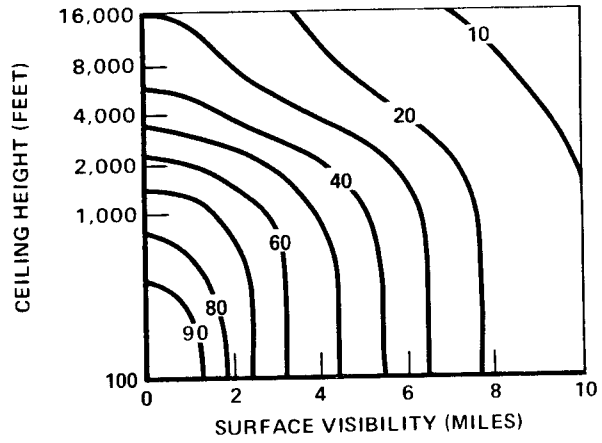


(c) Mid-winter, December-January, night

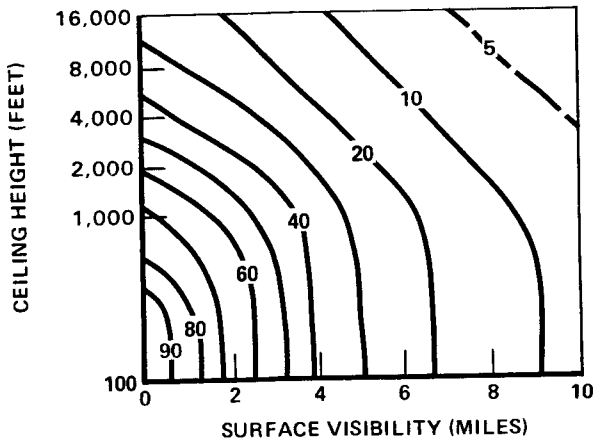
Fig. 17—Percent Frequency that Concurrent Ceiling and Visibility Values Are Equaled or Exceeded at Berlin



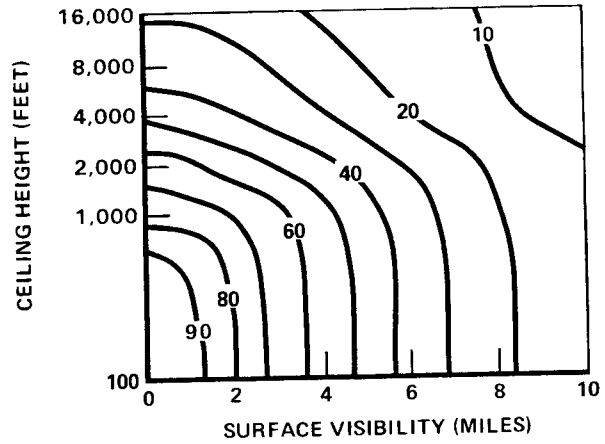
(d) Winter, November-February, day



(e) Winter, November-February, night

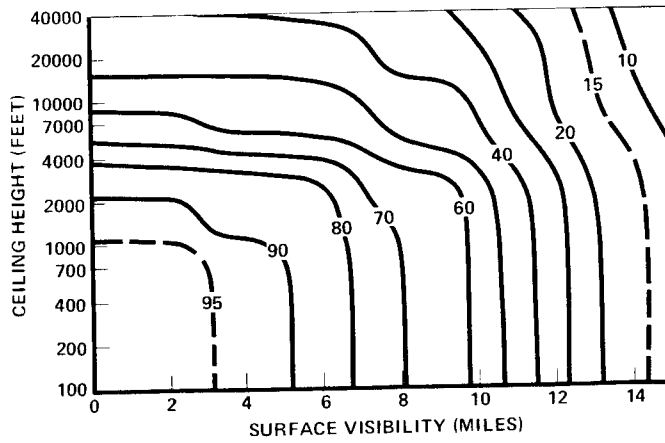


(f) Winter, November-February, forenoon

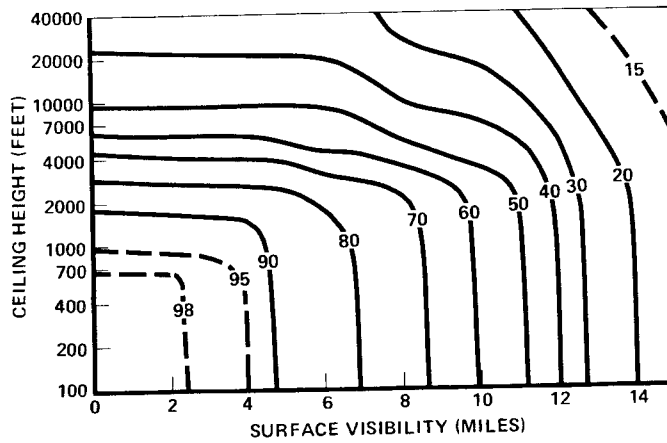


(g) Winter, November-February, afternoon

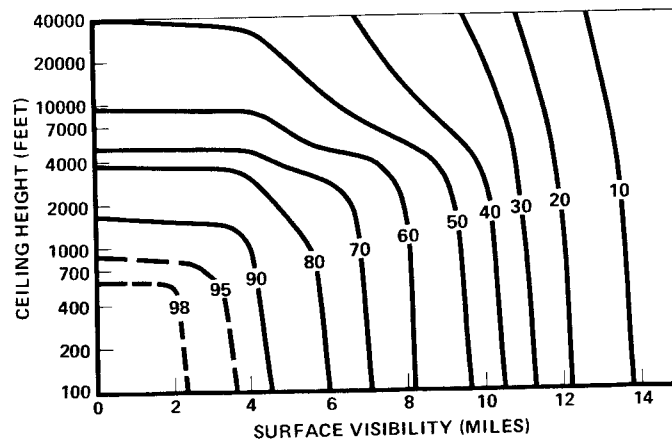
Fig. 17—Percent Frequency that Concurrent Ceiling and Visibility Values Are Equaled or Exceeded at Berlin



(h) Summer, May-August, all hours

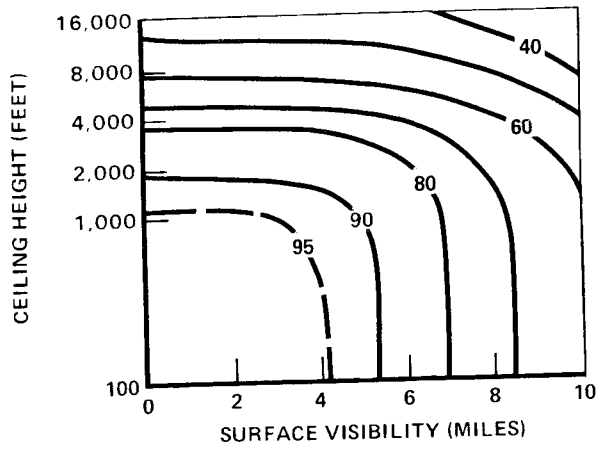


(i) Mid-summer, June-July, day

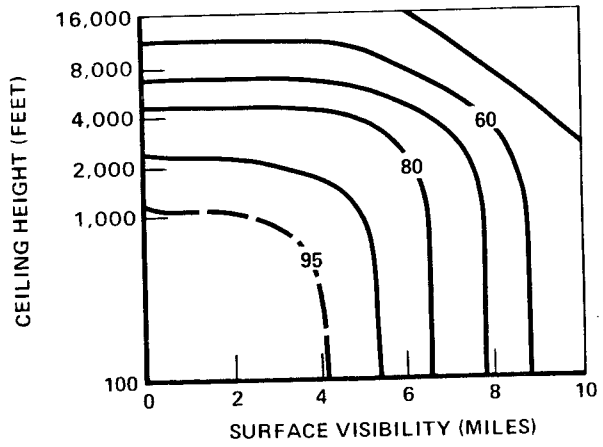


(j) Mid-summer, June-July, night

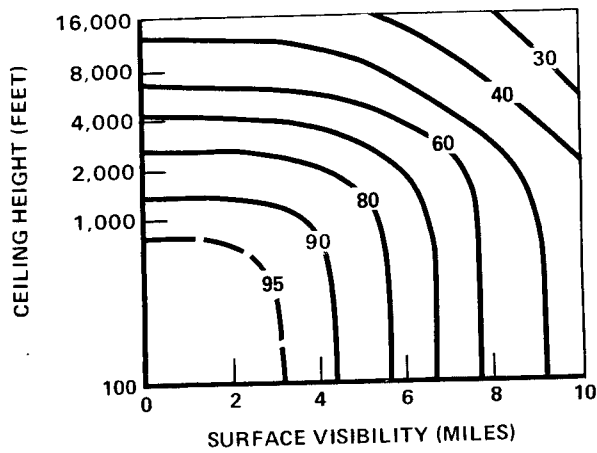
Fig. 17—Percent Frequency that Concurrent Ceiling and Visibility Values Are Equaled or Exceeded at Berlin



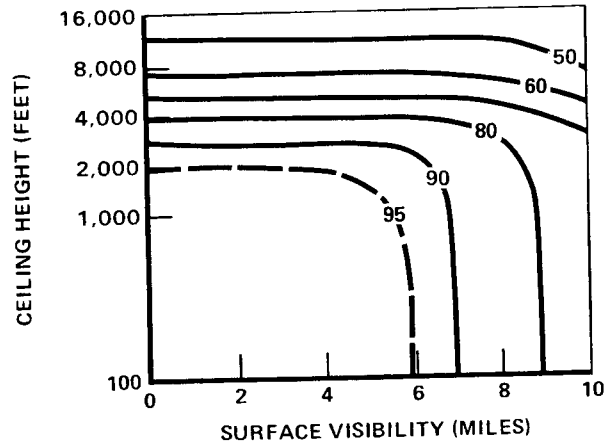
(k) Summer, May-August, day



(l) Summer, May-August, night

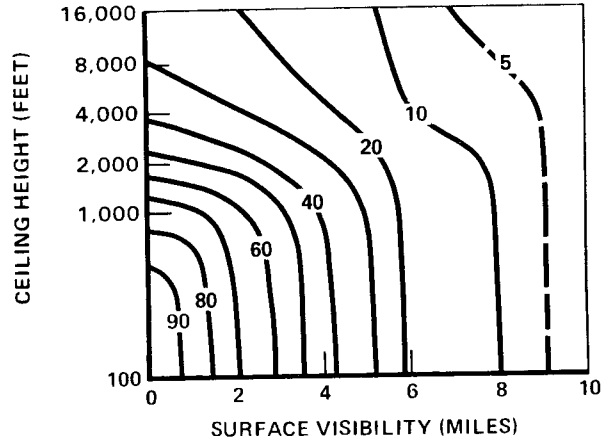


(m) Summer, May-August, forenoon

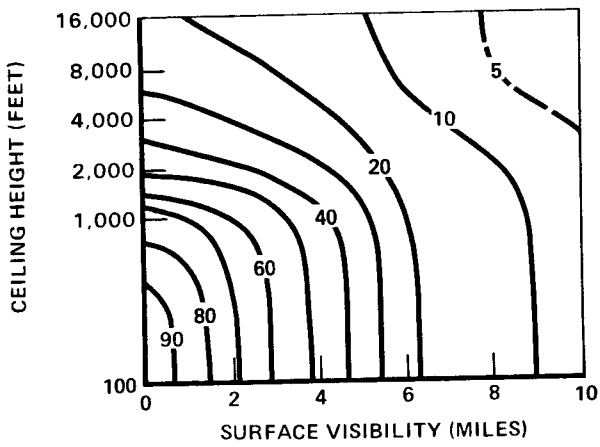


(n) Summer, May-August, afternoon

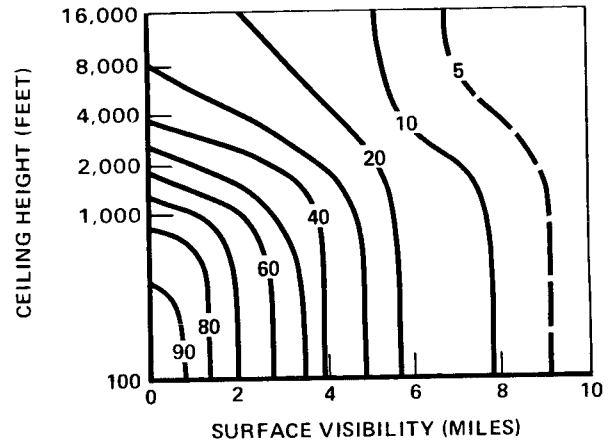
Fig. 17—Percent Frequency that Concurrent Ceiling and Visibility Values Are Equaled or Exceeded at Berlin



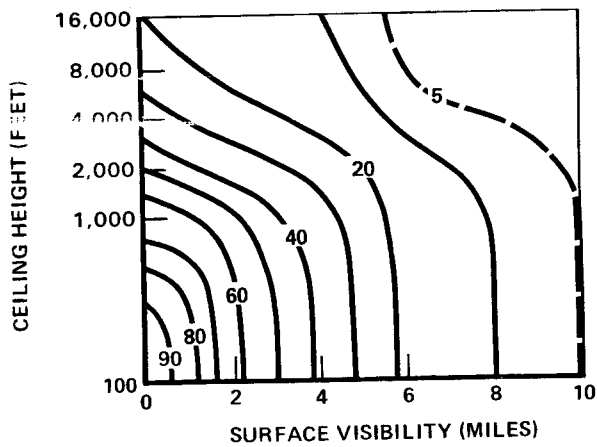
(a) Winter, November-February, all hours



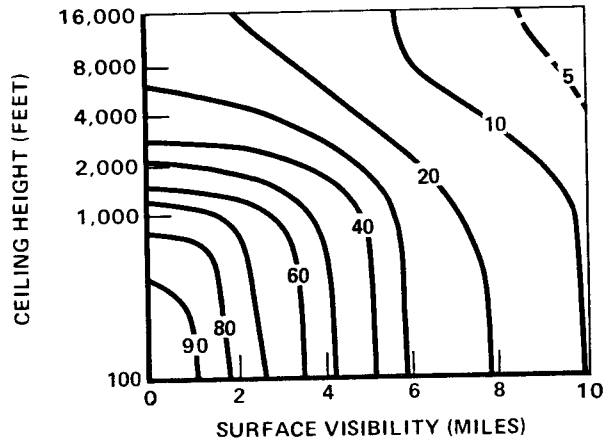
(b) Winter, November-February, day



(c) Winter, November-February, night

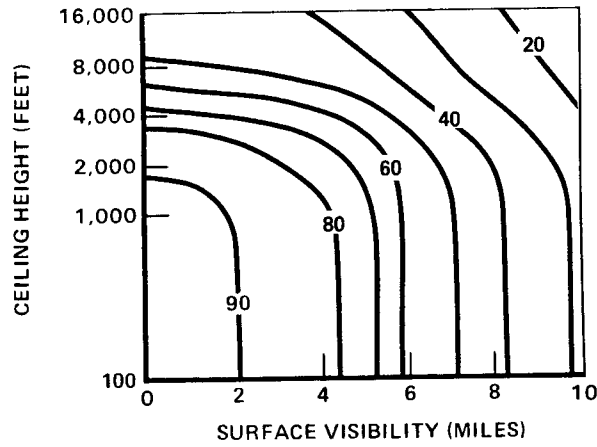


(d) Winter, November-February, forenoon

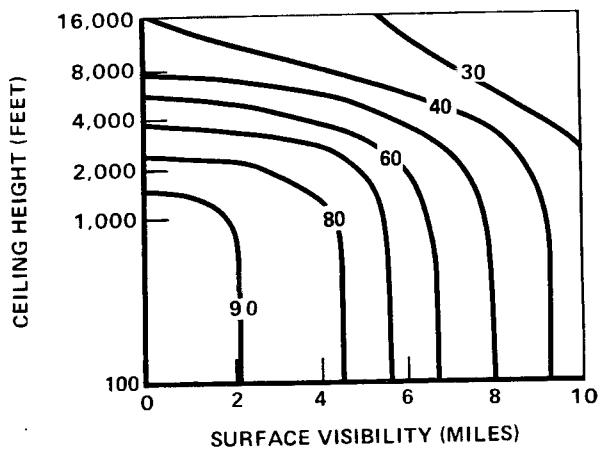


(e) Winter, November-February, afternoon

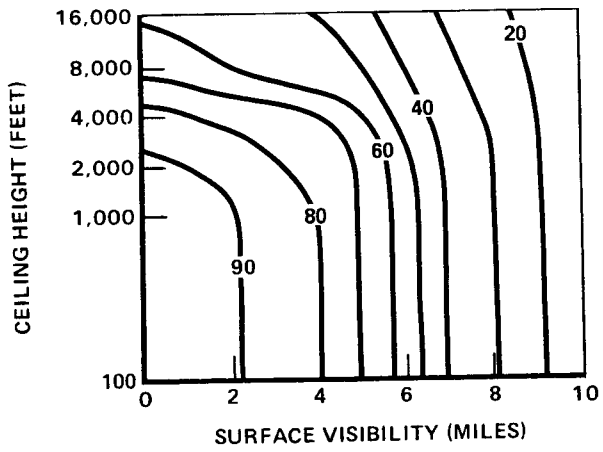
Fig. 18—Percent Frequency that Concurrent Ceiling and Visibility Values Are Equaled or Exceeded at Grafenwöhr



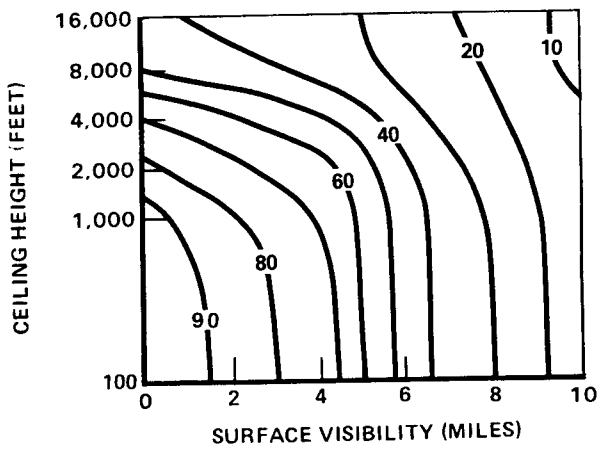
(f) Summer, May-August, all hours



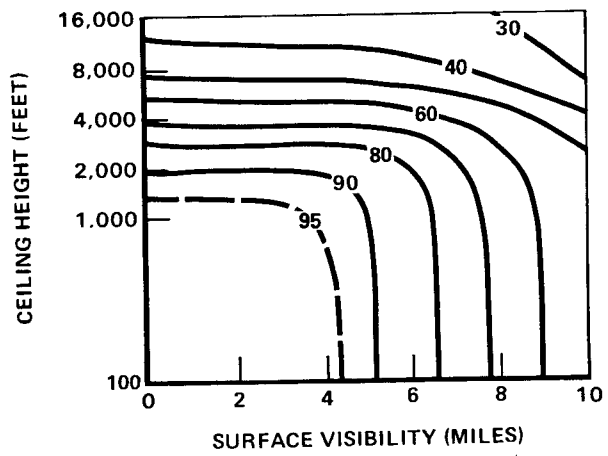
(g) Summer, May-August, day



(h) Summer, May-August, night

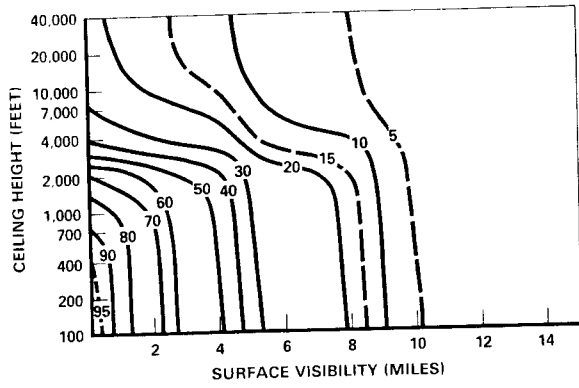


(i) Summer, May-August, forenoon

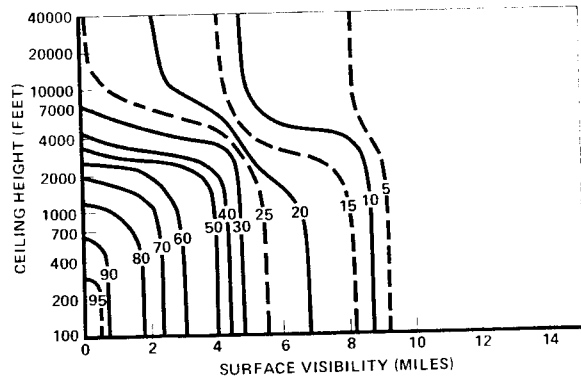


(j) Summer, May-August, afternoon

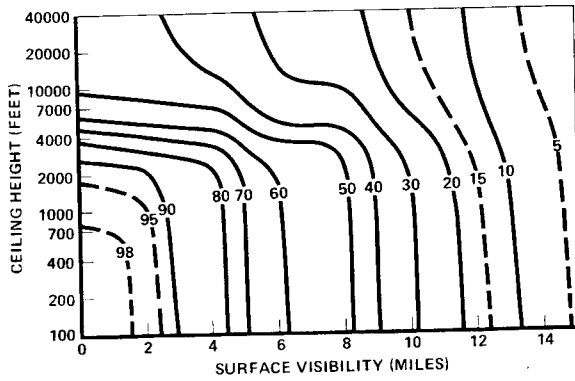
Fig. 18—Percent Frequency that Concurrent Ceiling and Visibility Values Are Equaled or Exceeded at Grafenwöhr



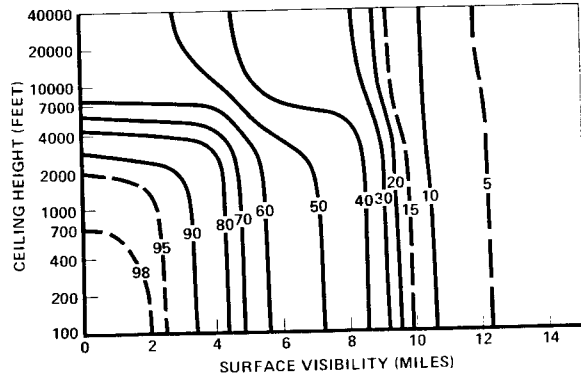
(a) Mid-winter, December-January, day



(b) Mid-winter, December-January, night

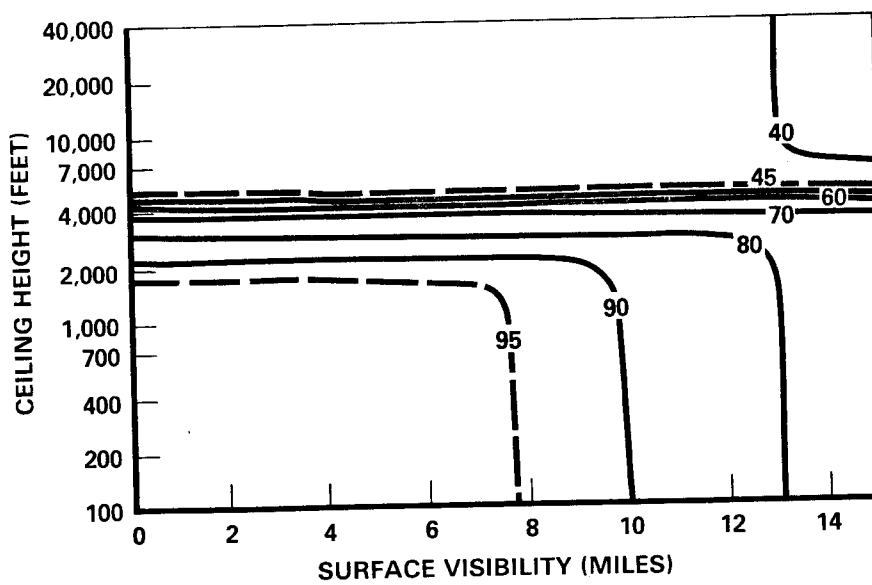


(c) Mid-summer, June-July, day

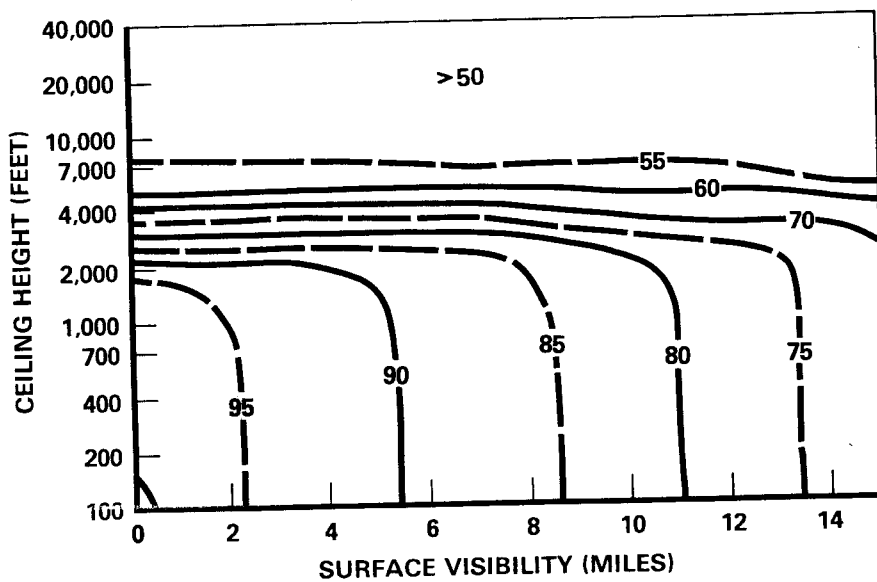


(d) Mid-summer, June-July, night

Fig. 19—Percent Frequency that Concurrent Ceiling and Visibility Values Are Equaled or Exceeded at Heidelberg

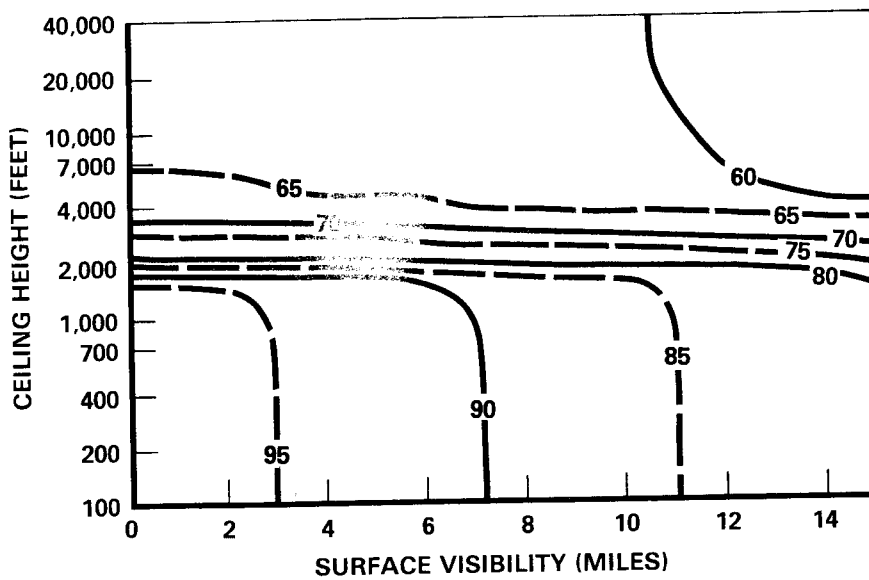


(a) Winter, November-February, all hours

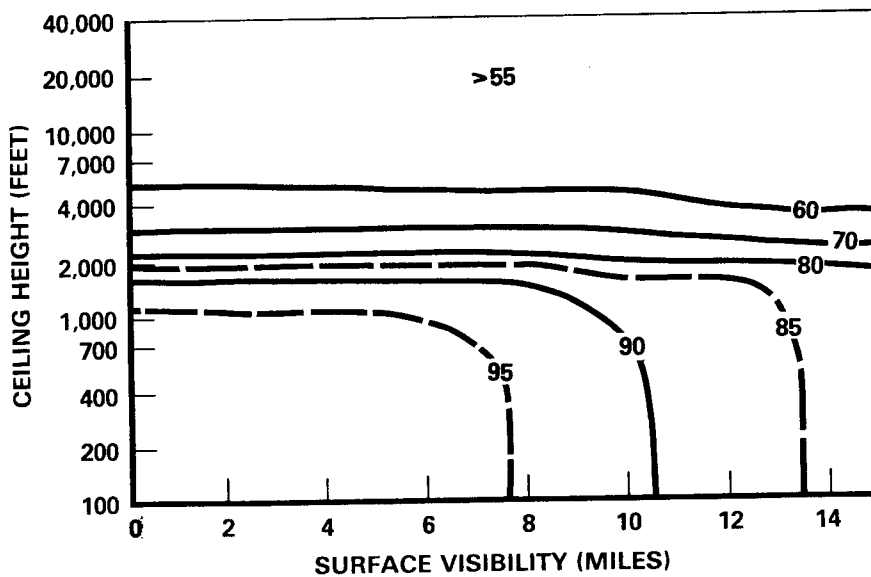


(b) Summer, May-August, all hours

Fig. 20—Percent Frequency that Concurrent Ceiling and Visibility Values Are Equaled or Exceeded at Bardufoss



(a) Winter, November-February, all hours



(b) Summer, May-August, all hours

Fig. 21—Percent Frequency that Concurrent Ceiling and Visibility Values Are Equaled or Exceeded at Kirkenes

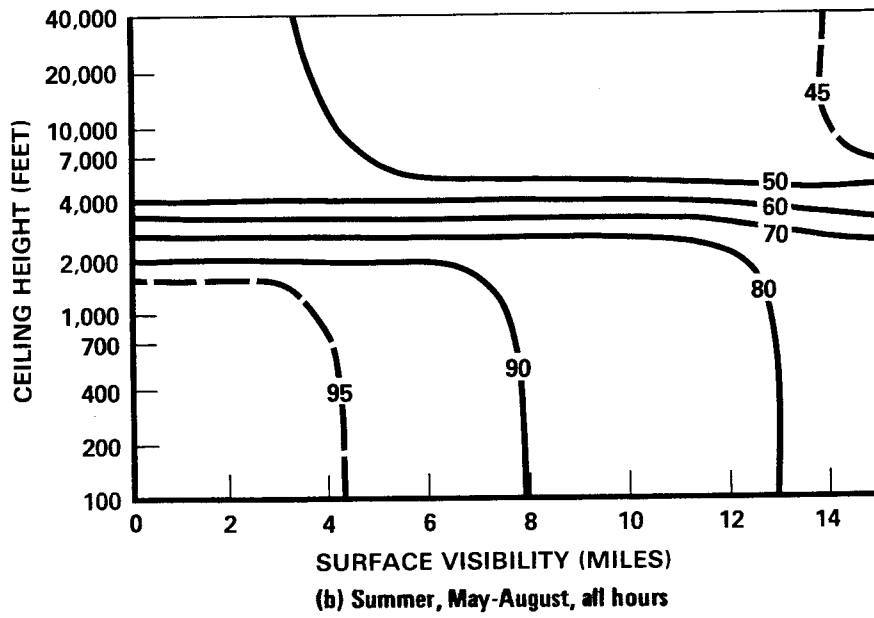
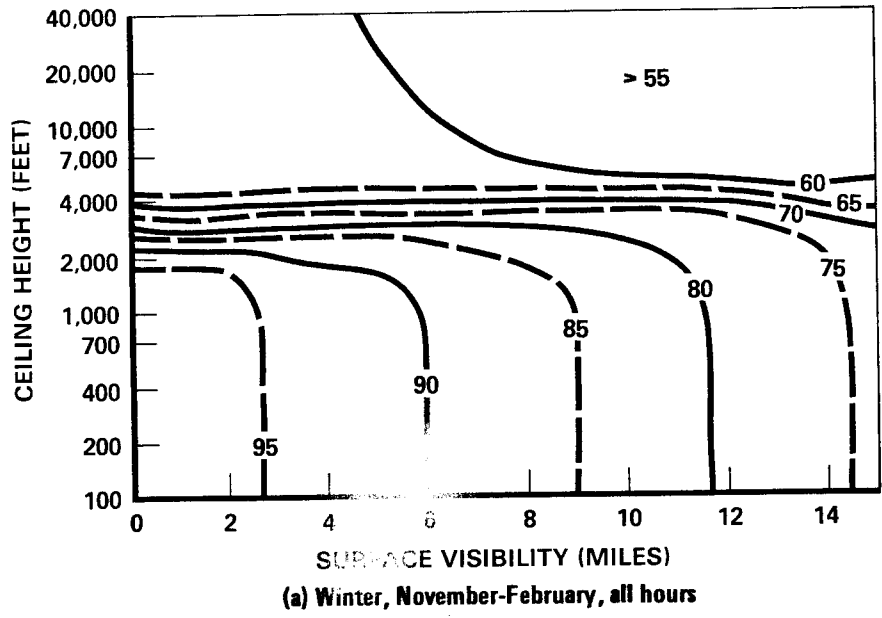
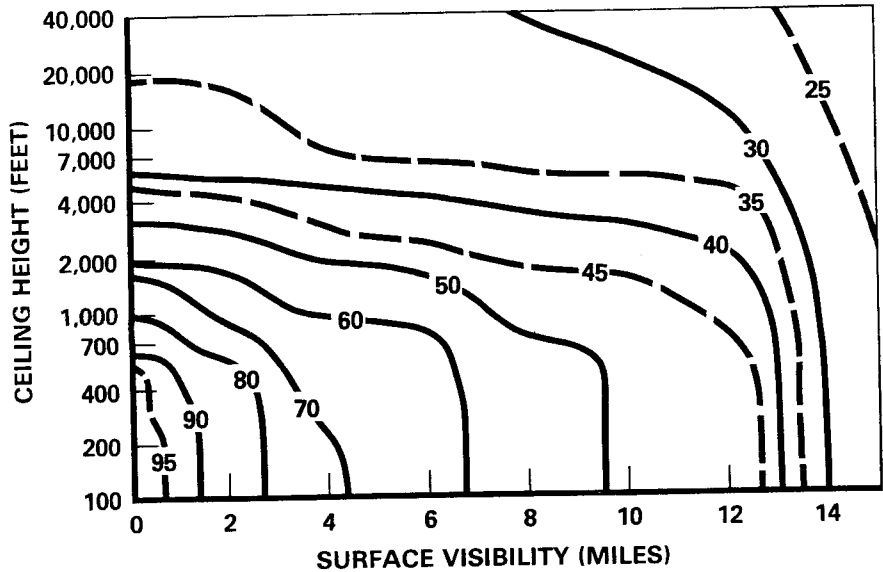
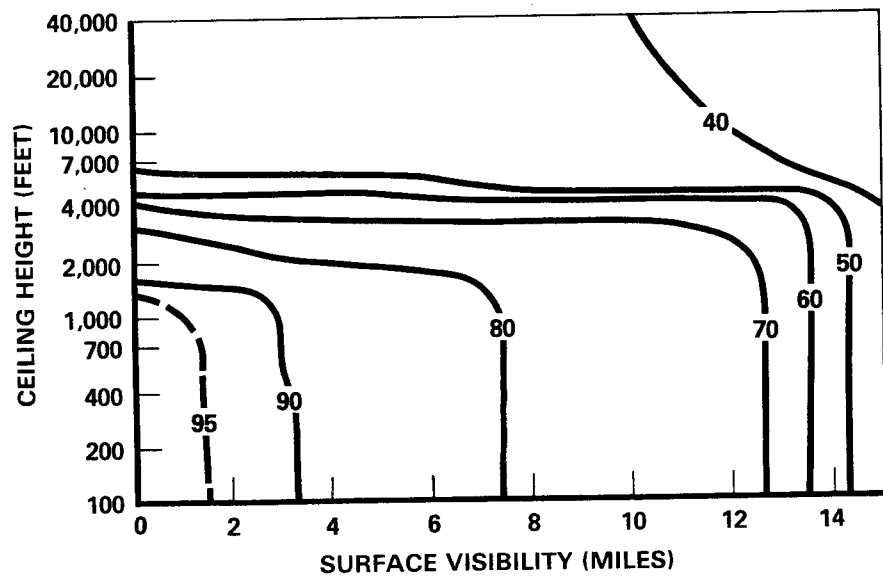


Fig. 22—Percent Frequency that Concurrent Ceiling and Visibility Values Are Equaled or Exceeded at Tromsø

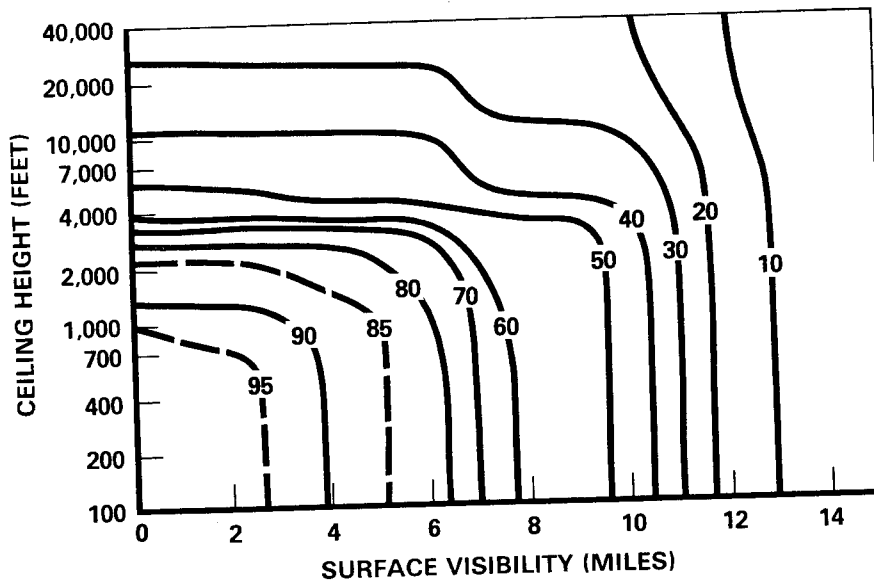


(a) Winter, November-February, all hours

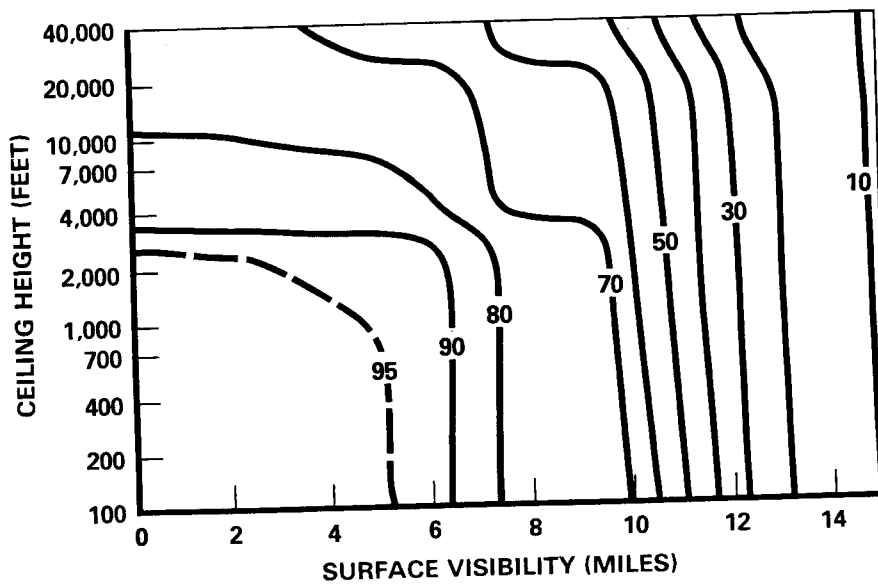


(b) Summer, May-August, all hours

Fig. 23—Percent Frequency that Concurrent Ceiling and Visibility Values Are Equaled or Exceeded at Sodankyla



(a) Winter, November-February, all hours



(b) Summer, May-August, all hours

Fig. 24—Percent Frequency that Concurrent Ceiling and Visibility Values Are Equaled or Exceeded at Istanbul

5. HOURLY-MONTHLY CEILING AND VISIBILITY FREQUENCIES AT BERLIN

Tabulations of hour-by-hour ceiling and visibility frequencies for each month of the year at Berlin-Tempelhof are presented in Tables 5 and 6. The data used for these calculations extend over a ten-year, nine-month period—from April 1946 through December 1956.²

Note that hours are stated in Greenwich Mean Time (GMT) in these tables—add one hour for local standard time. In Table 4, the last column, "Unlimited," gives the frequencies of observations when the total cloud amount $\leq 5/10$ or $\leq 4/8$, that is, when there is no "ceiling." In both Tables 5 and 6, the bottom rows, "All Hours," give the frequency distributions for the months as a whole.

The temporal detail of these tabulations permits a close examination of the diurnal and annual variations of ceiling and visibility, independently, as illustrated in Figs. 25-27. Figure 25 shows how the frequency of low visibility is significantly greater near dawn than in mid-afternoon, year-round. Figures 26 and 27 illustrate the complementary annual cycles of low and high ceilings and visibilities.

² A comparison was made of these frequency data with the frequencies shown in Fig. 17, which were calculated using a 17-year, 9-month period of Berlin data, from April 1946 through December 1963. The ceiling frequencies show no significant differences between the subset (April 1946 through December 1956) and the full set (April 1946 through December 1963). Visibility frequencies, however, do show a small but systematic difference. The frequencies with which given visibilities are equaled or exceeded are about 5 percent higher using the subset than they are using the full set. Speculatively, this could reflect a trend of diminishing visibilities due to increasing German industrialization (and air pollution) during the post-WW II years.

Table 6

HOURLY-MONTHLY VISIBILITY FREQUENCIES AT BERLIN

Visibility Class Interval (statute miles)										TOTAL OBS
<.5	>.5 <1.0	>1.0 <2.0	>2.0 <3.0	>3.0 <5.0	>5.0 <7.0	> 7.0 <10.0	>10.0 <15.0	>15.0 <25.0	>25.0	

JANUARY

0	0.02	0.02	0.09	0.14	0.13	0.15	0.22	0.17	0.01	0.0	308
1	0.02	0.03	0.08	0.16	0.17	0.14	0.20	0.20	0.01	0.0	310
2	0.02	0.03	0.08	0.14	0.16	0.15	0.21	0.20	0.02	0.0	310
3	0.02	0.04	0.09	0.12	0.17	0.16	0.22	0.18	0.01	0.0	309
4	0.02	0.02	0.13	0.12	0.16	0.18	0.19	0.17	0.02	0.0	308
5	0.03	0.02	0.14	0.14	0.16	0.16	0.20	0.15	0.02	0.0	310
6	0.03	0.03	0.20	0.17	0.15	0.11	0.17	0.12	0.01	0.00	309
7	0.04	0.08	0.21	0.13	0.14	0.11	0.15	0.09	0.00	0.00	310
8	0.04	0.10	0.18	0.17	0.16	0.12	0.13	0.09	0.01	0.0	307
9	0.03	0.09	0.19	0.17	0.16	0.13	0.13	0.07	0.02	0.0	310
10	0.03	0.08	0.16	0.16	0.19	0.15	0.14	0.07	0.02	0.0	310
11	0.01	0.09	0.13	0.15	0.18	0.18	0.13	0.10	0.03	0.0	310
12	0.01	0.06	0.11	0.15	0.20	0.16	0.15	0.12	0.03	0.0	310
13	0.02	0.05	0.09	0.13	0.23	0.16	0.15	0.15	0.03	0.00	310
14	0.03	0.05	0.08	0.16	0.21	0.14	0.16	0.15	0.03	0.00	310
15	0.02	0.05	0.10	0.17	0.20	0.16	0.13	0.14	0.04	0.0	310
16	0.02	0.04	0.14	0.19	0.19	0.13	0.15	0.13	0.02	0.0	310
17	0.02	0.02	0.14	0.17	0.22	0.15	0.14	0.13	0.01	0.0	310
18	0.02	0.02	0.14	0.15	0.21	0.19	0.14	0.13	0.01	0.0	307
19	0.01	0.02	0.12	0.16	0.18	0.20	0.15	0.15	0.01	0.0	309
20	0.02	0.03	0.10	0.14	0.20	0.17	0.18	0.15	0.01	0.0	310
21	0.02	0.04	0.07	0.15	0.21	0.15	0.18	0.16	0.01	0.0	310
22	0.03	0.01	0.09	0.14	0.18	0.17	0.20	0.16	0.01	0.0	310
23	0.03	0.02	0.08	0.16	0.17	0.16	0.22	0.16	0.02	0.00	309
ALL	0.02	0.04	0.12	0.15	0.18	0.15	0.17	0.14	0.02	0.00	7426

FEBRUARY

0	0.04	0.02	0.10	0.10	0.24	0.17	0.19	0.10	0.04	0.0	283
1	0.04	0.01	0.13	0.11	0.17	0.20	0.19	0.11	0.04	0.0	283
2	0.04	0.03	0.10	0.12	0.19	0.18	0.18	0.12	0.04	0.0	283
3	0.05	0.05	0.10	0.13	0.18	0.18	0.16	0.12	0.04	0.0	283
4	0.04	0.05	0.12	0.14	0.18	0.17	0.16	0.11	0.03	0.0	283
5	0.05	0.07	0.18	0.15	0.12	0.16	0.17	0.08	0.02	0.0	283
6	0.06	0.12	0.17	0.16	0.11	0.18	0.11	0.05	0.04	0.0	283
7	0.07	0.14	0.20	0.18	0.15	0.10	0.10	0.03	0.03	0.0	283
8	0.07	0.14	0.20	0.17	0.16	0.11	0.08	0.04	0.02	0.0	283
9	0.05	0.10	0.19	0.19	0.21	0.10	0.08	0.04	0.03	0.0	283
10	0.03	0.09	0.17	0.18	0.20	0.14	0.09	0.07	0.03	0.0	283
11	0.02	0.06	0.13	0.19	0.19	0.17	0.11	0.09	0.04	0.0	283
12	0.01	0.05	0.12	0.15	0.19	0.19	0.14	0.10	0.04	0.0	283
13	0.01	0.05	0.09	0.12	0.20	0.17	0.18	0.12	0.05	0.0	283
14	0.01	0.06	0.07	0.14	0.17	0.18	0.17	0.14	0.06	0.0	283
15	0.02	0.04	0.08	0.17	0.21	0.14	0.15	0.15	0.05	0.0	283
16	0.01	0.04	0.12	0.17	0.24	0.12	0.14	0.10	0.06	0.0	283
17	0.01	0.03	0.13	0.19	0.29	0.12	0.12	0.06	0.04	0.0	283
18	0.01	0.04	0.14	0.17	0.27	0.13	0.13	0.06	0.04	0.0	283
19	0.02	0.02	0.13	0.16	0.26	0.17	0.14	0.06	0.04	0.0	283
20	0.03	0.02	0.13	0.14	0.27	0.16	0.12	0.10	0.04	0.0	283
21	0.03	0.03	0.10	0.15	0.25	0.18	0.12	0.09	0.05	0.0	283
22	0.04	0.02	0.12	0.10	0.26	0.18	0.15	0.08	0.05	0.0	283
23	0.03	0.02	0.11	0.11	0.26	0.16	0.16	0.16	0.04	0.00	283
ALL	0.03	0.05	0.13	0.15	0.21	0.16	0.14	0.09	0.04	0.00	6792

Table 6—continued

Visibility Class Interval (statute miles)										TOTAL OBS
<.5	>.5 <1.0	>1.0 <2.0	>2.0 <3.0	>3.0 <5.0	>5.0 <7.0	>7.0 <10.0	>10.0 <15.0	>15.0 <25.0	>25.0	

MARCH

0	0.03	0.02	0.05	0.06	0.12	0.13	0.28	0.25	0.06	0.00	310
1	0.04	0.02	0.06	0.06	0.11	0.14	0.26	0.26	0.05	0.00	310
2	0.04	0.02	0.05	0.07	0.11	0.16	0.23	0.27	0.05	0.00	310
3	0.05	0.02	0.06	0.08	0.11	0.17	0.23	0.23	0.05	0.00	310
4	0.05	0.03	0.08	0.11	0.14	0.14	0.18	0.22	0.05	0.00	310
5	0.05	0.05	0.10	0.11	0.17	0.10	0.18	0.18	0.05	0.00	310
6	0.04	0.08	0.12	0.15	0.18	0.12	0.15	0.13	0.05	0.00	310
7	0.04	0.09	0.15	0.11	0.18	0.13	0.14	0.13	0.03	0.00	309
8	0.04	0.08	0.15	0.11	0.17	0.15	0.14	0.13	0.04	0.00	309
9	0.02	0.07	0.11	0.11	0.13	0.21	0.14	0.16	0.06	0.00	309
10	0.02	0.04	0.10	0.09	0.15	0.15	0.19	0.17	0.08	0.00	310
11	0.00	0.04	0.10	0.10	0.10	0.15	0.16	0.24	0.11	0.00	310
12	0.01	0.03	0.08	0.08	0.11	0.10	0.18	0.26	0.15	0.01	310
13	0.00	0.03	0.05	0.09	0.08	0.10	0.19	0.25	0.19	0.01	310
14	0.01	0.02	0.06	0.05	0.08	0.10	0.15	0.30	0.21	0.02	310
15	0.01	0.02	0.04	0.09	0.07	0.09	0.17	0.26	0.24	0.03	310
16	0.01	0.03	0.05	0.09	0.07	0.14	0.14	0.24	0.22	0.02	310
17	0.01	0.02	0.09	0.08	0.12	0.12	0.18	0.21	0.16	0.01	310
18	0.01	0.02	0.10	0.10	0.13	0.13	0.21	0.21	0.09	0.01	310
19	0.00	0.02	0.10	0.07	0.11	0.16	0.22	0.23	0.07	0.01	310
20	0.01	0.02	0.09	0.08	0.10	0.14	0.26	0.22	0.07	0.01	309
21	0.02	0.02	0.08	0.06	0.11	0.15	0.25	0.26	0.06	0.00	310
22	0.03	0.02	0.07	0.05	0.12	0.15	0.25	0.26	0.06	0.00	310
23	0.03	0.02	0.05	0.06	0.11	0.14	0.23	0.29	0.06	0.00	311
ALL	0.02	0.03	0.08	0.09	0.12	0.14	0.20	0.22	0.09	0.01	7437

APRIL

0	0.00	0.00	0.02	0.02	0.06	0.10	0.25	0.39	0.15	0.00	330
1	0.00	0.01	0.02	0.03	0.05	0.11	0.25	0.38	0.15	0.00	330
2	0.00	0.01	0.02	0.02	0.06	0.10	0.25	0.39	0.14	0.00	330
3	0.01	0.01	0.03	0.04	0.08	0.09	0.25	0.35	0.12	0.00	330
4	0.01	0.02	0.03	0.06	0.09	0.13	0.22	0.30	0.13	0.00	330
5	0.02	0.01	0.05	0.06	0.13	0.18	0.21	0.21	0.12	0.02	330
6	0.01	0.02	0.07	0.08	0.14	0.18	0.18	0.20	0.11	0.01	330
7	0.01	0.01	0.07	0.07	0.14	0.18	0.20	0.21	0.11	0.01	330
8	0.00	0.00	0.05	0.06	0.13	0.14	0.20	0.25	0.13	0.02	330
9	0.00	0.01	0.03	0.05	0.10	0.13	0.17	0.31	0.18	0.03	330
10	0.00	0.00	0.02	0.04	0.09	0.11	0.16	0.32	0.23	0.04	329
11	0.00	0.00	0.02	0.04	0.09	0.11	0.16	0.32	0.23	0.04	330
12	0.00	0.00	0.00	0.04	0.07	0.11	0.13	0.34	0.28	0.05	330
13	0.00	0.00	0.01	0.02	0.04	0.07	0.11	0.33	0.37	0.06	330
14	0.00	0.00	0.01	0.02	0.05	0.05	0.10	0.29	0.39	0.09	330
15	0.00	0.00	0.01	0.02	0.04	0.06	0.11	0.28	0.38	0.11	330
16	0.00	0.00	0.01	0.02	0.04	0.05	0.12	0.28	0.37	0.11	330
17	0.00	0.00	0.00	0.02	0.06	0.05	0.13	0.32	0.32	0.09	330
18	0.00	0.00	0.00	0.03	0.06	0.08	0.17	0.36	0.24	0.06	330
19	0.00	0.00	0.01	0.03	0.07	0.09	0.25	0.32	0.21	0.02	330
20	0.00	0.00	0.02	0.02	0.07	0.09	0.24	0.35	0.19	0.01	330
21	0.00	0.00	0.01	0.02	0.08	0.11	0.23	0.36	0.18	0.01	330
22	0.00	0.00	0.01	0.02	0.05	0.12	0.25	0.37	0.16	0.01	329
23	0.00	0.00	0.02	0.02	0.05	0.12	0.25	0.38	0.16	0.00	330
ALL	0.00	0.00	0.02	0.03	0.08	0.10	0.19	0.32	0.21	0.03	7918

Table 6—continued

Visibility Class Interval (statute miles)										TOTAL OBS
<.5	>.5 <1.0	>1.0 <2.0	>2.0 <3.0	>3.0 <5.0	>5.0 <7.0	>7.0 <10.0	>10.0 <15.0	>15.0 <25.0	>25.0	

MAY

0	0.0	0.0	0.01	0.01	0.02	0.08	0.21	0.51	0.14	0.02	341
1	0.0	0.00	0.01	0.01	0.03	0.09	0.24	0.49	0.12	0.02	340
2	0.00	0.0	0.0	0.04	0.04	0.10	0.25	0.43	0.13	0.01	341
3	0.01	0.0	0.01	0.02	0.07	0.12	0.24	0.40	0.12	0.01	341
4	0.00	0.00	0.01	0.04	0.06	0.15	0.26	0.33	0.12	0.01	341
5	0.00	0.00	0.01	0.03	0.09	0.19	0.24	0.30	0.13	0.01	341
6	0.00	0.0	0.01	0.03	0.09	0.18	0.26	0.30	0.10	0.02	341
7	0.00	0.0	0.01	0.04	0.07	0.15	0.20	0.37	0.14	0.01	341
8	0.0	0.0	0.01	0.01	0.05	0.11	0.21	0.35	0.23	0.02	341
9	0.0	0.0	0.00	0.01	0.04	0.09	0.18	0.37	0.26	0.04	341
10	0.0	0.0	0.01	0.01	0.03	0.17	0.13	0.39	0.31	0.06	341
11	0.0	0.0	0.00	0.00	0.02	0.04	0.13	0.39	0.36	0.06	340
12	0.0	0.0	0.00	0.0	0.01	0.02	0.13	0.38	0.39	0.07	341
13	0.0	0.0	0.00	0.00	0.01	0.03	0.11	0.35	0.40	0.09	341
14	0.0	0.0	0.0	0.01	0.01	0.03	0.09	0.35	0.43	0.09	340
15	0.0	0.0	0.0	0.0	0.01	0.02	0.11	0.31	0.45	0.10	340
16	0.0	0.0	0.0	0.0	0.02	0.02	0.12	0.27	0.48	0.10	339
17	0.0	0.0	0.0	0.01	0.01	0.04	0.11	0.30	0.43	0.11	341
18	0.0	0.0	0.0	0.01	0.02	0.04	0.15	0.33	0.37	0.09	341
19	0.0	0.0	0.00	0.01	0.02	0.06	0.17	0.37	0.31	0.06	340
20	0.0	0.0	0.00	0.00	0.02	0.08	0.19	0.44	0.23	0.04	340
21	0.00	0.0	0.00	0.01	0.02	0.07	0.18	0.49	0.19	0.04	341
22	0.0	0.0	0.01	0.01	0.01	0.11	0.19	0.50	0.18	0.03	341
23	0.0	0.00	0.00	0.02	0.02	0.07	0.19	0.52	0.16	0.02	341
ALL	0.00	0.00	0.00	0.01	0.03	0.08	0.18	0.39	0.26	0.05	8176

JUNE

0	0.0	0.00	0.01	0.01	0.03	0.06	0.26	0.42	0.19	0.01	328
1	0.00	0.00	0.01	0.02	0.04	0.10	0.26	0.39	0.17	0.01	327
2	0.0	0.00	0.01	0.02	0.06	0.15	0.25	0.33	0.16	0.01	328
3	0.00	0.0	0.01	0.03	0.11	0.17	0.25	0.25	0.16	0.01	328
4	0.0	0.00	0.01	0.05	0.12	0.20	0.22	0.26	0.14	0.01	328
5	0.0	0.0	0.02	0.03	0.12	0.21	0.22	0.26	0.13	0.01	328
6	0.0	0.0	0.01	0.04	0.11	0.22	0.20	0.28	0.13	0.01	328
7	0.0	0.0	0.01	0.03	0.09	0.20	0.18	0.31	0.17	0.02	328
8	0.0	0.0	0.02	0.03	0.07	0.14	0.17	0.32	0.24	0.01	328
9	0.0	0.0	0.02	0.02	0.05	0.09	0.16	0.34	0.30	0.02	329
10	0.0	0.0	0.00	0.02	0.04	0.08	0.15	0.35	0.32	0.03	328
11	0.0	0.0	0.01	0.02	0.04	0.06	0.12	0.34	0.35	0.06	326
12	0.0	0.0	0.01	0.02	0.03	0.04	0.11	0.31	0.41	0.07	328
13	0.0	0.0	0.0	0.02	0.03	0.03	0.09	0.36	0.39	0.09	328
14	0.0	0.0	0.00	0.02	0.04	0.02	0.06	0.37	0.39	0.10	328
15	0.0	0.00	0.0	0.02	0.03	0.02	0.06	0.32	0.44	0.10	328
16	0.0	0.0	0.01	0.02	0.03	0.03	0.06	0.30	0.45	0.10	328
17	0.0	0.0	0.00	0.02	0.02	0.03	0.08	0.30	0.44	0.11	328
18	0.0	0.00	0.00	0.02	0.06	0.02	0.12	0.30	0.41	0.08	328
19	0.0	0.00	0.00	0.02	0.05	0.05	0.14	0.29	0.37	0.07	328
20	0.0	0.00	0.01	0.02	0.03	0.07	0.20	0.35	0.28	0.05	328
21	0.0	0.00	0.01	0.02	0.02	0.11	0.17	0.39	0.25	0.03	328
22	0.0	0.00	0.01	0.02	0.04	0.09	0.21	0.39	0.22	0.02	328
23	0.00	0.0	0.01	0.02	0.02	0.08	0.23	0.44	0.18	0.01	327
ALL	0.00	0.00	0.01	0.02	0.05	0.09	0.17	0.33	0.28	0.04	7869

Table 6—continued

Visibility Class Interval (statute miles)										TOTAL OBS
<.5	>.5 <1.0	>1.0 <2.0	>2.0 <3.0	>3.0 <5.0	>5.0 <7.0	>7.0 <10.0	>10.0 <15.0	>15.0 <25.0	>25.0	

JULY

0	0.0	0.0	0.01	0.01	0.03	0.10	0.19	0.46	0.21	0.00	340
1	0.0	0.0	0.01	0.01	0.05	0.07	0.21	0.45	0.19	0.0	341
2	0.0	0.0	0.11	0.01	0.08	0.10	0.24	0.41	0.15	0.00	341
3	0.0	0.0	0.00	0.03	0.07	0.16	0.26	0.32	0.14	0.01	341
4	0.0	0.0	0.01	0.04	0.11	0.18	0.22	0.28	0.15	0.01	341
5	0.0	0.0	0.02	0.04	0.10	0.18	0.25	0.25	0.13	0.02	341
6	0.0	0.01	0.01	0.04	0.10	0.15	0.27	0.29	0.12	0.01	340
7	0.0	0.0	0.01	0.03	0.07	0.14	0.24	0.35	0.15	0.01	341
8	0.0	0.0	0.01	0.03	0.05	0.11	0.18	0.40	0.21	0.01	341
9	0.0	0.0	0.00	0.01	0.04	0.07	0.15	0.42	0.28	0.02	341
10	0.0	0.0	0.0	0.01	0.02	0.08	0.10	0.42	0.33	0.04	341
11	0.0	0.00	0.00	0.01	0.01	0.07	0.09	0.38	0.38	0.05	341
12	0.0	0.0	0.00	0.01	0.02	0.07	0.09	0.37	0.41	0.04	341
13	0.0	0.0	0.00	0.00	0.02	0.06	0.09	0.33	0.44	0.05	341
14	0.0	0.0	0.01	0.01	0.01	0.04	0.07	0.35	0.45	0.07	341
15	0.0	0.00	0.0	0.00	0.02	0.03	0.08	0.34	0.43	0.09	341
16	0.0	0.0	0.0	0.01	0.01	0.04	0.06	0.33	0.47	0.09	341
17	0.0	0.0	0.0	0.01	0.02	0.03	0.06	0.32	0.46	0.10	341
18	0.0	0.0	0.0	0.01	0.02	0.04	0.09	0.31	0.43	0.09	341
19	0.0	0.0	0.0	0.02	0.01	0.05	0.14	0.35	0.37	0.06	341
20	0.0	0.0	0.0	0.02	0.03	0.08	0.14	0.37	0.34	0.03	341
21	0.0	0.0	0.0	0.01	0.02	0.08	0.18	0.39	0.30	0.02	341
22	0.0	0.0	0.0	0.01	0.03	0.07	0.19	0.41	0.27	0.01	341
23	0.0	0.0	0.01	0.01	0.04	0.06	0.19	0.45	0.24	0.0	339
ALL	0.0	0.00	0.00	0.02	0.04	0.09	0.16	0.37	0.29	0.04	8180

AUGUST

0	0.00	0.0	0.01	0.01	0.05	0.07	0.27	0.44	0.15	0.00	341
1	0.01	0.00	0.01	0.01	0.05	0.07	0.29	0.42	0.14	0.0	341
2	0.01	0.01	0.02	0.02	0.05	0.11	0.29	0.38	0.11	0.0	341
3	0.01	0.0	0.02	0.05	0.09	0.16	0.25	0.33	0.09	0.0	341
4	0.01	0.0	0.02	0.06	0.15	0.18	0.23	0.27	0.08	0.0	341
5	0.01	0.01	0.01	0.06	0.19	0.18	0.23	0.22	0.10	0.0	341
6	0.00	0.00	0.04	0.04	0.19	0.21	0.20	0.22	0.09	0.00	341
7	0.00	0.01	0.03	0.04	0.12	0.23	0.23	0.24	0.10	0.00	341
8	0.00	0.01	0.02	0.04	0.07	0.17	0.24	0.31	0.13	0.01	341
9	0.0	0.0	0.01	0.03	0.06	0.11	0.21	0.38	0.19	0.02	341
10	0.0	0.00	0.00	0.02	0.03	0.08	0.16	0.43	0.25	0.02	341
11	0.0	0.0	0.01	0.01	0.02	0.05	0.16	0.43	0.28	0.04	341
12	0.0	0.0	0.01	0.0	0.02	0.03	0.12	0.45	0.32	0.05	341
13	0.0	0.0	0.0	0.01	0.01	0.03	0.12	0.42	0.36	0.06	341
14	0.0	0.0	0.0	0.01	0.02	0.03	0.09	0.39	0.40	0.06	341
15	0.0	0.0	0.00	0.00	0.01	0.04	0.09	0.39	0.40	0.07	341
16	0.0	0.0	0.00	0.01	0.02	0.04	0.07	0.36	0.42	0.08	341
17	0.0	0.0	0.01	0.01	0.03	0.06	0.07	0.34	0.42	0.07	341
18	0.0	0.00	0.01	0.01	0.04	0.07	0.15	0.34	0.32	0.06	341
19	0.0	0.00	0.00	0.01	0.06	0.08	0.20	0.34	0.28	0.02	341
20	0.0	0.0	0.01	0.01	0.05	0.08	0.20	0.40	0.23	0.01	341
21	0.00	0.0	0.0	0.01	0.06	0.09	0.21	0.43	0.20	0.01	341
22	0.00	0.0	0.00	0.02	0.05	0.10	0.20	0.43	0.18	0.00	341
23	0.00	0.0	0.00	0.02	0.04	0.09	0.25	0.43	0.16	0.00	341
ALL	0.00	0.00	0.01	0.02	0.06	0.10	0.19	0.37	0.23	0.02	8184

Table 6—continued

Visibility Class Interval (statute miles)										TOTAL OBS
<.5	>.5 <1.0	>1.0 <2.0	>2.0 <3.0	>3.0 <5.0	>5.0 <7.0	>7.0 <10.0	>10.0 <15.0	>15.0 <25.0	>25.0	

SEPTEMBER

0	0.0	0.01	0.02	0.03	0.09	0.12	0.28	0.39	0.07	0.0	330
1	0.01	0.00	0.02	0.03	0.09	0.12	0.30	0.36	0.07	0.0	329
2	0.02	0.01	0.02	0.02	0.11	0.10	0.28	0.34	0.06	0.0	330
3	0.02	0.02	0.05	0.06	0.09	0.15	0.27	0.37	0.05	0.0	336
4	0.03	0.01	0.04	0.09	0.14	0.17	0.23	0.25	0.04	0.00	333
5	0.02	0.02	0.06	0.11	0.20	0.21	0.16	0.17	0.05	0.00	330
6	0.01	0.02	0.06	0.13	0.17	0.23	0.16	0.17	0.05	0.00	330
7	0.01	0.00	0.06	0.11	0.16	0.23	0.18	0.20	0.05	0.00	330
8	0.01	0.01	0.02	0.07	0.17	0.17	0.22	0.27	0.07	0.00	330
9	0.01	0.01	0.01	0.04	0.08	0.19	0.21	0.33	0.11	0.02	330
10	0.01	0.01	0.02	0.02	0.06	0.13	0.18	0.40	0.18	0.02	330
11	0.0	0.0	0.0	0.03	0.03	0.08	0.15	0.45	0.24	0.02	330
12	0.0	0.0	0.01	0.01	0.03	0.06	0.13	0.47	0.27	0.03	330
13	0.0	0.0	0.0	0.01	0.02	0.06	0.08	0.46	0.33	0.04	330
14	0.0	0.0	0.01	0.01	0.02	0.05	0.09	0.41	0.37	0.05	330
15	0.0	0.0	0.01	0.01	0.02	0.04	0.12	0.37	0.38	0.05	330
16	0.0	0.0	0.01	0.02	0.03	0.06	0.14	0.37	0.34	0.03	330
17	0.0	0.0	0.00	0.02	0.05	0.09	0.18	0.38	0.25	0.02	330
18	0.0	0.00	0.0	0.03	0.06	0.12	0.22	0.41	0.15	0.01	330
19	0.0	0.0	0.00	0.02	0.10	0.12	0.23	0.41	0.11	0.01	330
20	0.00	0.0	0.00	0.02	0.11	0.13	0.23	0.42	0.17	0.00	330
21	0.00	0.0	0.01	0.02	0.09	0.12	0.23	0.43	0.09	0.0	330
22	0.00	0.01	0.00	0.02	0.09	0.12	0.25	0.43	0.08	0.00	330
23	0.0	0.01	0.02	0.01	0.09	0.12	0.27	0.41	0.07	0.0	330
ALL	0.00	0.00	0.02	0.04	0.09	0.13	0.20	0.36	0.15	0.01	7919

OCTOBER

0	0.05	0.01	0.04	0.06	0.13	0.14	0.24	0.37	0.02	0.0	340
1	0.05	0.02	0.04	0.07	0.13	0.14	0.21	0.32	0.02	0.0	340
2	0.05	0.02	0.04	0.07	0.13	0.14	0.21	0.31	0.02	0.0	340
3	0.04	0.02	0.06	0.09	0.11	0.15	0.22	0.28	0.02	0.0	340
4	0.04	0.02	0.10	0.12	0.12	0.18	0.18	0.22	0.02	0.0	339
5	0.05	0.04	0.12	0.13	0.19	0.12	0.16	0.16	0.03	0.0	340
6	0.04	0.07	0.13	0.14	0.18	0.16	0.13	0.11	0.04	0.0	340
7	0.05	0.06	0.14	0.15	0.19	0.14	0.14	0.11	0.03	0.0	340
8	0.05	0.06	0.11	0.15	0.18	0.15	0.14	0.13	0.03	0.0	340
9	0.03	0.05	0.08	0.11	0.19	0.14	0.16	0.18	0.06	0.0	337
10	0.01	0.04	0.09	0.05	0.20	0.13	0.16	0.24	0.08	0.0	338
11	0.01	0.01	0.06	0.07	0.14	0.16	0.15	0.27	0.11	0.00	340
12	0.0	0.01	0.05	0.06	0.11	0.14	0.16	0.30	0.15	0.01	340
13	0.0	0.02	0.03	0.06	0.09	0.14	0.15	0.33	0.18	0.01	340
14	0.0	0.02	0.03	0.05	0.09	0.13	0.17	0.32	0.18	0.02	339
15	0.00	0.01	0.05	0.05	0.15	0.08	0.23	0.24	0.18	0.01	339
16	0.00	0.01	0.06	0.06	0.16	0.14	0.20	0.22	0.14	0.01	340
17	0.00	0.01	0.06	0.07	0.18	0.17	0.20	0.24	0.05	0.01	340
18	0.00	0.01	0.06	0.06	0.20	0.16	0.21	0.24	0.04	0.01	340
19	0.01	0.01	0.07	0.07	0.18	0.15	0.23	0.26	0.04	0.0	337
20	0.01	0.02	0.07	0.05	0.15	0.18	0.22	0.27	0.03	0.0	339
21	0.02	0.02	0.06	0.06	0.16	0.17	0.21	0.29	0.02	0.0	340
22	0.04	0.02	0.04	0.06	0.14	0.16	0.22	0.29	0.02	0.0	340
23	0.04	0.01	0.06	0.05	0.14	0.15	0.23	0.30	0.02	0.0	338
ALL	0.03	0.03	0.07	0.08	0.15	0.15	0.19	0.25	0.06	0.00	8146

Table 6—continued

Visibility Class Interval (statute miles)										TOTAL OBS
<.5	>.5 ≤1.0	>1.0 ≤2.0	>2.0 ≤3.0	>3.0 ≤5.0	>5.0 ≤7.0	>7.0 ≤10.0	>10.0 ≤15.0	>15.0 ≤25.0	>25.0	

NOVEMBER

0	0.08	0.02	0.12	0.09	0.17	0.15	0.22	0.14	0.01	0.00	330
1	0.07	0.03	0.11	0.10	0.16	0.16	0.21	0.15	0.02	0.00	330
2	0.06	0.03	0.11	0.11	0.16	0.15	0.22	0.14	0.02	0.00	330
3	0.07	0.04	0.12	0.12	0.15	0.15	0.19	0.15	0.02	0.00	330
4	0.06	0.05	0.12	0.14	0.16	0.14	0.19	0.12	0.02	0.00	330
5	0.07	0.05	0.17	0.12	0.18	0.15	0.16	0.08	0.02	0.00	330
6	0.06	0.09	0.18	0.15	0.15	0.13	0.14	0.08	0.02	0.00	330
7	0.07	0.14	0.20	0.14	0.19	0.08	0.09	0.08	0.02	0.00	330
8	0.05	0.16	0.19	0.16	0.17	0.09	0.09	0.08	0.01	0.00	330
9	0.04	0.13	0.19	0.18	0.18	0.11	0.07	0.09	0.01	0.00	330
10	0.03	0.10	0.17	0.16	0.22	0.13	0.08	0.08	0.04	0.00	330
11	0.02	0.07	0.15	0.14	0.20	0.17	0.11	0.10	0.04	0.00	330
12	0.01	0.07	0.11	0.16	0.21	0.16	0.14	0.12	0.04	0.00	330
13	0.02	0.07	0.10	0.12	0.21	0.17	0.12	0.14	0.05	0.00	330
14	0.02	0.05	0.13	0.11	0.23	0.18	0.10	0.12	0.05	0.00	330
15	0.02	0.03	0.17	0.17	0.22	0.14	0.11	0.10	0.04	0.00	330
16	0.02	0.05	0.15	0.19	0.24	0.13	0.12	0.08	0.03	0.00	330
17	0.02	0.06	0.15	0.15	0.23	0.16	0.12	0.09	0.03	0.00	330
18	0.03	0.05	0.15	0.13	0.24	0.16	0.13	0.10	0.02	0.00	330
19	0.03	0.05	0.12	0.14	0.24	0.15	0.14	0.11	0.02	0.00	330
20	0.04	0.04	0.10	0.13	0.22	0.18	0.15	0.12	0.02	0.00	329
21	0.03	0.04	0.11	0.13	0.19	0.18	0.16	0.13	0.02	0.00	329
22	0.05	0.03	0.11	0.12	0.20	0.18	0.17	0.13	0.02	0.00	329
23	0.05	0.04	0.12	0.09	0.18	0.16	0.19	0.14	0.01	0.00	330
ALL	0.04	0.06	0.14	0.13	0.20	0.15	0.14	0.11	0.02	0.00	7917

DECEMBER

0	0.04	0.06	0.12	0.13	0.17	0.13	0.16	0.16	0.02	0.00	340
1	0.05	0.05	0.14	0.10	0.17	0.14	0.18	0.16	0.02	0.00	340
2	0.05	0.05	0.13	0.12	0.17	0.13	0.17	0.17	0.01	0.00	340
3	0.05	0.07	0.11	0.13	0.14	0.14	0.19	0.16	0.01	0.00	340
4	0.04	0.06	0.15	0.11	0.15	0.14	0.19	0.14	0.01	0.00	340
5	0.06	0.06	0.16	0.12	0.14	0.12	0.19	0.12	0.01	0.00	340
6	0.06	0.11	0.18	0.12	0.12	0.13	0.14	0.12	0.01	0.00	338
7	0.08	0.15	0.19	0.12	0.14	0.11	0.11	0.08	0.02	0.00	340
8	0.08	0.14	0.21	0.15	0.11	0.12	0.09	0.07	0.02	0.00	340
9	0.08	0.15	0.16	0.15	0.16	0.13	0.07	0.08	0.01	0.00	340
10	0.07	0.13	0.15	0.15	0.15	0.13	0.08	0.09	0.01	0.00	340
11	0.06	0.11	0.17	0.13	0.19	0.11	0.09	0.12	0.02	0.00	340
12	0.05	0.08	0.17	0.13	0.20	0.12	0.10	0.12	0.02	0.00	339
13	0.04	0.08	0.16	0.14	0.19	0.13	0.12	0.12	0.02	0.00	340
14	0.03	0.08	0.18	0.14	0.18	0.13	0.14	0.09	0.03	0.00	340
15	0.04	0.07	0.19	0.14	0.19	0.13	0.12	0.09	0.02	0.00	339
16	0.04	0.08	0.20	0.12	0.21	0.13	0.11	0.09	0.02	0.00	340
17	0.04	0.08	0.18	0.12	0.22	0.14	0.12	0.09	0.02	0.00	340
18	0.03	0.07	0.19	0.13	0.19	0.16	0.11	0.10	0.02	0.00	340
19	0.02	0.09	0.17	0.14	0.16	0.15	0.14	0.10	0.02	0.00	340
20	0.03	0.07	0.16	0.11	0.19	0.16	0.14	0.11	0.02	0.00	340
21	0.04	0.07	0.16	0.11	0.17	0.16	0.12	0.14	0.02	0.00	340
22	0.05	0.06	0.15	0.12	0.17	0.14	0.14	0.14	0.02	0.00	339
23	0.04	0.07	0.13	0.12	0.19	0.12	0.16	0.15	0.02	0.00	338
ALL	0.05	0.09	0.16	0.13	0.17	0.13	0.13	0.12	0.02	0.00	8153

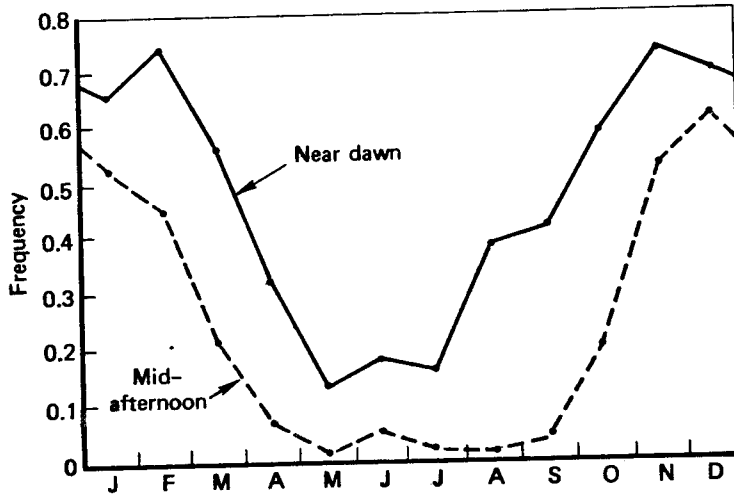


Fig. 25—Monthly Frequencies of Low Visibility (< 5 mi) at Two Times of Day at Berlin

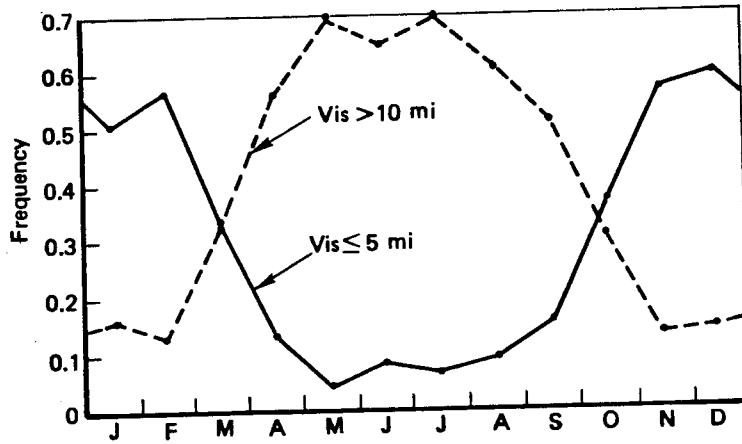


Fig. 26—Monthly Frequencies of High and Low Visibilities at Berlin

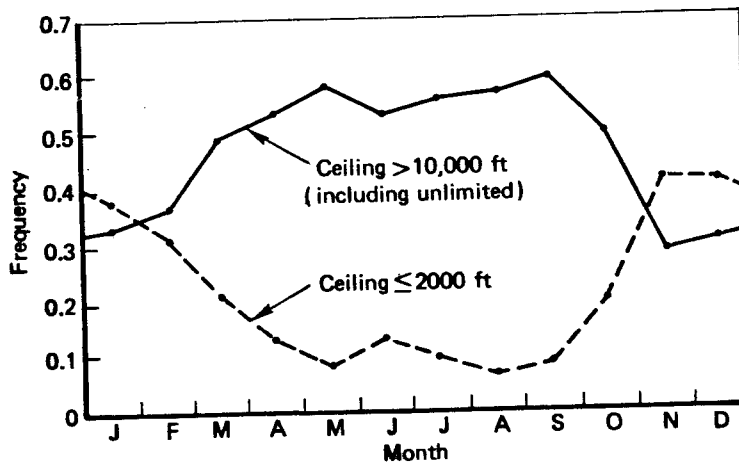


Fig. 27—Monthly Frequencies of High and Low Ceilings at Berlin

6. DURATIONS OF ADVERSE CEILING AND VISIBILITY AT THREE GERMAN LOCATIONS

The expected duration of a weather state is frequently of interest. Three sets of calculations of low ceiling and visibility durations were made using Berlin, Bitburg, and Heidelberg data. The analyses were done for different reasons and had different ground rules. "Bad weather" is a term of convenience in referring to the weather states that are considered.

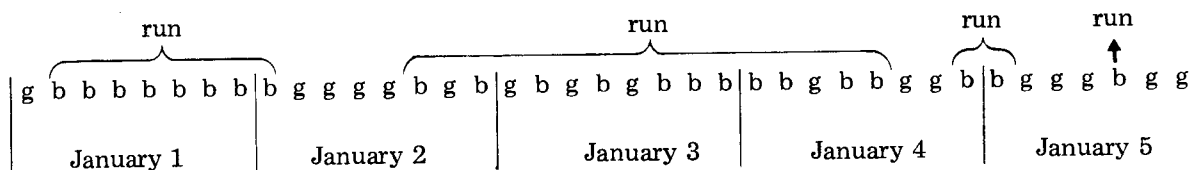
a. Berlin: Random Encounter with Bad Weather, Seasonal Durations

The first calculations answered the question: If the weather sequence were entered at random and a ceiling < 1000 ft or visibility < 1 mi were encountered, what would be the probability that either or both of these conditions would continue for H hours? The question is answered for three seasons, winter (November through February), summer (May through August), and spring/fall (March, April, September, and October); and is also answered for the durations of ceiling < 4000 ft or visibility < 4 mi in winter. (See Fig. 28.) These calculations were made using hourly weather observations at Berlin (Tempelhof) from April 1946 through December 1963.

b. Berlin: Length of Daytime Bad Weather Runs in January

The second analysis looked at the duration of "runs" of adverse weather. The question answered is the following (which is quite different from the previous question): Given that "good" weather turns to "bad," what is the probability that the bad weather continues for H hours or D days? The question is answered, in Figs. 29-31, only for runs beginning in the month of January (using 10 yr of Berlin data, from 1954 through 1963) and is only concerned with daylight hours (the original problem having to do with the utility of daylight visual systems). If the first weather event in any of the 10 Januarys was bad weather, it was assumed that that was the beginning of a bad weather run; therefore, the results are slightly biased toward shorter runs. However, each run that extended beyond the end of January ran to completion, and was accounted for. Consequences of the biasing assumption have not been examined.

Two definitions of "bad weather run" were used. In Fig. 29, a bad weather run is a consecutive string of daylight hours that contains no consecutive pair of good weather hours. Bad weather is a ceiling < 1200 ft or visibility < 3 mi. A sunset hour and the following sunrise hour are taken as consecutive hours. The definition is illustrated below. Runs of duration > 90 hr were not tabulated.



The dots in Fig. 29 are the computed hour-by-hour duration probabilities, approximated by the smooth curve.

Figure 30 shows cumulative duration probabilities for runs of "bad weather days," given that a bad weather day occurs following a good weather day, where a bad weather day is one in which a ceiling < 1200 ft or visibility < 3 mi occurs the majority of daylight hours. The raw frequency distribution of the durations of runs of bad weather days in Berlin, starting in January, from 1954 through 1963, is shown in Fig. 31.

c. Bitburg and Heidelberg: Lengths of Bad Weather Runs in Four Seasons

The question answered by this analysis is straightforward: Given a bad weather hour following a good weather hour, what is the probability that bad weather will persist for H hours (all hours, day and night, included)? The two weather states examined are (1) ceiling < 1000 ft or visibility < 3 mi and (2) ceiling < 5000 ft or visibility < 3 mi. The results are graphed in Figs. 32 and 33.

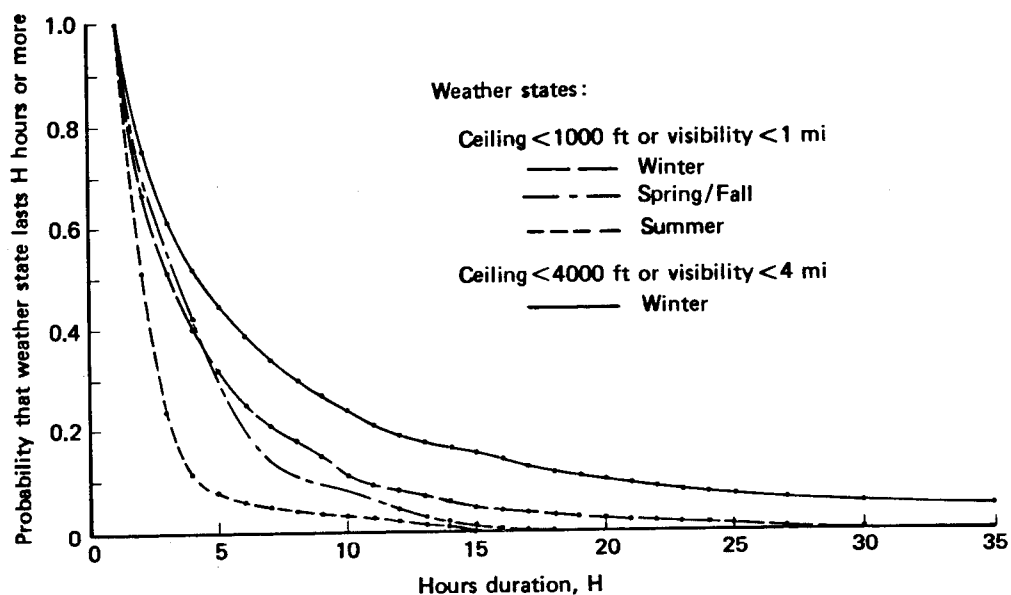


Fig. 28—Weather State Duration Probabilities, Given Random Encounter with Weather State: Berlin, January 1946-1953

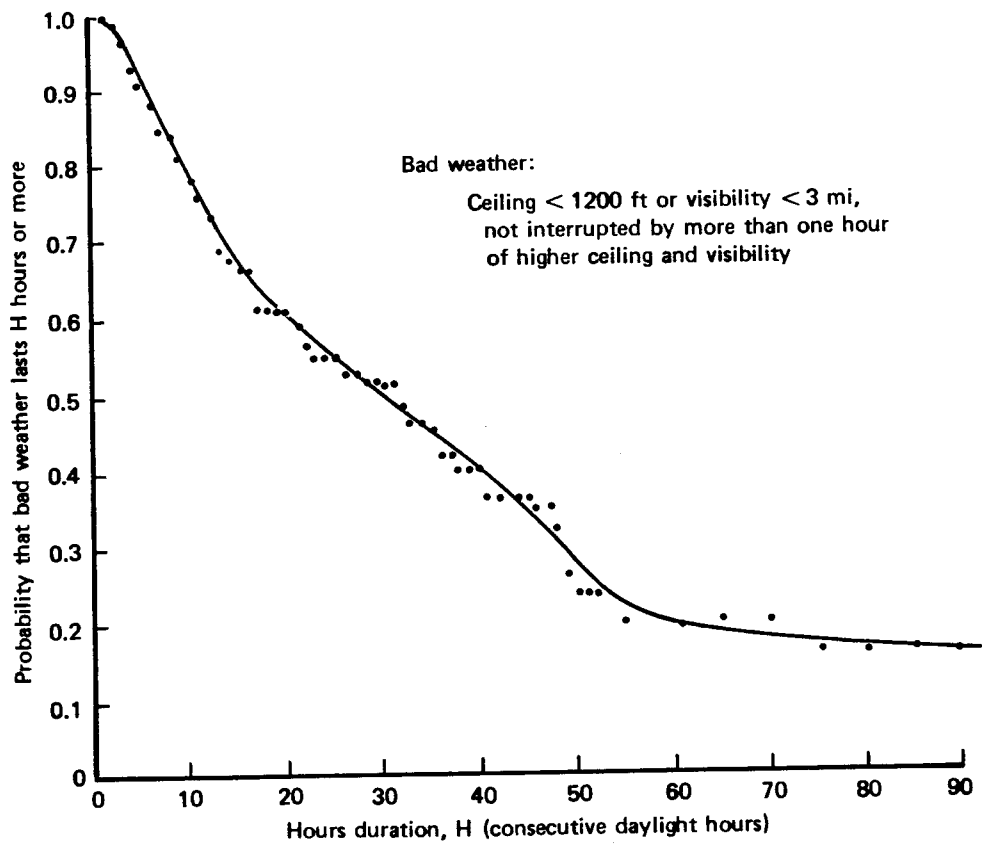


Fig. 29—Bad Weather Duration Probability, Number of Daylight Hours: Berlin, January 1954-1963

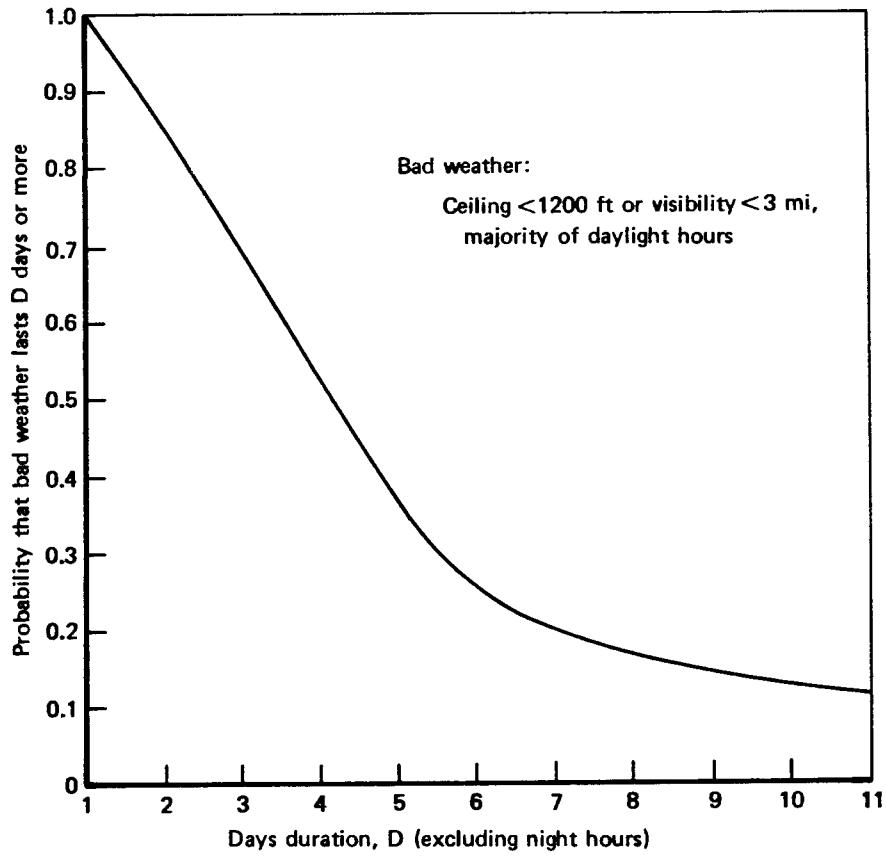


Fig. 30—Bad Weather Duration Probability, Number of Days:
Berlin, January 1954-1963

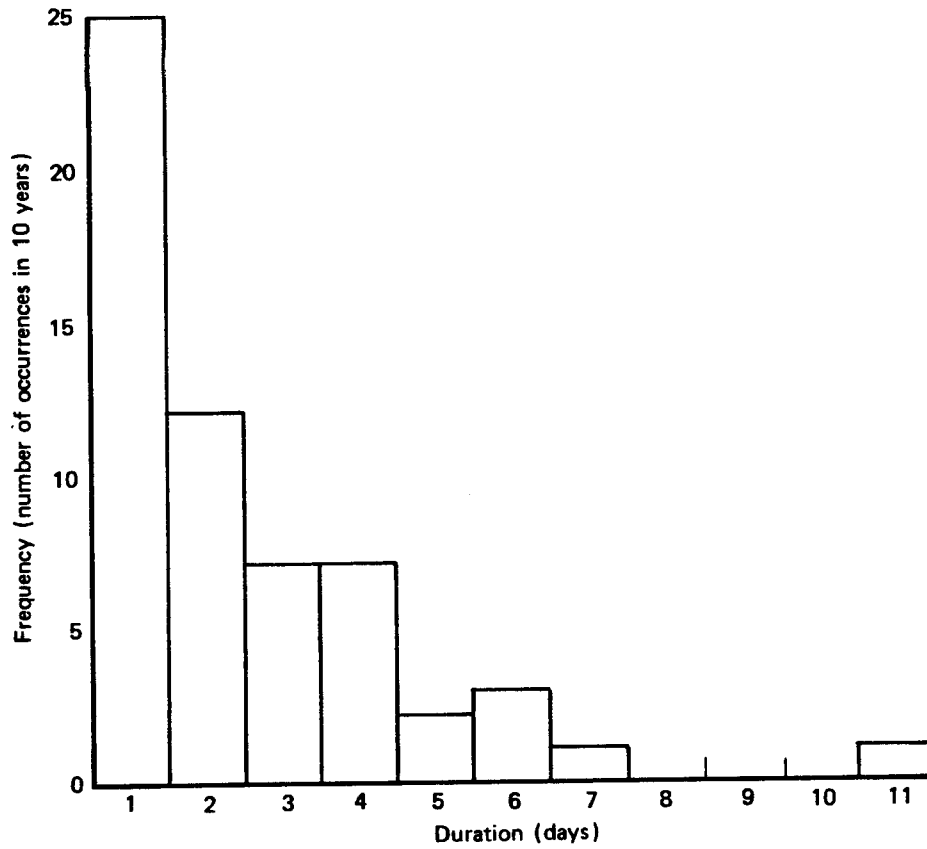


Fig. 31—Frequency Distribution of Durations of Runs of Consecutive "Bad Weather Days" (Defined as in Fig. 30): Berlin, January 1954-1963

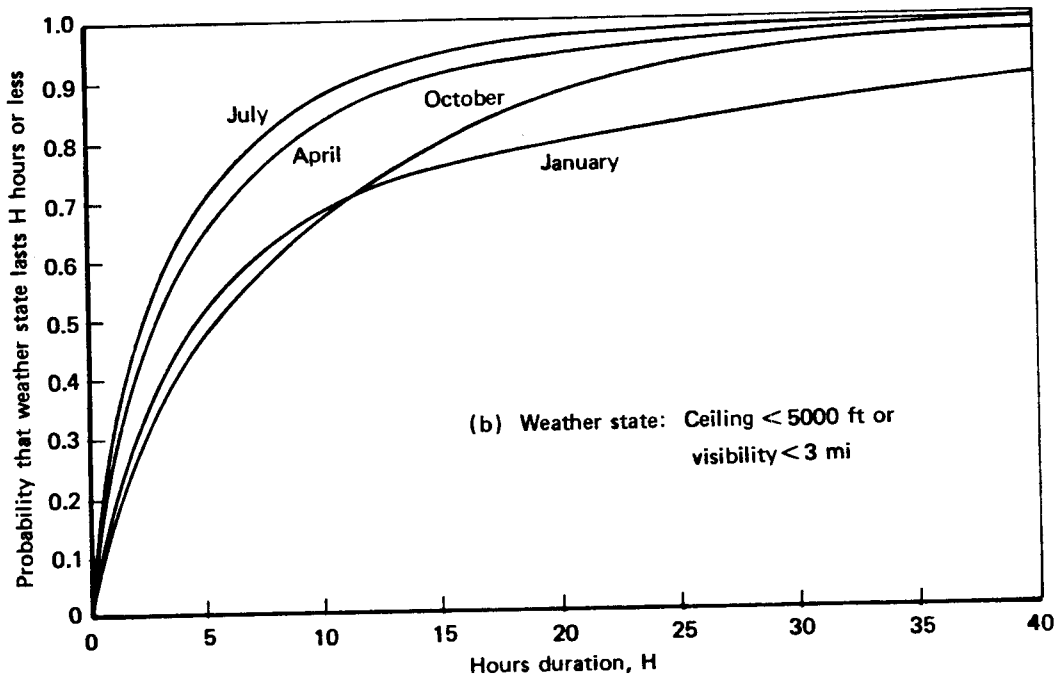
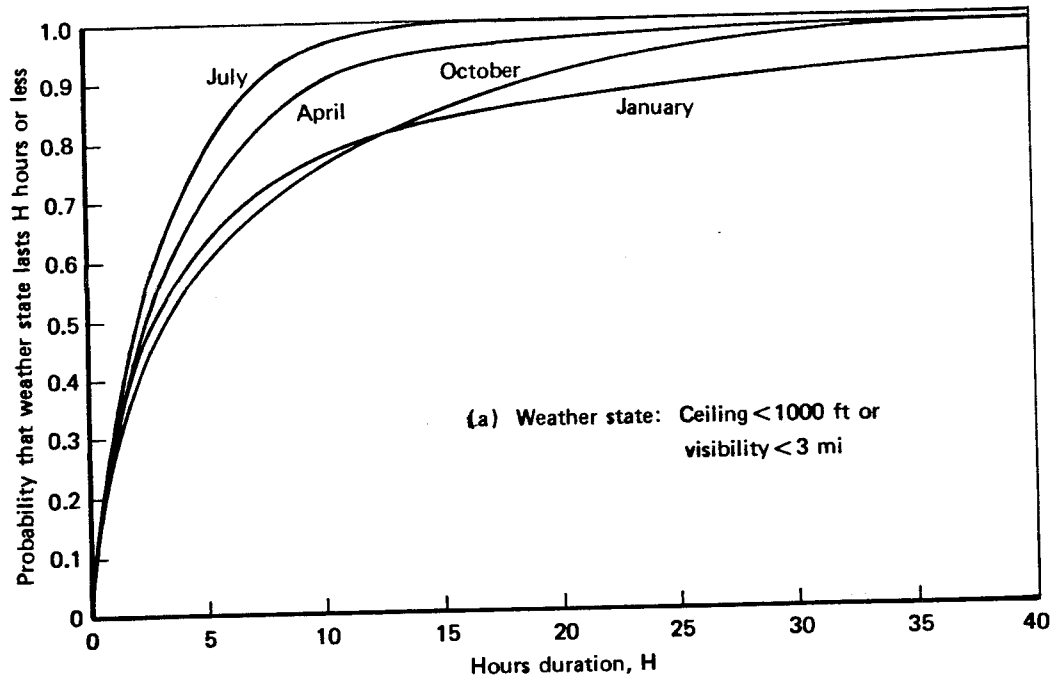


Fig. 32—Weather State Duration Probabilities: Bitburg, 1963-1967

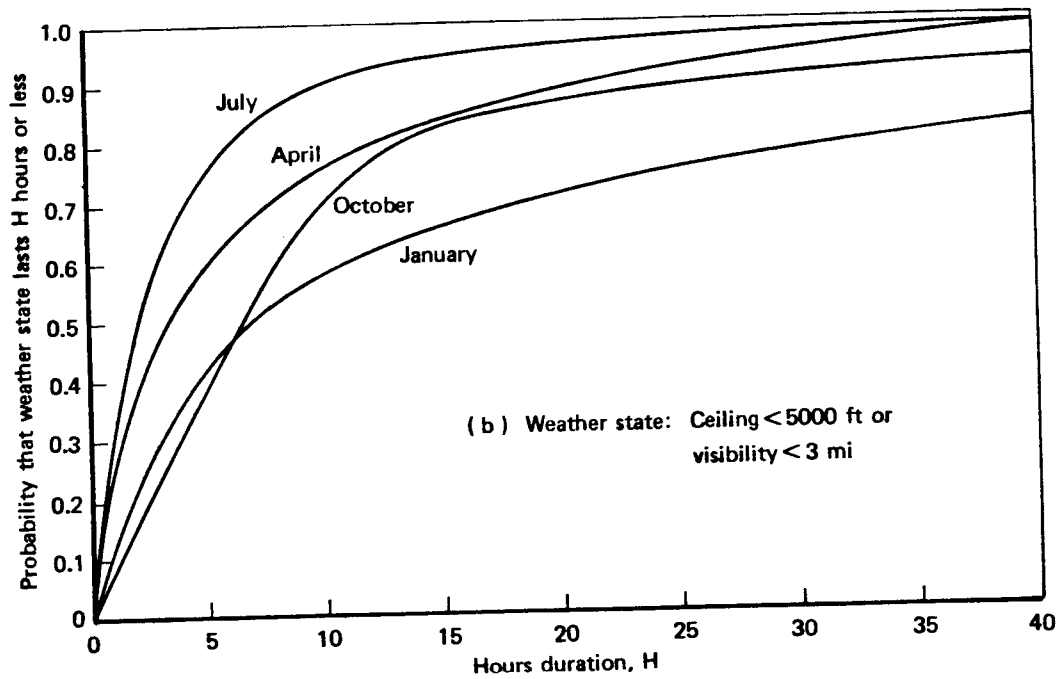
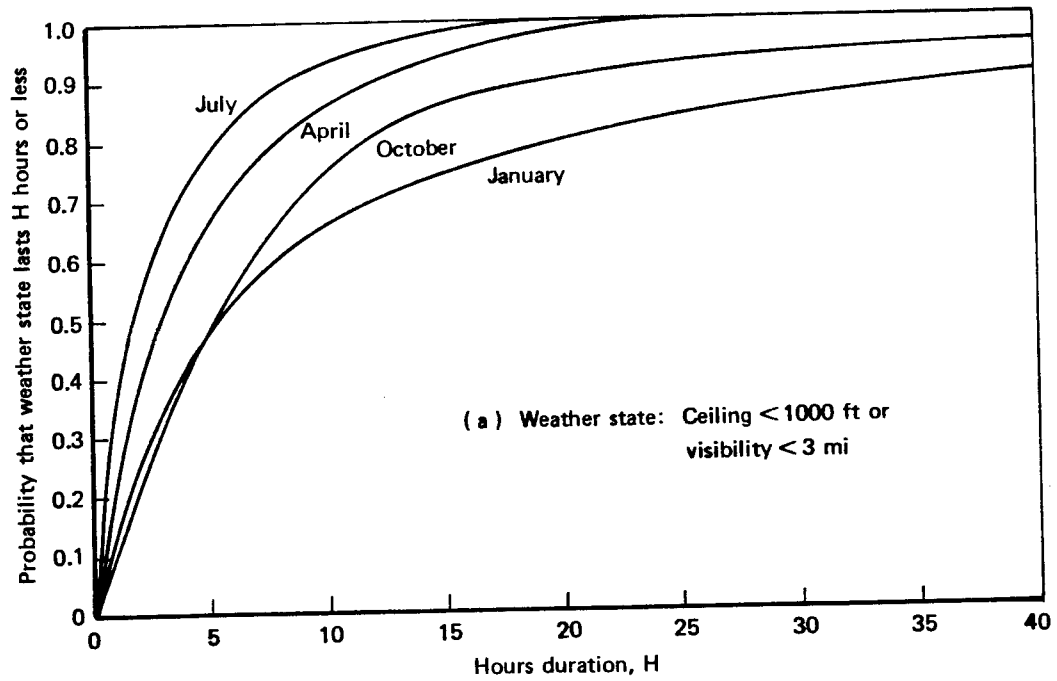


Fig. 33—Weather State Duration Probabilities: Heidelberg, 1963-1967

7. MONTHLY VISIBILITY FREQUENCIES AT FULDA

Table 7 presents monthly visibility by quartiles at Fulda, FRG. Quartiles are calculated by ordering all n values of a variable, usually from highest to lowest, and then dividing the ordered set into four subsets (quartiles), each containing equal numbers ($n/4$) of the values. The internal boundaries of the quartiles, the quartile points (Q_1 , Q_2 , Q_3), correspond to the 25 percent, 50 percent, and 75 percent points on the cumulative frequency distributions of the values.

In the calculations for Table 7, the values of visibility at Fulda were ordered from lowest to highest; hence, the first quartiles contain the lowest 25 percent of visibility values, and so on. The quartile points tend to be repetitive because of the biased coarseness of the reported visibility values. The averages shown are the averages of all values in each quartile and (last column) the average of all visibility values each month.

A four-month sample of Fulda visibility frequency distributions is shown in Fig. 34. The absence of visibility values in the 16 to 18 km and 22 to 24 km ranges illustrates a problem mentioned earlier: Reported visibilities are biased by the unique availability of visibility check points (hills, towers, etc.) at every observing site.

Table 7
MONTHLY VISIBILITY QUANTILES AT FULDA

Month	QUANTILE										ALL	
	First (lowest)		Second		Third		Fourth (highest)		Average			
	Minimum	Average	Q ₁	Average	Q ₂	Average	Q ₃	Average	Maximum	Average		
				VISIBILITY (km)								
Jan	0	1.5	2.8	3.8	4.8	7.5	10.0	16.0	24.0	7.2		
Feb	0	1.6	2.8	4.5	7.0	8.8	13.0	16.4	24.0	7.9		
Mar	0	2.6	4.8	6.6	8.0	11.3	15.0	19.5	35.0	10.0		
Apr	0	3.4	7.0	8.6	13.0	15.8	21.0	22.0	35.0	12.5		
May	0	5.0	8.0	12.4	15.0	19.3	21.0	22.7	24.0	14.8		
Jun	0	5.0	8.0	12.1	15.0	19.5	21.0	22.4	24.0	14.8		
Jul	0	4.6	8.0	11.4	15.0	18.7	21.0	22.5	35.0	14.3		
Aug	0	3.9	8.0	11.2	15.0	19.4	21.0	22.7	35.0	14.3		
Sep	0	1.8	4.8	7.7	10.0	15.3	18.0	22.5	35.0	11.8		
Oct	0	1.6	3.6	6.2	8.0	11.3	15.0	20.4	35.0	9.9		
Nov	0	1.5	3.6	5.2	7.0	9.6	13.0	19.3	35.0	8.9		
Dec	0	1.4	2.6	3.7	4.8	8.2	13.0	17.3	35.0	7.7		

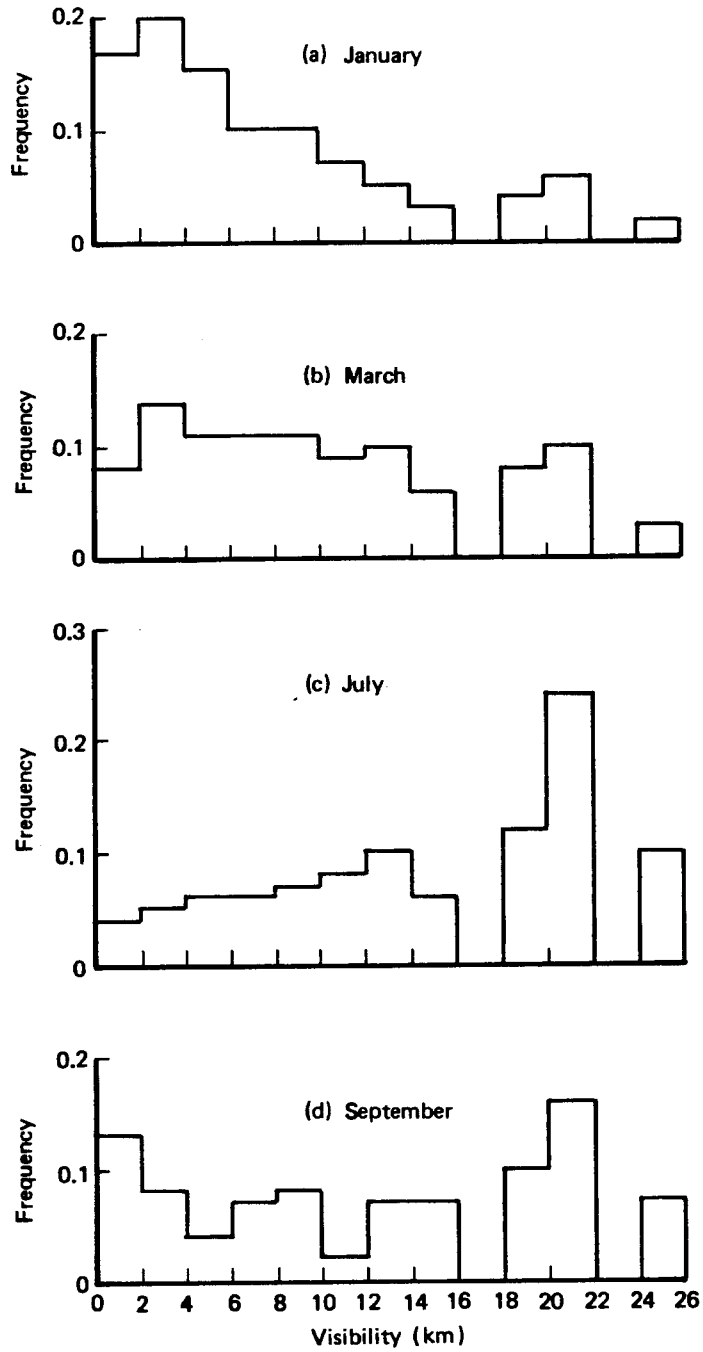


Fig. 34—Mid-season Frequency Distributions of Visibility at Fulda

8. SEASONAL CLOUD AMOUNT FREQUENCY VERSUS ALTITUDE AT BERLIN

The frequencies of cloud amounts between the surface and any altitude up to 16,000 ft over Berlin are given in Fig. 35. These are "daytime" frequencies (0600 to 1800 hr local time) for the four seasons of the year.

All possible cloud amounts are represented by the four mutually exclusive categories—overcast, broken, scattered, and no clouds. Cloud amount categories are defined in terms of total cloud amount, N , in the atmospheric layer from the surface to the indicated altitude:

Category	N		
No clouds			$N = 0/8$
Scattered	$1/8$	\leq	$N < 6/8$
Broken	$6/8$	\leq	$N < 8/8$
Overcast	$8/8$	$=$	N

The curves are plotted in cumulative fashion. The curves, and their vertical separation, are interpreted as shown on Fig. 35(a). For example, in winter, between the ground and 6000 ft altitude, overcast clouds exist 49 percent of the time, broken or overcast clouds 63 percent of the time (broken 14 percent of the time), scattered or broken or overcast 69 percent of the time (scattered 6 percent of the time), and no clouds (clear) the remaining 31 percent of the time.

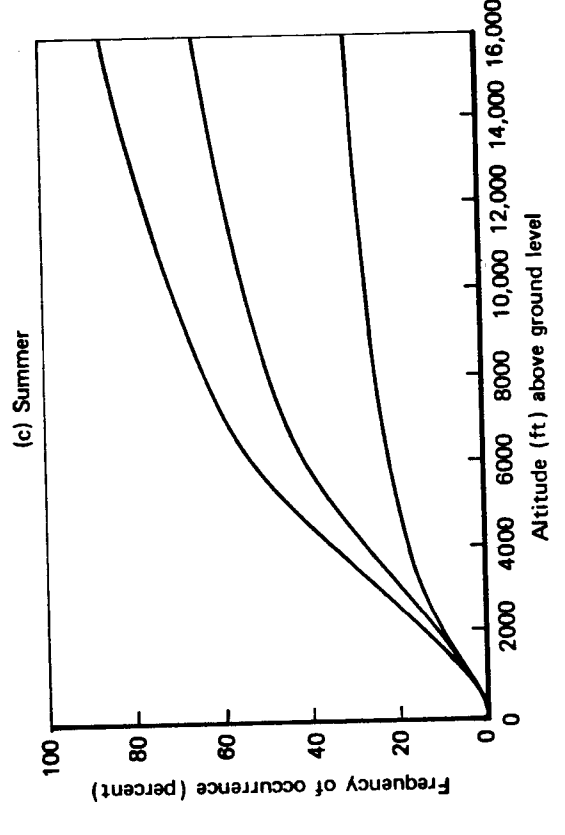
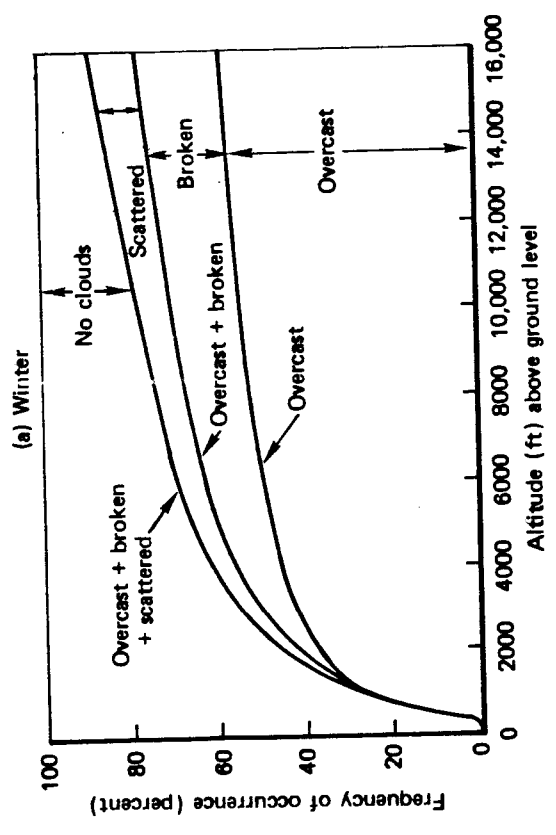
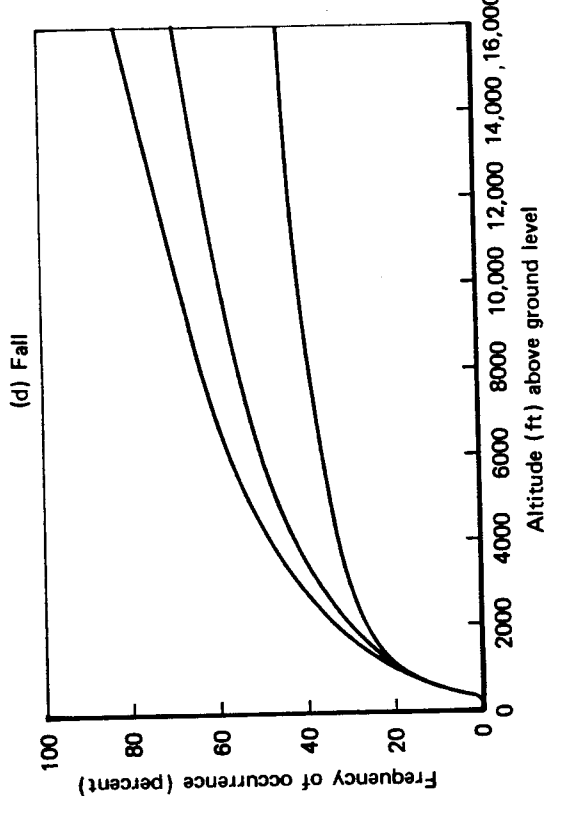
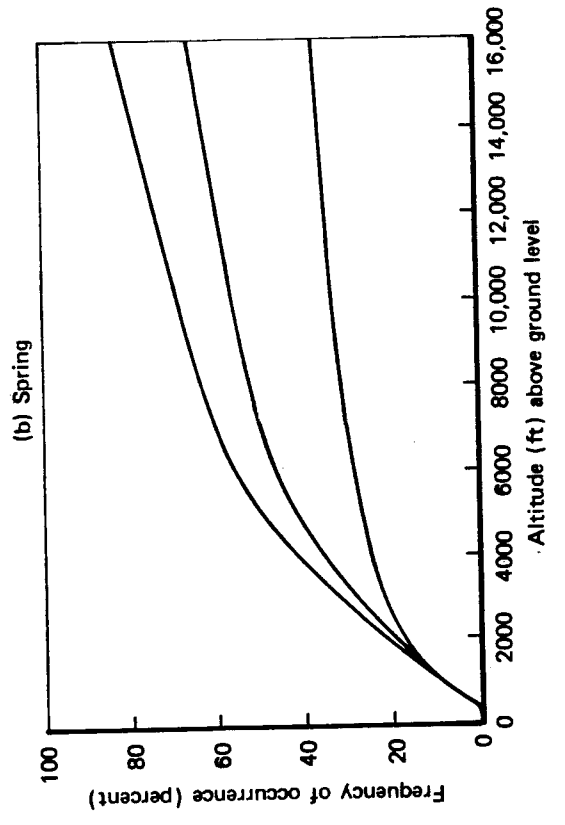


Fig. 35—Seasonal Frequencies of Cloud Amount as a Function of Altitude at Berlin

9. MONTHLY CLOUD AMOUNT FREQUENCY VERSUS ALTITUDE AT 21 LOCATIONS IN WEST AND CENTRAL EUROPE

The following cloud-amount frequency data, Table 8, are based on observations at 0700, 1300, and 1900 hr local standard time (LST) taken over a five-year period during the mid-1930s. The 21 stations were carefully selected to represent the various climatic regimes of west-central Europe.

The sky cover data include the total sky cover, the amount of low cloud, the height of the low cloud, and the presence or absence of middle clouds. Clouds below 8000 ft are classed as low clouds, and their heights are given from 0 to 8000 ft. The heights of middle clouds are not reported, but aircraft measurements in the area confirm a range of 8000 ft to 12,000 ft. Decision trees were devised to estimate the amount of cloud below the levels of 1000, 5000, 8000, 12,000, and 35,000 ft. It was assumed that all reported clouds were at or below 35,000 ft.

The decision to present data for less than 2/10 and greater than 5/10 coverage hinged on two factors. First, the specific operational problem dictated that less than 2/10 clouds generally correlates with good flying weather and 6/10 clouds or more are generally considered as inhibiting flight operations. Second, sky conditions tend toward extremes; that is, sky cover around 5/10 is less frequent than almost clear or almost overcast. The frequency of cloud cover between 2/10 and 6/10 below any level for any month is small. For example, at Klagenfurt, in July, the cloud distribution below 5000 ft was less than 2/10 sky cover 78 percent of the time, from 2/10 through 5/10 7 percent of the time, and greater than 5/10 15 percent of the time.

Table 8

MONTHLY CLOUD AMOUNT PERCENT FREQUENCIES FOR SELECTED ALTITUDES IN WEST CENTRAL EUROPE: 21 LOCATIONS

Month	Less than 0.2 clouds below:					Greater than 0.5 clouds below:				
	1000 ft	5000 ft	8000 ft	12,000 ft	35,000 ft	1000 ft	5000 ft	8000 ft	12,000 ft	35,000 ft
(a) Le Havre, France										
Jan	86	25	20	12	8	14	58	77	84	89
Feb	86	33	27	20	14	14	50	69	78	82
Mar	89	37	33	25	15	9	42	64	72	77
Apr	91	31	24	17	11	8	44	71	80	84
May	88	43	39	28	20	10	36	58	65	74
Jun	95	44	40	24	17	4	26	56	67	77
Jul	92	39	33	22	17	8	36	62	72	79
Aug	90	45	41	30	24	9	30	55	63	71
Sep	92	34	31	21	14	7	38	66	74	81
Oct	90	25	22	15	9	9	47	76	82	85
Nov	80	22	19	11	9	20	60	78	85	90
Dec	87	22	19	13	11	13	58	79	83	88

Table 8—continued

Month	Less than 0.2 clouds below:					Greater than 0.5 clouds below:				
	1000 ft	5000 ft	8000 ft	12,000 ft	35,000 ft	1000 ft	5000 ft	8000 ft	12,000 ft	35,000 ft
(b) Nancy, France										
Jan	77	23	22	13	9	22	62	78	84	88
Feb	76	27	26	17	10	23	54	73	79	84
Mar	89	51	47	31	24	11	32	50	61	72
Apr	87	19	16	6	6	13	64	83	93	94
May	97	43	38	28	20	2	31	60	69	74
Jun	90	44	39	28	16	8	33	57	66	78
Jul	96	41	38	28	21	4	29	60	68	72
Aug	95	42	40	28	20	5	27	58	67	75
Sep	88	38	34	21	14	11	37	64	62	80
Oct	81	24	22	11	7	16	58	78	86	90
Nov	77	23	22	14	13	20	54	78	83	86
Dec	63	17	17	7	4	37	71	83	90	94
(c) Paris, France										
Jan	77	29	26	16	10	22	54	73	82	87
Feb	83	35	32	25	17	16	47	67	74	78
Mar	89	47	44	33	24	10	35	55	63	71
Apr	93	33	29	19	12	6	44	70	79	83
May	91	43	40	31	19	8	34	58	66	73
Jun	97	47	39	25	17	3	26	55	69	77
Jul	94	41	35	25	18	4	33	63	72	77
Aug	95	53	44	29	20	5	23	51	64	74
Sep	93	47	40	23	17	7	32	57	71	79
Oct	89	40	34	21	15	11	43	64	74	80
Nov	74	32	28	16	12	25	56	71	81	86
Dec	77	26	24	13	10	21	57	75	83	88
(d) Tours, France										
Jan	71	36	27	19	14	26	50	65	79	84
Feb	75	42	36	27	21	23	44	59	71	76
Mar	86	51	46	35	25	11	32	50	61	67
Apr	89	44	35	23	16	9	31	58	73	79
May	91	51	42	31	22	7	28	51	64	71
Jun	91	50	40	28	17	7	23	51	66	73
Jul	90	52	42	29	23	7	25	50	62	72
Aug	93	58	48	34	25	6	21	44	59	67
Sep	89	51	43	29	21	9	28	49	65	72
Oct	85	44	33	25	17	12	37	60	72	77
Nov	70	39	34	26	20	17	46	63	71	76
Dec	64	29	25	15	11	22	59	72	81	86
(e) Vlissingen, Netherlands										
Jan	82	38	34	16	15	17	57	65	78	84
Feb	88	36	32	18	18	12	54	67	75	82
Mar	93	51	44	20	17	6	40	55	71	82
Apr	96	38	38	9	9	4	49	67	82	91
May	98	62	50	20	15	2	34	49	65	76
Jun	99	62	50	21	15	1	26	45	66	82
Jul	99	58	46	24	19	1	33	50	66	78
Aug	98	64	56	25	22	2	26	41	61	77
Sep	97	43	35	16	13	3	37	62	74	85
Oct	97	38	32	10	8	3	46	66	81	91
Nov	91	37	30	13	11	9	54	69	80	87
Dec	83	31	27	12	11	16	60	72	82	89

Table 8—continued

Month	Less than 0.2 clouds below:					Greater than 0.5 clouds below:				
	1000 ft	5000 ft	8000 ft	12,000 ft	35,000 ft	1000 ft	5000 ft	8000 ft	12,000 ft	35,000 ft
(f) Aachen, West Germany										
Jan	70	23	21	11	8	29	65	78	85	90
Feb	77	28	28	18	15	22	54	72	78	83
Mar	85	34	33	22	16	13	46	67	73	80
Apr	75	18	17	9	7	23	59	82	88	92
May	86	31	31	23	14	13	45	69	71	80
Jun	90	34	32	19	12	10	37	67	74	83
Jul	91	27	24	16	10	8	44	74	81	85
Aug	91	33	30	19	13	8	40	69	77	83
Sep	91	35	33	17	10	8	35	65	74	86
Oct	82	27	26	12	7	16	49	74	79	89
Nov	74	24	23	13	10	25	57	76	82	89
Dec	75	25	24	14	12	23	60	75	82	87
(g) Berlin, West Germany										
Jan	75	30	25	12	8	24	60	73	83	89
Feb	75	28	23	13	10	23	60	75	82	88
Mar	78	38	34	17	13	20	49	64	75	84
Apr	87	32	27	15	10	12	45	71	80	86
May	93	52	44	27	18	6	30	51	65	75
Jun	97	51	37	24	15	3	23	54	70	78
Jul	94	46	35	19	13	6	29	55	75	82
Aug	91	46	36	18	13	7	28	58	72	83
Sep	92	57	52	29	18	8	24	44	60	73
Oct	84	36	30	14	10	14	45	68	80	87
Nov	67	34	28	15	10	31	59	70	80	87
Dec	68	31	26	15	11	30	62	72	80	87
(h) Bremen, West Germany										
Jan	63	19	18	9	7	35	66	82	87	92
Feb	62	25	24	14	11	35	59	76	81	87
Mar	75	32	30	20	16	23	50	69	75	81
Apr	80	25	23	15	10	19	50	76	81	86
May	91	44	41	29	22	7	34	57	65	72
Jun	93	43	41	23	18	6	31	58	68	78
Jul	87	33	29	18	13	10	37	68	77	83
Aug	92	44	39	26	19	6	27	57	67	75
Sep	89	45	42	23	14	10	30	56	67	79
Oct	81	29	24	13	10	17	45	73	81	88
Nov	69	25	22	12	9	29	59	77	83	89
Dec	67	26	24	11	10	32	62	75	83	89
(i) Frankfurt am Main, West Germany										
Jan	82	17	16	9	8	17	66	84	89	91
Feb	88	29	28	18	16	11	56	72	77	82
Mar	95	38	36	24	20	5	44	64	70	76
Apr	96	30	25	13	9	4	44	72	81	88
May	98	45	40	28	21	2	27	56	66	73
Jun	98	45	38	26	17	10	26	56	68	76
Jul	97	38	32	21	16	3	25	63	72	80
Aug	95	45	36	22	17	5	26	57	71	80
Sep	94	44	40	19	14	5	29	56	69	81
Oct	91	29	25	14	9	9	51	72	79	87
Nov	79	20	17	9	9	21	63	82	87	91
Dec	75	16	13	8	7	23	70	85	90	92

Table 8—continued

Month	Less than 0.2 clouds below:					Greater than 0.5 clouds below:				
	1000 ft	5000 ft	8000 ft	12,000 ft	35,000 ft	1000 ft	5000 ft	8000 ft	12,000 ft	35,000 ft
(j) München, West Germany										
Jan	77	36	30	12	10	23	55	68	82	89
Feb	87	45	41	24	19	12	43	57	69	77
Mar	89	53	42	23	17	11	36	51	69	79
Apr	89	41	32	11	6	10	41	62	80	90
May	90	47	38	23	16	10	33	55	70	78
Jun	96	49	39	26	19	4	29	54	66	74
Jul	97	49	40	23	20	3	24	52	67	77
Aug	94	45	34	22	16	6	32	58	72	79
Sep	90	50	43	22	17	9	32	51	66	79
Oct	80	37	31	16	11	19	52	66	76	85
Nov	70	40	35	18	13	29	52	63	75	83
Dec	73	35	30	11	8	26	57	68	83	90
(k) Nürnberg, West Germany										
Jan	75	21	19	10	9	24	65	79	87	90
Feb	82	30	28	18	15	17	53	72	77	83
Mar	88	41	37	26	19	11	42	60	69	77
Apr	90	24	20	10	6	9	43	78	87	91
May	91	42	36	26	18	8	28	58	71	76
Jun	93	43	38	27	18	5	25	57	67	75
Jul	95	43	35	24	18	4	23	58	71	78
Aug	91	42	34	21	16	6	26	60	73	81
Sep	94	47	40	22	15	5	28	55	68	80
Oct	84	30	28	14	10	15	51	71	80	87
Nov	74	25	24	14	10	24	58	76	81	87
Dec	72	22	20	10	7	27	65	79	87	91
(l) Stuttgart, West Germany										
Jan	90	32	27	13	12	9	53	71	81	88
Feb	87	33	28	19	17	13	55	70	77	82
Mar	94	39	32	20	18	5	42	63	73	80
Apr	89	21	18	8	6	11	60	80	88	92
May	91	47	41	29	23	9	30	54	64	72
Jun	94	45	39	28	16	5	28	57	66	73
Jul	96	36	29	12	10	4	25	64	78	89
Aug	90	37	33	24	21	9	35	64	72	77
Sep	88	41	35	15	13	11	35	61	75	85
Oct	85	38	31	17	15	13	45	64	77	83
Nov	81	31	25	13	10	19	50	72	79	87
Dec	88	27	25	11	9	12	56	56	81	89
(m) Dresden, East Germany										
Jan	80	26	24	12	9	20	57	74	83	89
Feb	78	23	22	11	9	22	59	78	84	90
Mar	81	34	31	17	12	19	49	67	77	85
Apr	88	25	23	12	7	11	42	75	83	89
May	89	37	35	22	18	9	31	63	73	79
Jun	94	37	33	20	12	6	23	63	71	81
Jul	94	32	29	16	12	6	30	69	75	85
Aug	88	34	31	19	15	12	32	66	73	82
Sep	92	44	41	23	16	7	31	56	64	78
Oct	83	27	24	12	9	16	51	74	81	89
Nov	77	29	26	14	11	23	54	71	80	86
Dec	78	27	25	11	10	21	53	74	81	89

Table 8—continued

Month	Less than 0.2 clouds below:					Greater than 0.5 clouds below:				
	1000 ft	5000 ft	8000 ft	12,000 ft	35,000 ft	1000 ft	5000 ft	8000 ft	12,000 ft	35,000 ft
(n) Erfurt, East Germany										
Jan	91	25	23	11	9	9	55	76	85	90
Feb	89	22	21	14	11	10	57	78	83	87
Mar	87	33	29	20	15	13	48	68	77	82
Apr	91	26	22	11	7	9	49	75	84	90
May	92	41	36	25	17	7	36	61	69	77
Jun	98	43	39	25	17	2	29	58	67	76
Jul	98	38	35	18	14	1	33	62	73	82
Aug	97	40	33	18	15	3	30	62	71	82
Sep	98	46	42	24	15	2	26	55	66	78
Oct	94	29	28	14	11	6	46	71	81	86
Nov	83	25	24	13	11	17	59	75	83	88
Dec	79	24	22	12	10	20	61	77	85	89
(o) Krakow, Poland										
Jan	76	35	34	20	16	23	50	65	73	82
Feb	74	26	25	14	12	26	44	74	81	87
Mar	78	34	32	16	13	21	55	66	74	84
Apr	88	29	28	11	7	12	41	71	79	90
May	92	37	35	19	14	7	27	64	72	82
Jun	94	35	34	21	16	6	30	65	71	80
Jul	97	25	22	12	10	2	32	75	82	88
Aug	87	28	28	10	8	12	43	72	77	90
Sep	87	42	40	28	22	12	36	59	62	72
Oct	80	36	34	21	17	20	47	65	71	80
Nov	73	36	34	19	16	27	52	64	71	82
Dec	67	25	23	11	11	32	62	75	83	89
(p) Warsaw, Poland										
Jan	55	25	25	14	13	43	61	75	80	86
Feb	55	25	25	9	7	41	62	75	82	93
Mar	68	33	32	15	13	30	51	68	77	86
Apr	81	29	28	8	7	17	48	72	89	93
May	87	44	42	23	16	12	29	57	68	78
Jun	88	41	37	23	17	11	30	60	66	79
Jul	84	24	24	10	8	15	41	76	81	90
Aug	87	27	26	9	8	11	35	73	81	92
Sep	89	43	42	24	21	11	29	57	65	77
Oct	75	32	32	16	13	24	49	68	78	85
Nov	58	25	24	11	10	42	62	76	79	89
Dec	48	20	20	7	7	50	70	80	87	93
(q) Wroclaw, Poland										
Jan	84	34	28	17	15	14	53	69	79	83
Feb	87	28	22	13	11	12	55	74	82	87
Mar	85	36	32	16	12	14	47	65	76	85
Apr	94	37	24	13	11	6	44	66	82	87
May	95	52	39	23	17	5	25	51	67	79
Jun	95	53	41	26	21	5	21	50	65	75
Jul	96	43	30	16	14	3	27	60	76	84
Aug	92	48	34	19	16	7	27	55	71	81
Sep	93	56	43	28	24	6	24	47	61	72
Oct	86	35	29	16	14	12	46	68	76	84
Nov	80	32	28	13	11	17	51	68	78	87
Dec	80	31	25	13	12	20	57	73	81	87

Table 8—continued

Month	Less than 0.2 clouds below:					Greater than 0.5 clouds below:				
	1000 ft	5000 ft	8000 ft	12,000 ft	35,000 ft	1000 ft	5000 ft	8000 ft	12,000 ft	35,000 ft
(r) Praha, Czechoslovakia										
Jan	94	28	26	16	12	5	51	73	80	85
Feb	95	36	34	19	17	4	39	65	74	81
Mar	96	48	46	28	22	3	31	53	63	73
Apr	97	40	37	19	15	3	32	60	71	81
May	99	57	48	33	25	1	20	44	59	69
Jun	98	56	47	32	24	2	16	44	57	68
Jul	98	51	42	25	22	2	18	51	64	75
Aug	99	49	40	28	23	1	20	53	64	72
Sep	96	56	51	37	27	3	19	46	55	64
Oct	93	36	32	17	14	6	37	66	77	84
Nov	88	21	19	13	10	12	60	80	84	88
Dec	87	23	21	13	10	12	60	78	83	87
(s) Klagenfurt, Austria										
Jan	79	43	30	17	12	21	49	62	77	85
Feb	60	43	32	20	16	39	52	61	74	82
Mar	91	63	44	18	15	9	32	43	68	82
Apr	94	64	29	14	11	6	31	51	79	87
May	92	65	35	20	14	8	29	42	72	81
Jun	95	69	34	21	15	5	24	42	71	81
Jul	96	78	45	29	23	3	15	33	62	72
Aug	91	65	33	16	11	8	26	46	76	86
Sep	90	63	44	26	20	9	30	43	63	75
Oct	81	54	34	20	16	18	40	55	74	80
Nov	67	31	22	14	11	33	62	71	83	87
Dec	69	31	22	13	11	32	74	83	86	88
(t) Wien, Austria										
Jan	87	37	24	15	14	11	51	72	80	86
Feb	92	50	35	25	24	8	37	55	69	75
Mar	98	57	44	26	23	1	26	48	63	75
Apr	99	43	24	14	12	1	30	63	79	86
May	98	68	45	27	21	1	17	38	61	74
Jun	99	64	42	29	24	1	18	42	61	72
Jul	99	70	40	22	19	1	11	37	66	78
Aug	99	57	29	16	14	1	20	49	75	84
Sep	98	66	48	37	32	1	17	38	54	63
Oct	92	43	28	17	15	7	39	61	76	83
Nov	81	35	23	15	13	19	53	70	79	86
Dec	74	24	20	13	12	24	63	78	82	87
(u) Kaliningrad, USSR										
Jan	67	27	25	15	15	30	62	74	80	85
Feb	70	26	21	10	7	28	63	76	86	91
Mar	75	33	31	20	12	23	53	69	75	82
Apr	88	35	27	9	6	11	37	68	81	91
May	95	51	44	24	16	5	21	51	64	78
Jun	91	52	45	21	14	9	22	49	63	80
Jul	87	31	27	11	8	10	32	70	79	89
Aug	93	38	31	9	5	12	25	64	79	91
Sep	95	48	42	21	17	4	27	55	68	79
Oct	83	28	17	10	7	14	49	76	85	90
Nov	66	26	21	13	10	32	62	76	82	89
Dec	55	17	15	8	7	43	74	84	88	93

10. THUNDERSTORM FREQUENCY IN NORTHERN GERMANY

Figures 36 and 37 were developed from special summaries entitled *World Distribution of Thunderstorm Days* (1956) and *Hourly Probability of World-Wide Thunderstorm Occurrence* (1971). Thunderstorm activity is described by a unit called a "thunderstorm day" that, by international agreement, is defined as a local calendar day on which thunder is heard. A thunderstorm day is recorded regardless of the actual number of thunderstorms observed on that day. Lightning seen without thunder being heard is not recorded as a thunderstorm.

As seen in Fig. 36, across the plains of northern Germany less than one-half thunderstorm day per month is reported, on the average, during the months of November through February. Thunderstorms during these months are associated with occasional fronts or low pressure systems moving through northern Germany. In July, the month of maximum occurrence, only five thunderstorm days are recorded on the average. Summer (June, July, August) thunderstorms usually occur during the early afternoon (Fig. 37) when heating and convection are at a maximum within the unstable summer air mass. Based on an observer's audible range of about 20 km, there is, however, only slightly better than a 1 percent probability of having a thunderstorm within 20 km of a given point, even during the hours of maximum occurrence. Occurrences before 1200 or after 2000 hr GMT may be due to an occasional weather front or low pressure system similar to those in winter. These summer disturbances are usually very weak. However, they may generate squall lines similar to those experienced through the U.S. midwest, which normally develop during the afternoon and reach a maximum during the evening and early morning hours.

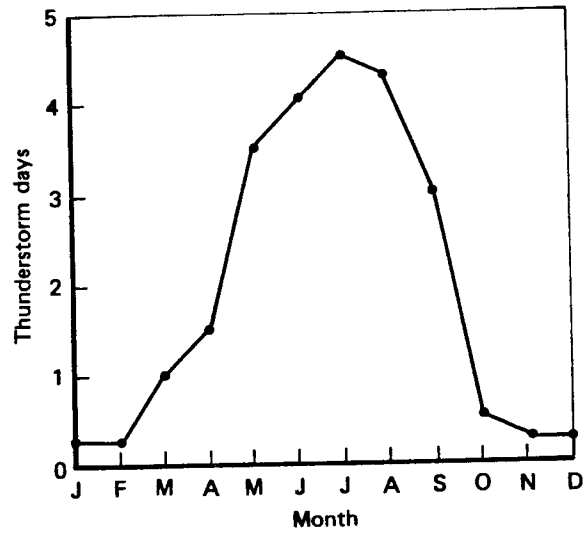


Fig. 36—Thunderstorm Days per Month in Northern Germany

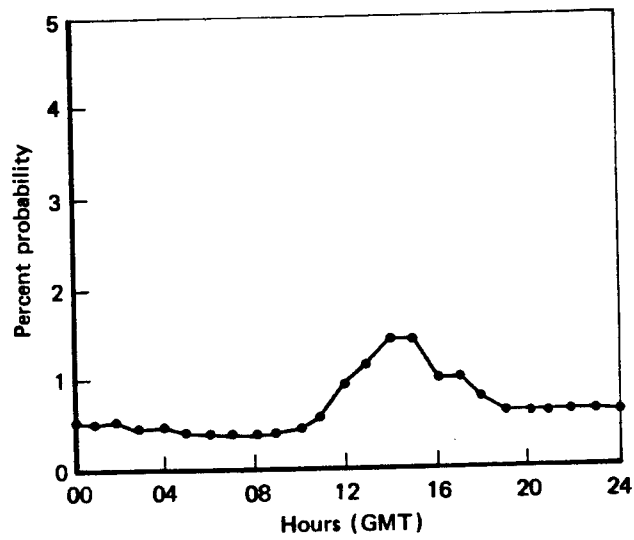


Fig. 37—Hourly Probability of Thunderstorms within 20 km, June-August in Northern Germany

11. SURFACE WINDS AT THREE GERMAN AIRFIELDS

The character of the surface winds in the foothills of western Germany is documented for Bitburg, Ramstein, and Spangdahlem. These wind distributions were compiled from hourly surface wind observations during the mid-season months of January, April, July, and October, taken throughout the day, under all weather conditions, from the various periods of record documented in the *Revised Uniform Summary of Surface Weather Observations*.

The "wind rose" format is used to present the wind speed and direction frequencies. The wind data for the three airfields, shown in Figs. 38, 39, and 40, also contain peak gust data for 1961 through 1970. The orientation of the major runway at each of these locations is shown to permit estimates of possible crosswind situations.

Table 9 indicates that, at Bitburg and Spangdahlem, wind speeds are less than 17 knots about 95 percent of the time and, at Ramstein, about 98 percent of the time. Gale force winds (≥ 28 knots) occur less than one-half of one percent of the time at all of these locations.

Table 9
PERCENT FREQUENCY OF SURFACE WIND SPEEDS AT THREE
AIR BASES IN GERMANY

Base	January	April	July	October
≥ 17 kn				
Bitburg	8.2	3.9	2.4	2.7
Ramstein	3.5	1.2	1.0	0.9
Spangdahlem	8.1	2.8	2.1	1.8
≥ 22 kn				
Bitburg	2.4	0.6	0.4	0.5
Ramstein	0.8	0.2	0.1	0.1
Spangdahlem	2.4	0.2	0.4	0.4
≥ 28 to 33 kn				
Bitburg	0.2	< 0.5	< 0.5	0.1
Ramstein	0.1	< 0.5	< 0.5	0
Spangdahlem	0.3	0	< 0.5	0.1
≥ 34 to 40 kn				
Bitburg	< 0.5	0	0	0
Ramstein	0	0	0	0
Spangdahlem	0.1	0	0	0

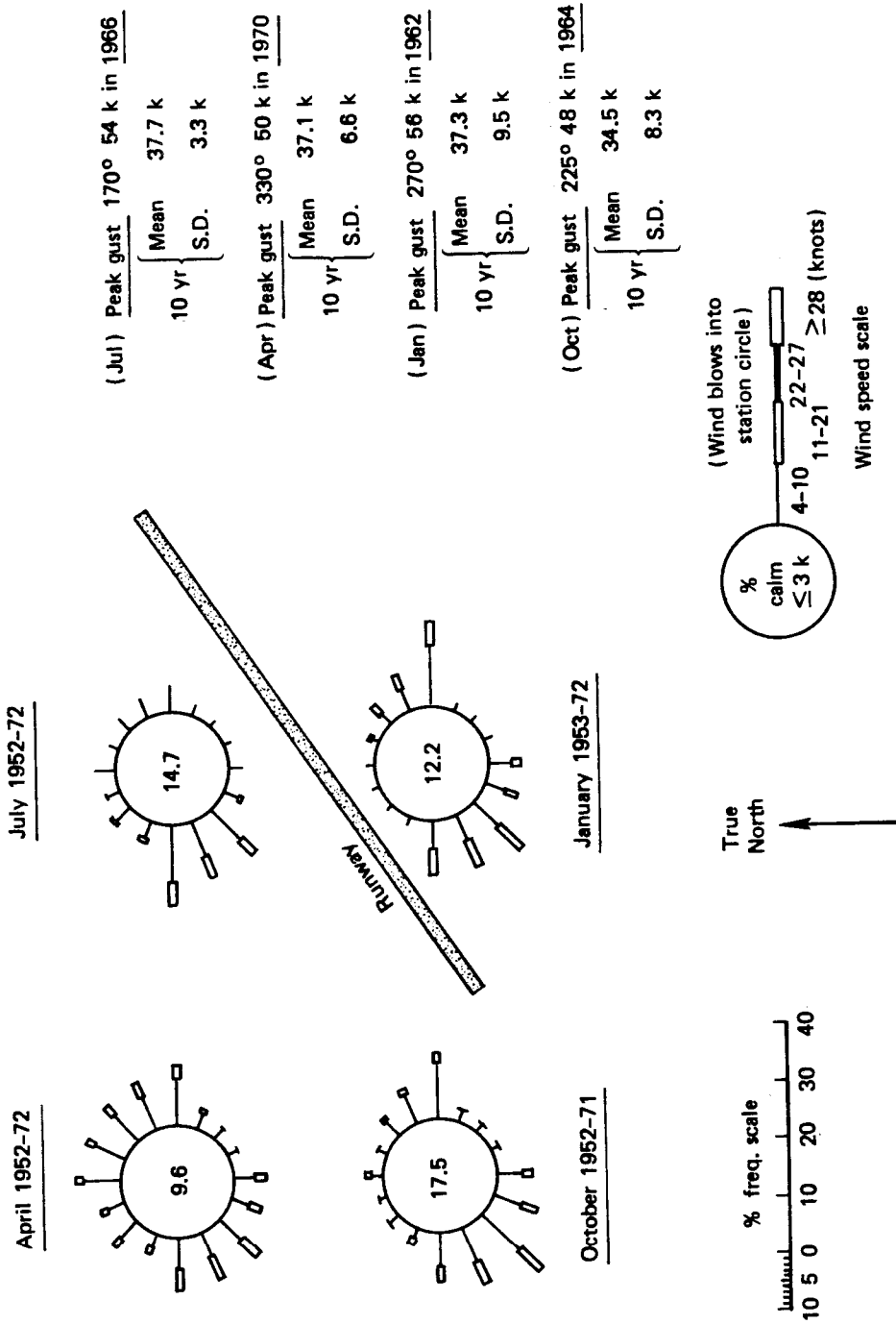


Fig. 38—Surface Wind Data for Bitburg

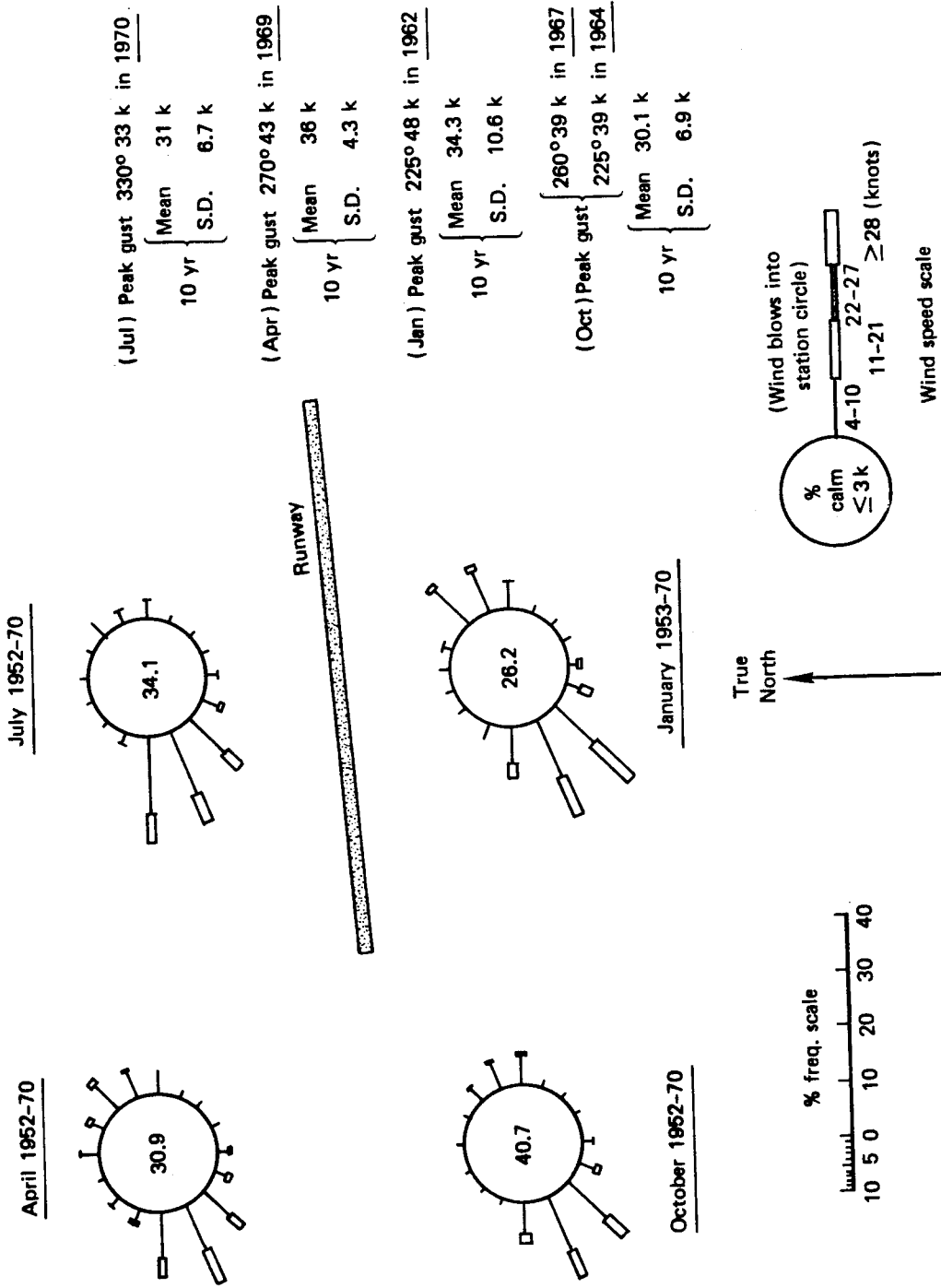


Fig. 39—Surface Wind Data for Ramstein

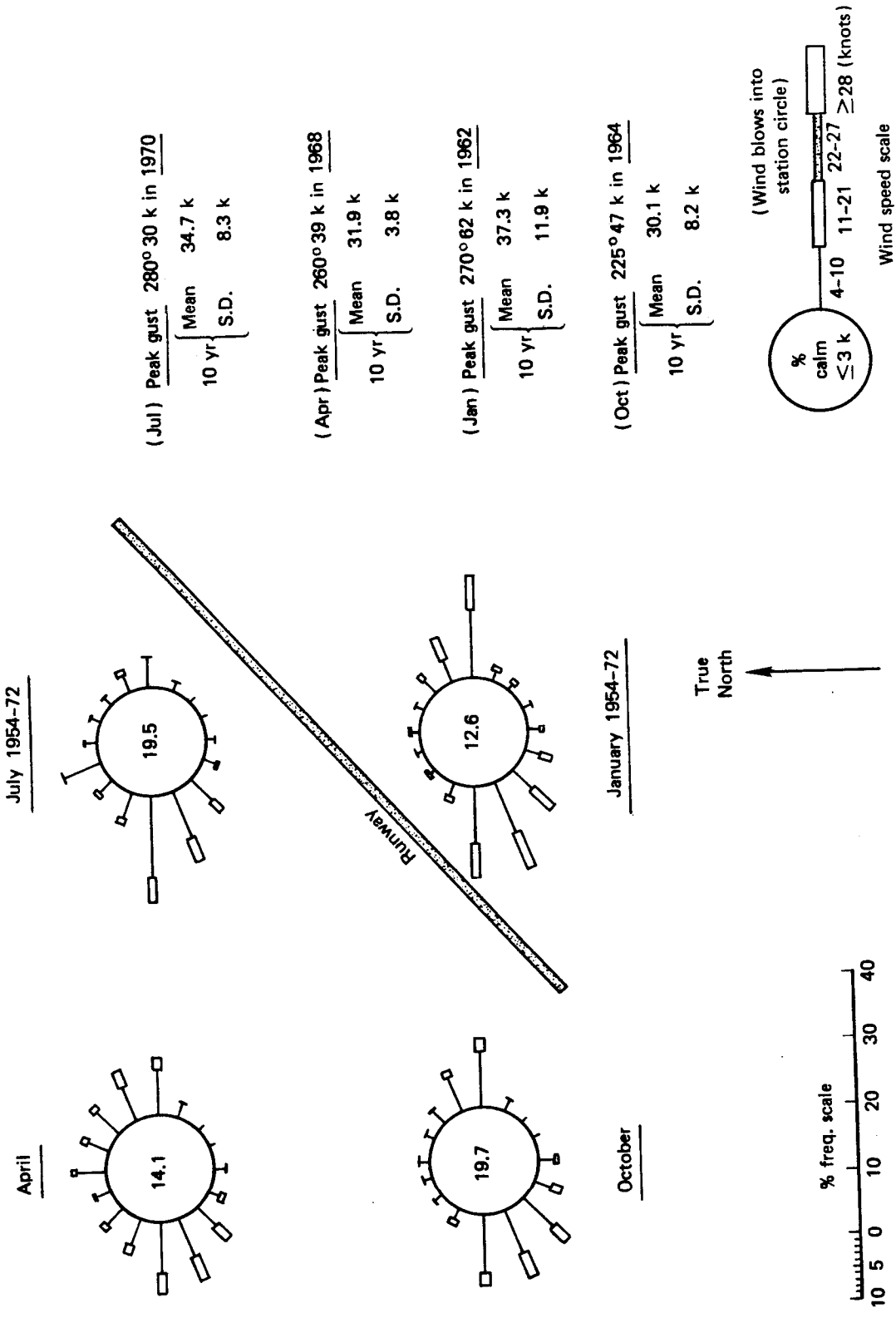


Fig. 40—Surface Wind Data for Spangdahlem

III. TARGET DETECTION AND ATMOSPHERIC TRANSMISSION MODEL CALCULATIONS

1. INTRODUCTION AND GUIDE

The standard weather observables—such as cloud heights and visibilities, for which many statistics are presented in Sec. II—simply do not suffice to evaluate the performance of visual and infrared sensor systems. The principal variables that are needed are the atmospheric transmission of visible contrast and the atmospheric transmission of 8-12 μm IR radiation.¹

The visible target-to-background *inherent* contrast, C_o , is defined by the expression

$$C_o \equiv \left| \frac{L_g - L_t}{L_g} \right| ,$$

where L_g and L_t are the luminances (brightnesses) of the background and target, as observed with no atmosphere between the observer and the target scene. Because of light scattering by atmospheric particles, contrast is always diminished in transit through the atmosphere from target scene to distant sensor. The contrast received at a remote sensor, C_R , is a function of the range, R (km), from target to sensor, the atmospheric visible extinction coefficient, β (neper km^{-1}), and the ratio of the luminance of the horizon sky to the luminance of the ground, L_s/L_g , which parameterizes the effect of light scattered into the field of view (and which is known in the trade as the "sky-ground ratio"):

$$C_R = \frac{C_o}{1 + \frac{L_s}{L_g} \left(e^{\beta R} - 1 \right)} .$$

The reciprocal of the denominator on the right-hand side of the above equation is the contrast transmission, T_C , which ranges in value from zero to one.

The received intensity of 8-12 μm radiation, I_R , after propagation through the atmosphere, is assumed to follow Bouguer's (Beer's) law:

$$I_R = I_o e^{-\gamma R},$$

where I_o is the intensity at the source and γ is the total atmospheric extinction coefficient in the 8-12 μm band. The 8-12 μm transmission $\tau = e^{-\gamma R}$. For estimation purposes, γ is broken down into its three major components,

$$\gamma = \gamma_m + \gamma_c + \gamma_a,$$

¹ The imaging IR sensors of Air Force tactical interest all operate in the 8-12 μm atmospheric "window."

γ_m being the H₂O molecular absorption coefficient, γ_c the H₂O continuum absorption coefficient, and γ_a the aerosol extinction (primarily scattering) coefficient.

To make the calculations presented in the following sections of this report, it was necessary to devise a method for estimating values for the above normally unobserved quantities (β , L_s/L_g , γ_m , γ_c , and γ_a) from the normally observed quantities that appear in weather records. The method was developed in Huschke (1976), which describes the deduction algorithms and rationale in detail; it also describes the visual and imaging infrared target detection models used to calculate target detection probabilities. The combination of algorithms for deducing the transmission variables and estimating detection probabilities is a "model," known as WETTA (weather effects on tactical target acquisition). All of the transmission and target detection calculations presented in Sec. III of this report were made using WETTA.

An important attribute of WETTA is its computational simplicity, permitting the statistical evaluation of visible and IR transmission from large samples of historical weather data at fairly low cost. Its accuracy should be adequate at least to produce realistic frequency distributions of the transmission variables. Data against which to judge models of this type either do not exist or are just beginning to become available in small quantities.

Data on visual contrast transmission along with the standard "predictor" weather variables do not exist. There are models of radiative transfer that are physically much more sophisticated than WETTA (e.g., Monte Carlo multiple Mie scattering models and parameterizations thereof) against which WETTA contrast transmission predictions can be compared. The USAF Environmental Technical Applications Center (ETAC) recently completed such a comparison (Breitling, 1979). The ETAC conclusion was that WETTA did a reasonably good job of reproducing the contrast transmission results of the "better" models under a variety of parameter variations. They decided, therefore, to use WETTA as the basis for an experimental, operational, contrast prediction methodology.

A good quality set of IR transmission and weather data is just beginning to emerge from Project OPAQUE (Optical Atmospheric Quantities in Europe) (Fenn, 1978). A sample of these data, for two winter months (December 1976 and February 1977) at the USAF-sponsored OPAQUE measurement site at Meppen, West Germany, were acquired, and the WETTA predictions of 8-12 μm extinction were compared with measurements. The WETTA algorithm requires temperature, dew-point, visibility (or visible extinction coefficient), and precipitation (intensity and whether occurring). All are in the OPAQUE data set, except that precipitation data are not yet available. (For preliminary comparisons, therefore, precipitation was assumed *not* to be occurring.) Comparisons were run against OPAQUE measurements in both the 8.0-12.1 μm band and 8.25-13.2 μm band. The results, in terms of measured and predicted cumulative frequency distributions of total extinction coefficient, are shown in Fig. 41; the ordinate is the relative frequency that the abscissa value of extinction is equaled or exceeded. (There are as-yet-unexplained differences in the frequency distributions of the measurements in the two slightly different wavelength bands.) Until precipitation data are obtained from the OPAQUE program, and until comparisons can be run for other seasons of the year and other locations, judgment of WETTA 8-12 μm extinction predictions must be tentative. However, these preliminary results indicate that statistical predictions using WETTA will approximate reality.

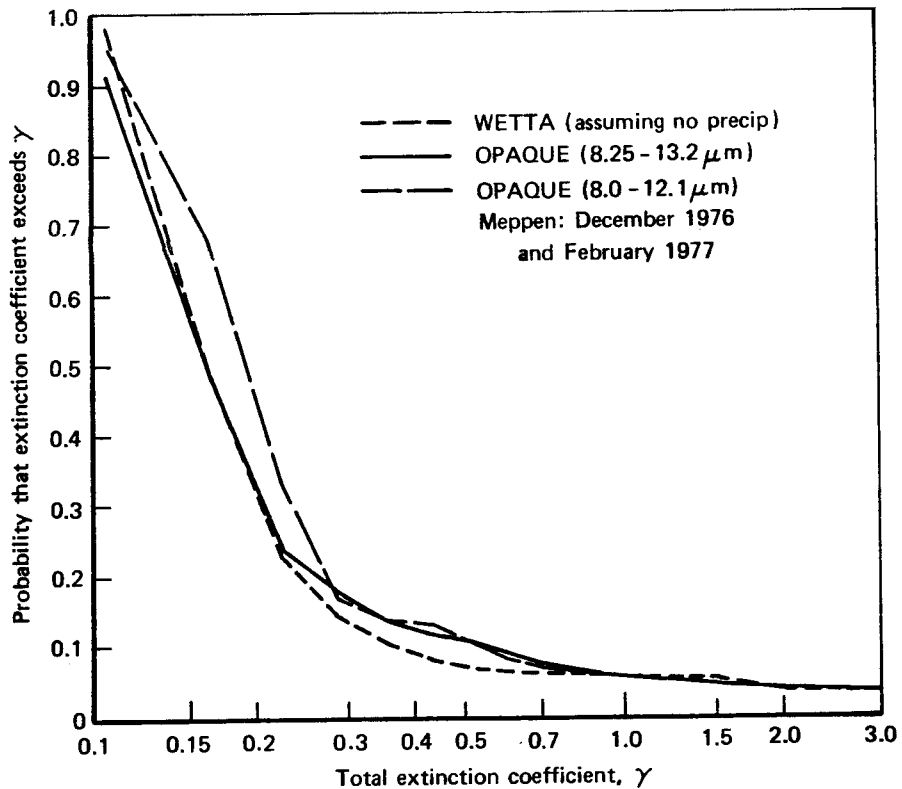


Fig. 41—Comparison of WETTA Predictions and OPAQUE Measurements of Total Atmospheric Extinction in the 8-13 μm Region

The remainder of Sec. III consists of four sets of WETTA model calculations on target detection and the atmospheric transmission of visible and 8-12 μm radiation in Germany; the contents are summarized in the following paragraphs.

- | Section | Title/Description |
|---------|--|
| 2. | <i>Visual Ground-to-Ground Target Detection Probabilities in December and July at Leinefelde.</i> Tables are presented of target detection probability as a function of the unaided eye and six-power binoculars, for three values of target-to-background contrast, and for tank and APC targets. The tables represent "typical" July and December months and are subdivided according to the best, middle, and worst one-third of target acquisition conditions in each month. |
| 3. | <i>Visual and IIR Target Detection Comparison in January and July at Four German Locations.</i> The detection performance of visual and IIR target seekers is simplified to a "pass or fail" dichotomy (based on $P_D < 0.5$ or $P_D \geq 0.5$). Joint pass or fail frequencies are presented for Hamburg, Han- |

nover, Kitzingen, and Grafenwöhr, for day, night, and all hours, based on six Januarys and six Julys.

4. *Diurnal and Seasonal Visible Contrast Transmission Probabilities at Low Altitudes at Kitzingen.* Curves of exceedance probabilities for visual contrast transmission as a function of range are presented for summer (May through August) and winter (November through February), and for all daylight hours, worst hours, and best hours in each season.
5. *Intra-Annual 8-12 μm Extinction Coefficient Probabilities for the Surface Layer at Four German Locations.* Cumulative probability distributions of 8-12 μm extinction coefficient are graphed for Hamburg, Hannover, Kitzingen, and Grafenwöhr, based on six years of weather data at each location. Included are the annual (all months combined) probability distributions and enveloping distributions representing best months and worst months for IR transmission.

2. VISUAL GROUND-TO-GROUND TARGET DETECTION PROBABILITIES IN DECEMBER AND JULY AT LEINEFELDE

Ground-to-ground target detection probability tables were calculated for the following situations:

- The probabilities represent winter and summer weather conditions in the Fulda Gap region (Leinefelde, East Germany), calculated for the best, middle, and worst thirds of target detection weather.
- Sensors are the unaided eye and the eye with 6-power (6X) binoculars.
- Targets are tanks and APCs, with inherent target-to-background contrasts representing the range from "dirty" to "clean" vehicles. Tanks are designated by a characteristic dimension (L_{\min}) of 3 m, and APCs by a dimension of 2 m. The inherent target-to-background contrasts (C_o) for both types of vehicles are 0.1 (very low contrast), 0.2 (low contrast), and 0.5 (medium-high contrast). C_o values commonly assumed for these targets range from 0.2 to 0.6.
- The degree of target discrimination required (modeled) is about midway between simple "blob" detection and target class recognition (e.g., tank versus truck). This is equivalent to requiring six resolution lines (three line pairs) to cross the minimum dimension of the target, per the well-known criteria of Johnson (1958) for target discrimination. Johnson's criterion for detection is one line pair and for recognition four line pairs, across the target.
- Probabilities are single-glimpse detection probabilities;² therefore, the probabilities of a glimpse falling on a target (in general, the probabilities related to searching for a target) are excluded from these tables.
- No problems due to battlefield dust and smoke are considered.

The visual contrast portion of the Rand WETTA model, along with an adaptation of the Bailey (1970) visual target acquisition model (both documented in Huschke, 1976), was used to make these calculations.

December (1959) and July (1953) were selected on the basis that their ceiling and visibility statistics closely matched the long-term (9 yr) statistics for those months in that area, as shown in Fig. 42. Note the wide variation in the interannual statistics. This indicates that no month in a single year can really be called "typical."

A total of 120 daytime weather observations at Leinefelde were used for each month (each table), and 120 detection probabilities calculated for each observation—2 target types \times 5 combinations of magnification and inherent contrast \times 12 ranges. For each month, the "weather" was ranked from best to worst using as the criterion the sum of the visual target detection probabilities for all ranges for the unaided eye, $C_o = 0.1$, tank target cases, as calculated for each weather observation. Average detection probabilities by range were then calculated for the upper, middle, and lower one-third of the observations for each target type, magnification,

² The probability that an observer will detect a target given that the target is within his foveal field of view during one glimpse of his multi-glimpse scan of the target scene.

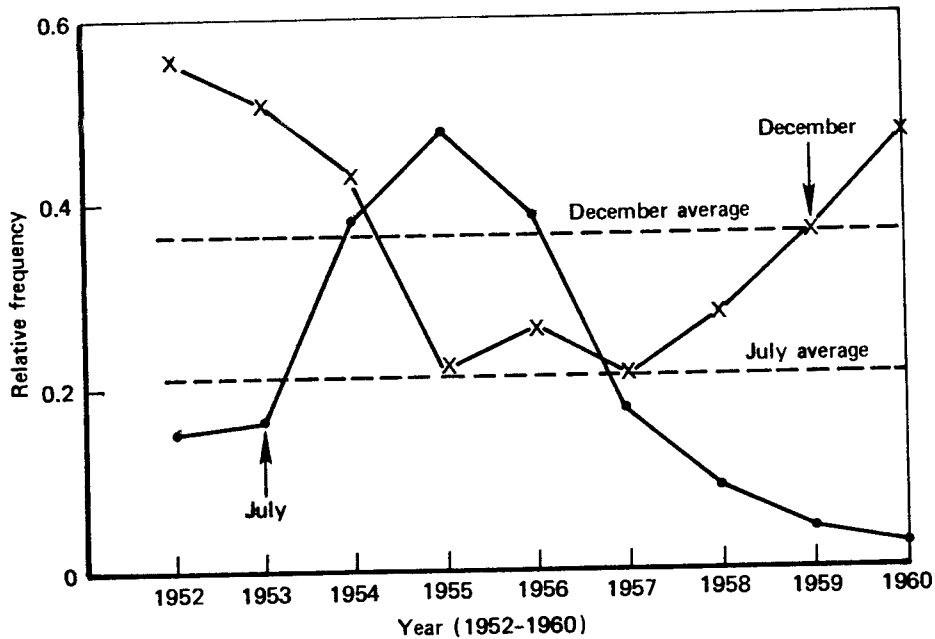


Fig. 42—Monthly Relative Frequencies of Ceiling < 500 ft or Visibility < 3 mi at Leinefelde; (arrows indicate months used in study)

and inherent contrast. These are the values tabulated in Table 10, December 1959, and Table 11, July 1953.

There are some interesting relationships among these sets of detection probabilities. (1) The strong influence of apparent target size is seen in a comparison of the probabilities for tank versus APC targets and for unaided eye versus 6X binocular sensors. (2) The effects of different target-to-background contrasts appear small at short ranges (< 1000 m) but become quite large when long detection ranges can be attained, as with binoculars. (3) The probabilities for the best third of July and December weather conditions are not very different, and those for the best and middle thirds of July weather are almost identical. The greatest differences between best and worst conditions are found in December. These relationships are illustrated in Fig. 43, which shows average target detection probabilities further averaged over all ranges from 500 m to 3000 m (the maximum range of the TOW missile); as indicated, these are for a very low contrast tank target sought with six-power binoculars.

Table 11

NEAR-GROUND VISUAL TARGET DETECTION PROBABILITIES AT LEINEFELDE,
JULY 1953

Range (m)	Best				Middle				Worst				
	One-Third of Weather				One-Third of Weather				One-Third of Weather				
	Unaided Eye		Binoculars		Unaided Eye		Binoculars		Unaided Eye		Binoculars		
	$C_o =$	$C_o =$	$C_o =$	$C_o =$	$C_o =$	$C_o =$	$C_o =$	$C_o =$	$C_o =$	$C_o =$	$C_o =$	$C_o =$	$C_o =$
	0.1	0.2	0.5	0.1	0.5	0.1	0.5	0.1	0.5	0.1	0.5	0.1	0.5
Tank Target ($L_{min} = 3 m$)													
250	0.99	0.99	0.99	1.0	1.0	0.99	0.99	1.0	1.0	0.98	0.99	0.99	1.0
500	0.81	0.81	0.81	1.0	1.0	0.81	0.81	1.0	1.0	0.66	0.81	0.81	0.94
1,000	0.34	0.42	0.42	1.0	1.0	0.32	0.42	1.0	1.0	0.15	0.32	0.41	0.69
1,500	0.09	0.22	0.22	0.95	0.99	0.08	0.21	0.94	0.99	0.03	0.11	0.18	0.45
2,000	0.02	0.09	0.12	0.76	0.95	0.02	0.09	0.71	0.95	0.01	0.03	0.09	0.26
2,500	0.01	0.03	0.07	0.52	0.89	0	0.03	0.09	0.12	0	0.01	0.04	0.14
3,000	0	0.01	0.04	0.32	0.81	0.01	0.01	0.45	0.89	0	0	0.01	0.08
3,500			0.02	0.19	0.73	0	0.02	0.26	0.81		0	0	0.04
4,000			0.01	0.11	0.66	0	0	0.14	0.73		0	0	0.04
5,000			0	0.04	0.52	0	0	0.08	0.66				0.01
7,000				0.01	0.23	0	0	0.03	0.52				0
10,000				0	0.03	0	0	0.01	0.19				0
				0	0.03	0	0	0	0.02				0
APC Target ($L_{min} = 2 m$)													
250	0.92	0.92	0.92	1.0	1.0	0.92	0.92	1.0	1.0	0.90	0.92	0.92	1.0
500	0.58	0.59	0.59	1.0	1.0	0.58	0.59	1.0	1.0	0.43	0.56	0.59	0.92
1,000	0.13	0.22	0.22	0.99	0.99	0.12	0.22	0.99	0.99	0.05	0.15	0.21	0.64
1,500	0.02	0.08	0.09	0.84	0.92	0.02	0.07	0.82	0.92	0.01	0.03	0.07	0.36
2,000	0	0.02	0.04	0.56	0.81	0	0.02	0.51	0.81	0	0.01	0.02	0.18
2,500		0	0.02	0.32	0.69	0	0	0.27	0.69		0	0	0.08
3,000			0	0.17	0.59	0	0	0.13	0.59		0	0	0.04
3,500				0.09	0.49	0	0	0.07	0.49				0.02
4,000				0.05	0.42	0	0	0.04	0.42				0.01
5,000				0.02	0.29	0	0	0.01	0.29				0
7,000				0	0.08	0	0	0	0.06				0
10,000				0	0.01	0	0	0	0				0

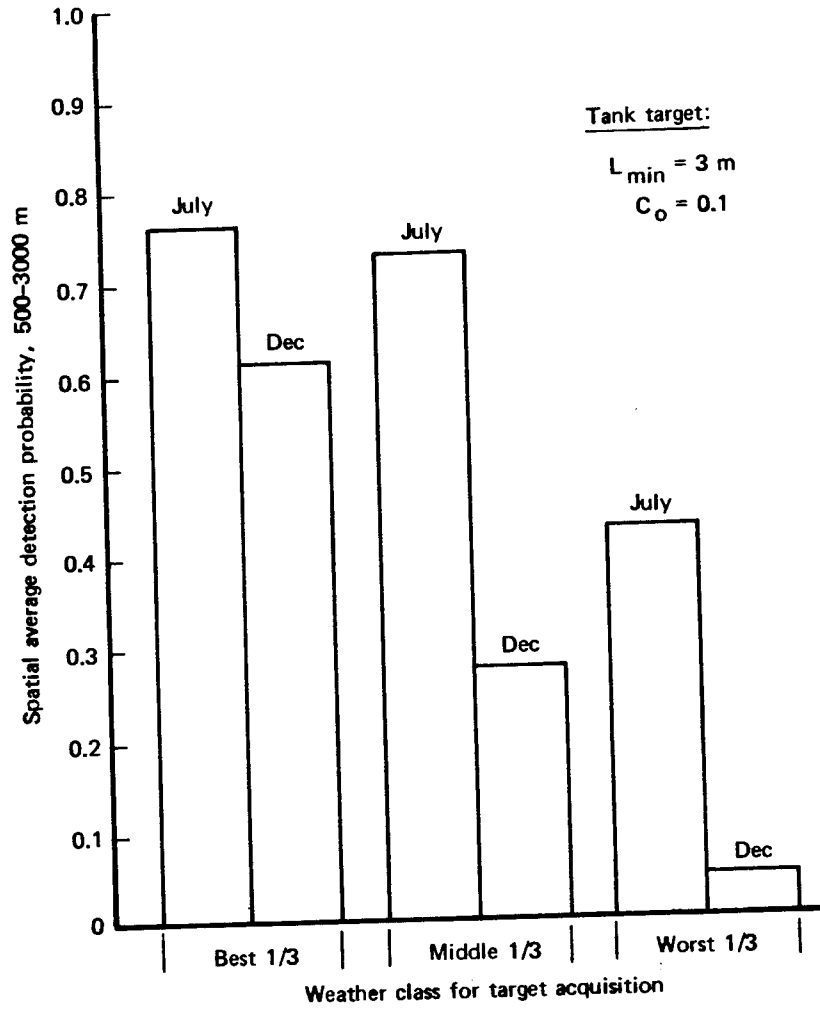


Fig. 43—Visual Target Detection Probabilities (6-power binoculars) Averaged over 500 m to 3000 m Range: Leinefelde, July 1953 and December 1959

3. VISUAL AND IIR TARGET DETECTION COMPARISON IN JANUARY AND JULY AT FOUR GERMAN LOCATIONS

The WETTA atmospheric transmission model (Huschke, 1976) and the Bailey-Mundie target acquisition equations (Bailey, 1970) were used to make a joint comparison of the air-to-ground target detection capabilities of visual and IIR target detection systems in the German environment. The parameters of the problem were highly simplified, as follows:

- *Conversion range*—7500 ft was assumed as the minimum conversion range (the range by which the target must be detected to permit time for a successful attack).
- *Dive angle*—10°.
- *Minimum cloud (ceiling) height*—1800 ft, based on a shallow pop-up maneuver and terrain considerations.
- *Target*—The target is an armored vehicle having a characteristic dimension of 3 m, an inherent visual target-to-background contrast of 0.4, and an inherent IR target-to-background temperature difference of 2°C.³ The background visible reflectance (albedo) is 0.1.
- *Visual seeker*—The human eye, as modeled by Bailey, has a threshold contrast of 0.087 for the given target size and minimum conversion range.
- *IIR seeker*—Sensitivity, resolution, etc. correspond to those of a low-quality forward-looking infrared (FLIR) device: noise equivalent temperature difference (NETD) is 0.1°C; resolution is 0.25 mrad.
- *Recognition*—Only simple detection of an object that might be a target is required: one resolution line pair across the minimum target dimension, per Johnson's criteria (Johnson, 1958).
- *Search*—The seekers, eye and IIR, were assumed to have been cued to look in the direction of the target—i.e., no search was required.

The analysis was further simplified into a pass/fail dichotomy. If the target detection probability ≥ 0.5 , the system "passed," otherwise it "failed." Also, if the cloud ceiling was below the 1800 ft minimum, it was assumed that there was no cloud-free line of sight, and both systems "failed." However, if scattered clouds occurred below 1800 ft, a cloud-free line of sight was assumed.

All weather observations (at 1-hr or 3-hr intervals) for six Januarys and six Julys, from 1965 through 1970, were used for calculating target detection probabilities at Hamburg, Hannover, Kitzingen, and Grafenwöhr in West Germany. Results were tabulated as joint probabilities of "pass" or "fail" for the visual and IIR seekers, separating night and day results (visual seekers always fail at night; that is, no artificial illumination was considered).

Tables 12 (January) and 13 (July) summarize the findings: (1) The most striking result of these calculations is that the visual seeker never "passes" when the IIR seeker "fails." Given the simplifications of the analysis and the usual modeling uncertainties, these results nevertheless speak well for the potential of IIR systems.

³ These assumed visual and IR target contrast values are "typical" values averaged over the projected area of the target. In reality, they vary widely from target to target, background to background, and from spot to spot on a given target. A sense of the sensitivity of visual P_D to target-to-background contrast can be gotten from Tables 10 and 11.

(2) Both types of seekers, but especially the eye, "pass" much more frequently in July than in January. (3) In January, the IIR seeker appears to perform better at night than during the day. (4) Differences among the four locations are not large, except that Grafenwöhr represents the least favorable weather for both seeker types and Kitzingen the best weather for visual systems.

All of the entries in Tables 12 and 13 are joint probabilities to be interpreted according to the following guide:

Joint Probability							
All Hours				Day			Night
Visual		IIR		Visual		IIR	IIR Total
Pass	Fail	Total		Pass	Fail	Total	
Location							
IIR Pass	a	b	a + b	a	b	a + b	a + b
IIR Fail	c	d	c + d	c	d	c + d	c + d
Visual Total	a + c	b + d	1.00	a + c	b + d	1.00	1.00

- where a = joint probability that both seekers pass,
- b = joint probability that visual fails but IIR passes,
- c = joint probability that visual passes but IIR fails,
- d = joint probability that both seekers fail,
- a + b = probability that IIR passes,
- c + d = probability that IIR fails,
- a + c = probability that visual passes,
- b + d = probability that visual fails, and
- a + b + c + d = 1.00.

Table 12

COMPARISON OF VISUAL AND IIR TARGET SEEKER UTILITY IN GERMANY:
JANUARY 1965-1970; DETECTION AT 7500 FEET

	Joint Probability						
	All Hours			Day			Night
	Visual		IIR Total	Visual		IIR Total	IIR Total ^a
	Pass	Fail		Pass	Fail		
All Locations							
IIR Pass	0.04	0.55	0.59	0.10	0.37	0.47	0.67
IIR Fail	0.00	0.41	0.41	0.00	0.53	0.53	0.33
Visual Total	0.04	0.96	1.00	0.10	0.90	1.00	1.00
Hamburg							
IIR Pass	0.03	0.52	0.55	0.09	0.33	0.42	0.63
IIR Fail	0.00	0.45	0.45	0.00	0.58	0.58	0.37
Visual Total	0.03	0.97	1.00	0.09	0.91	1.00	1.00
Hannover							
IIR Pass	0.04	0.59	0.63	0.11	0.39	0.50	0.71
IIR Fail	0.00	0.37	0.37	0.00	0.50	0.50	0.29
Visual Total	0.04	0.96	1.00	0.11	0.89	1.00	1.00
Kitzingen							
IIR Pass	0.06	0.60	0.66	0.17	0.42	0.59	0.71
IIR Fail	0.00	0.34	0.34	0.00	0.41	0.41	0.29
Visual Total	0.06	0.94	1.00	0.17	0.83	1.00	1.00
Grafenwöhr							
IIR Pass	0.02	0.51	0.53	0.05	0.34	0.39	0.61
IIR Fail	0.00	0.47	0.47	0.00	0.61	0.61	0.39
Visual Total	0.02	0.98	1.00	0.05	0.95	1.00	1.00

^aVisual always fails at night.

Table 13
 COMPARISON OF VISUAL AND IIR TARGET SEEKER UTILITY IN GERMANY:
 JULY 1965-1970; DETECTION AT 7500 FEET

	Joint Probability						
	All Hours			Day			Night
	Visual		IIR Total	Visual		IIR Total	IIR Total ^a
	Pass	Fail		Pass	Fail		
All Locations							
IIR Pass	0.36	0.51	0.87	0.58	0.27	0.85	0.88
IIR Fail	<u>0.00</u>	<u>0.13</u>	<u>0.13</u>	<u>0.00</u>	<u>0.15</u>	<u>0.15</u>	<u>0.12</u>
Visual Total	0.36	0.64	1.00	0.58	0.42	1.00	1.00
Hamburg							
IIR Pass	0.37	0.48	0.85	0.59	0.23	0.82	0.91
IIR Fail	<u>0.00</u>	<u>0.15</u>	<u>0.15</u>	<u>0.00</u>	<u>0.18</u>	<u>0.18</u>	<u>0.09</u>
Visual Total	0.37	0.63	1.00	0.59	0.41	1.00	1.00
Hannover							
IIR Pass	0.35	0.51	0.86	0.55	0.28	0.83	0.90
IIR Fail	<u>0.00</u>	<u>0.14</u>	<u>0.14</u>	<u>0.00</u>	<u>0.17</u>	<u>0.17</u>	<u>0.10</u>
Visual Total	0.35	0.65	1.00	0.55	0.45	1.00	1.00
Kitzingen							
IIR Pass	0.41	0.50	0.91	0.68	0.23	0.91	0.90
IIR Fail	<u>0.00</u>	<u>0.09</u>	<u>0.09</u>	<u>0.00</u>	<u>0.09</u>	<u>0.09</u>	<u>0.10</u>
Visual Total	0.41	0.59	1.00	0.68	0.32	1.00	1.00
Grafenwöhr							
IIR Pass	0.30	0.54	0.84	0.51	0.34	0.85	0.82
IIR Fail	<u>0.00</u>	<u>0.16</u>	<u>0.16</u>	<u>0.00</u>	<u>0.15</u>	<u>0.15</u>	<u>0.18</u>
Visual Total	0.30	0.70	1.00	0.51	0.49	1.00	1.00

^aVisual always fails at night.

4. DIURNAL AND SEASONAL VISIBLE CONTRAST TRANSMISSION PROBABILITIES AT LOW ALTITUDES AT KITZINGEN

Occurrence frequencies of visual contrast transmission as a function of range were calculated for a representative location in south-central West Germany. Kitzingen, about 70 mi east-southeast of Frankfurt, experiences monthly median visible contrast transmission that is very close to the values experienced elsewhere in Germany—slightly better, in fact, than the other three locations compared in Fig. 44.

The WETTA model algorithms (Huschke, 1976) were used to calculate the visible contrast transmission for every daytime weather observation at Kitzingen over the 6-yr period from 1965 through 1970. It was calculated for eight slant ranges from 1000 to 14,400 ft. With the assumption of low-level attack (altitude ≤ 600 ft), it was also assumed that the line of sight from aircraft to target lay entirely within the lowest "mixed layer" of the atmosphere in which, it is further assumed, the visibility is constant with height and equal to the reported surface visibility. We crudely accounted for the effect of clouds in the line of sight (not very frequent at such low altitudes) by setting the transmission equal to zero if a cloud ceiling was (a) less than 300 ft for ranges out to 7000 ft and (b) less than 600 ft for ranges greater than 7000 ft.

To obtain information on seasonal and sunrise-to-sunset variations, the data were stratified by season (summer, spring/fall, and winter) and by morning and afternoon solar elevation angle. Table 14 is one example of the complete set of 24 cumulative frequency tabulations (8 ranges \times 3 seasons) of visible contrast transmission as a function of solar elevation angle.

The tabulated data were then transformed into curves of cumulative contrast transmission probability vs. range for two seasons—summer and winter—and three periods during the day—all daylight hours, worst hours (early daylight), and best hours (early afternoon). Those curves are given in Figs. 45(a) through 45(f).

By relating visual target detection probability (P_D) to visible contrast transmission, using a target detection model, we can use the curves of Fig. 45 to determine how frequently a given P_D can be expected to be exceeded—a useful temporal measure of effectiveness often referred to as "utility." Appendix A presents a set of relationships that can be used for this purpose: graphical relationships between range, target size, inherent target-to-background contrast, contrast transmission, and detection probability.

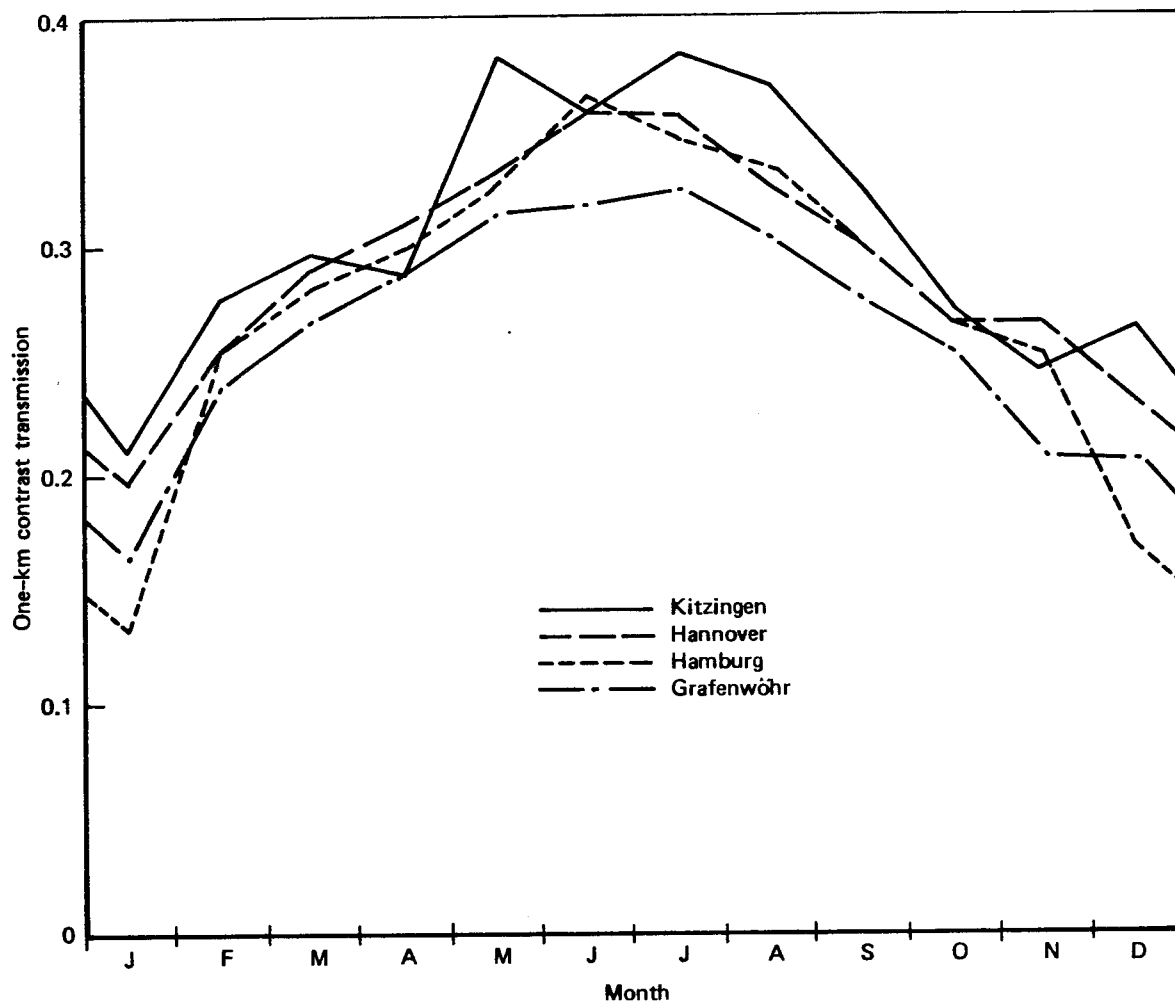


Fig. 44—Monthly Median Values of 1-km Visible Contrast Transmission in Germany

Table 14

CUMULATIVE PROBABILITY OF VISIBLE CONTRAST TRANSMISSION AS A
FUNCTION OF MORNING AND AFTERNOON SOLAR ELEVATION ANGLE AT
KITZINGEN; SUMMER (MAY-AUGUST); 5000 FT RANGE

Solar Elevation Angle, ϵ (deg)	Contrast Transmission, $T_C \geq$														
	0	0.05	0.10	0.15	0.20	0.25	0.30	0.35	0.40	0.45	0.50	0.55	0.60	0.65	0.70
<u>Morning</u>															
$1 \leq \epsilon < 10$	0.98 ^a	0.87	0.74	0.54	0.34	0.17	0.08	0.05	0	0	0	0	0	0	0
$10 \leq \epsilon < 20$	0.98	0.89	0.77	0.67	0.45	0.25	0.15	0.07	0	0	0	0	0	0	0
$20 \leq \epsilon < 30$	0.99	0.90	0.79	0.70	0.52	0.30	0.19	0.12	0	0	0	0	0	0	0
$30 \leq \epsilon < 40$	1.0	0.95	0.84	0.78	0.65	0.43	0.28	0.22	0.08	0.05	0	0	0	0	0
$40 < \epsilon < 50$	1.0	0.98	0.93	0.85	0.72	0.53	0.43	0.32	0.11	0.07	0	0	0	0	0
$50 \leq \epsilon$	1.0	0.99	0.97	0.94	0.83	0.67	0.57	0.49	0.22	0.19	0.13	0.10	0.02	0	0
<u>Afternoon</u>															
$50 \leq \epsilon$	1.0	0.99	0.98	0.97	0.89	0.76	0.67	0.58	0.21	0.20	0.14	0.12	0.02	0	0
$40 \leq \epsilon < 50$	1.0	1.0	0.99	0.99	0.92	0.78	0.69	0.57	0.19	0.15	0	0	0	0	0
$30 \leq \epsilon < 40$	1.0	0.99	0.98	0.98	0.93	0.82	0.71	0.59	0.22	0.13	0	0	0	0	0
$20 \leq \epsilon < 30$	1.0	0.99	0.99	0.97	0.90	0.81	0.67	0.47	0	0	0	0	0	0	0
$10 \leq \epsilon < 20$	1.0	1.0	0.98	0.97	0.88	0.74	0.51	0.29	0	0	0	0	0	0	0
$1 \leq \epsilon < 10$	1.0	1.0	0.97	0.92	0.73	0.47	0.34	0.25	0	0	0	0	0	0	0
All $\epsilon > 1$	1.0	0.96	0.92	0.86	0.74	0.57	0.45	0.35	0.10	0.08	0.03	0.03	0.01	0	0

^aProbability that contrast transmission \geq column value and ceiling \geq 300 ft.

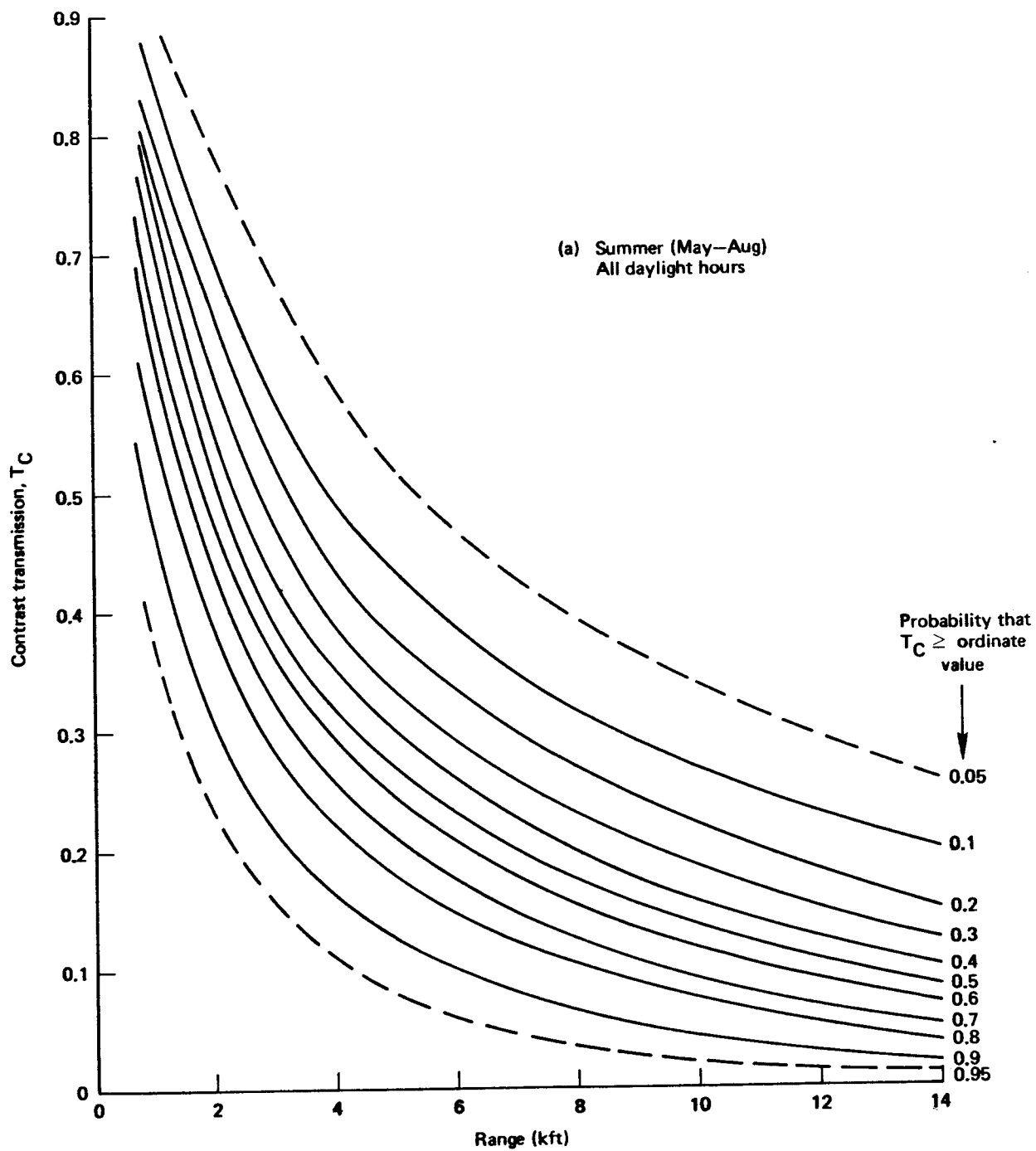


Fig. 45—Curves of Cumulative Contrast Transmission Probability vs. Range at Kitzingen

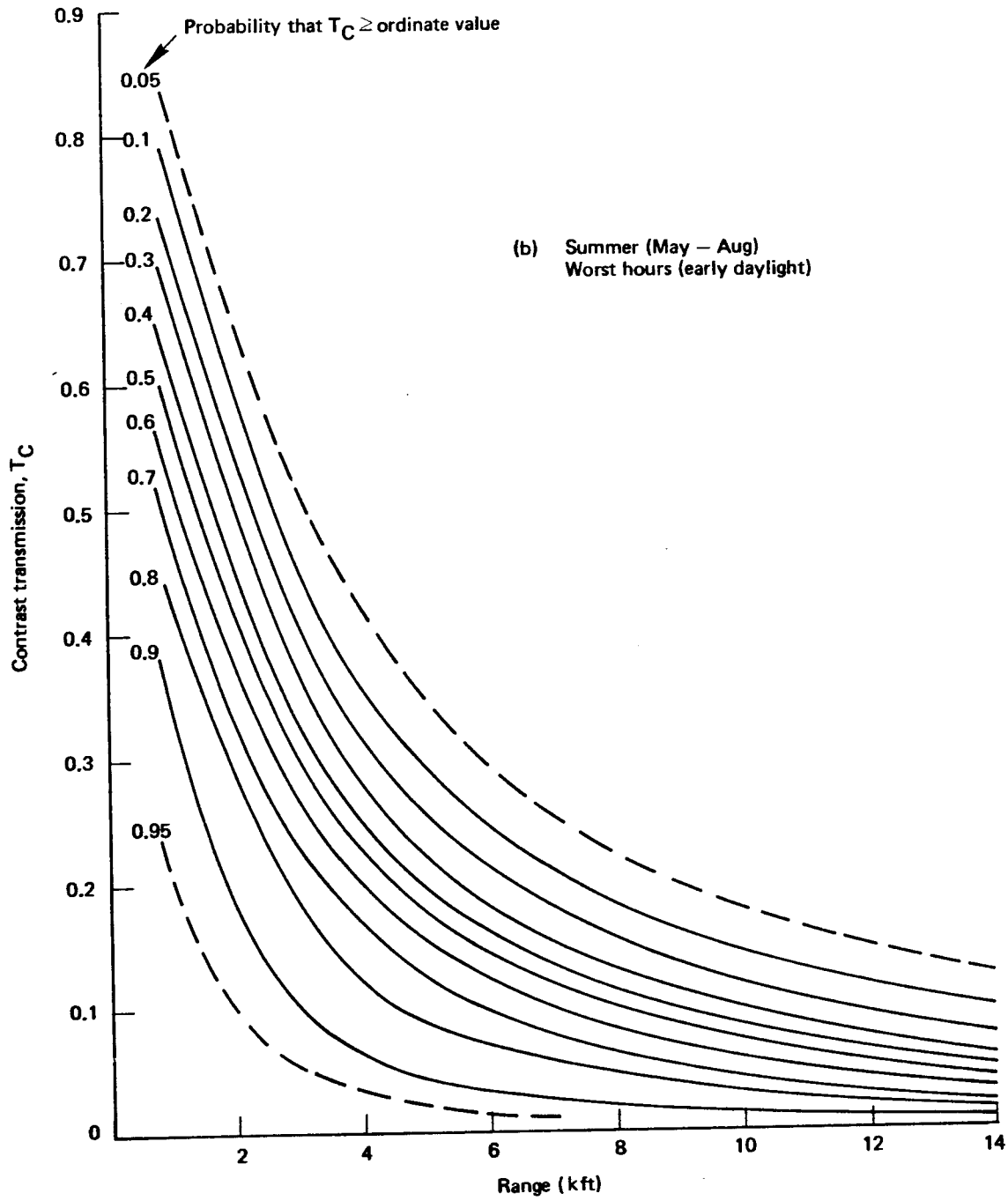


Fig. 45—Curves of Cumulative Contrast Transmission Probability vs. Range at Kitzingen

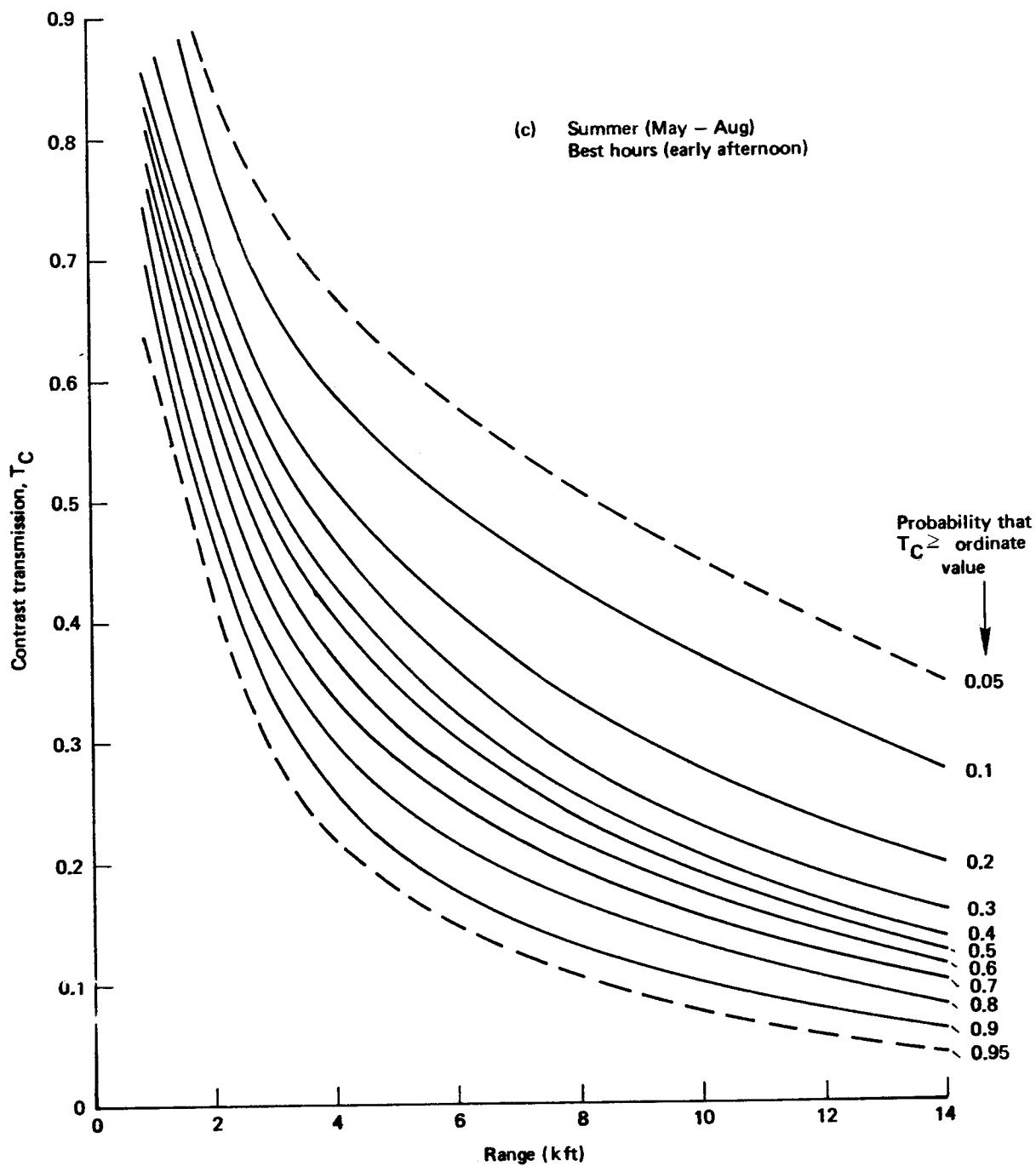


Fig. 45—Curves of Cumulative Contrast Transmission Probability vs. Range at Kitzingen

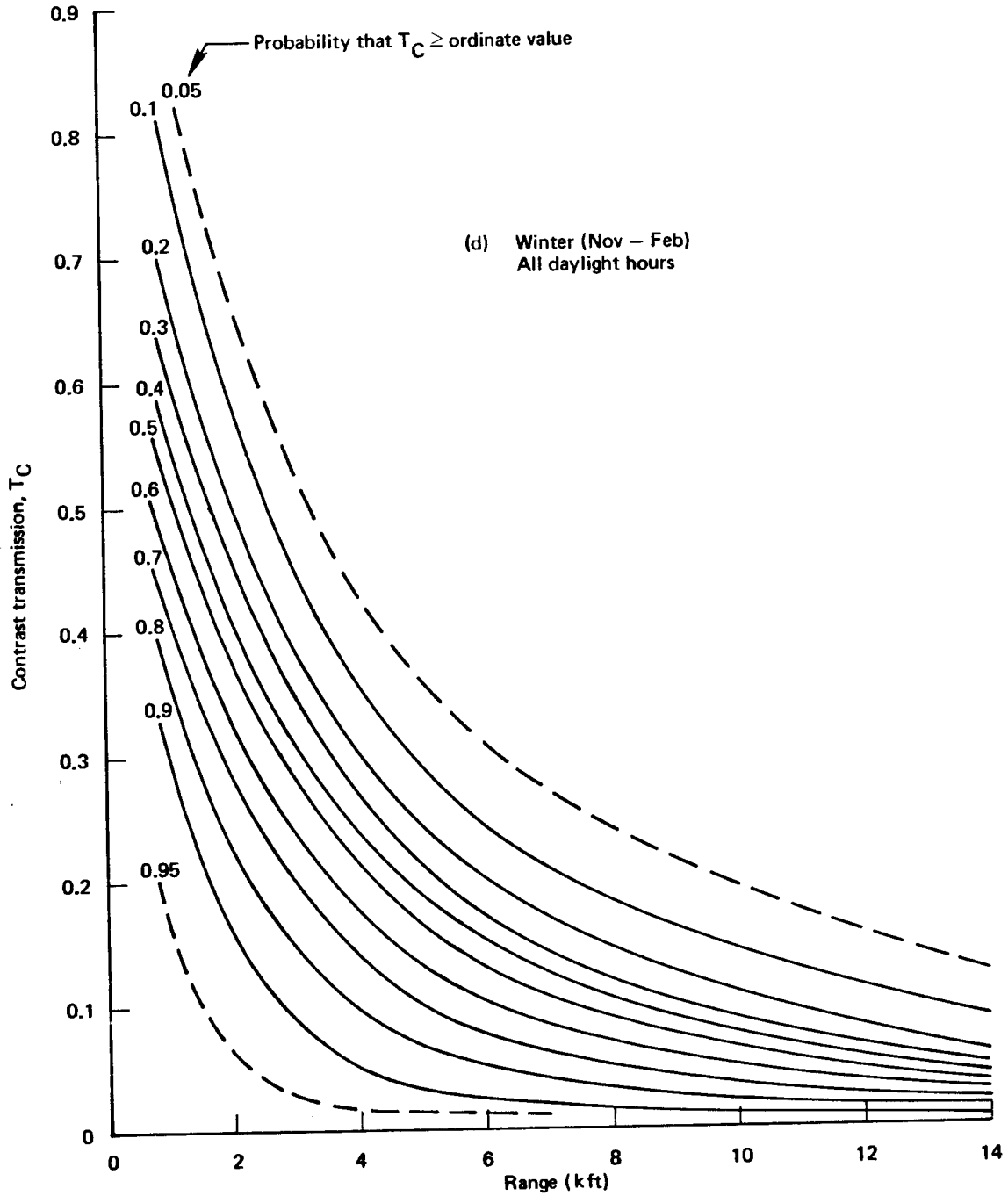


Fig. 45—Curves of Cumulative Contrast Transmission Probability vs. Range at Kitzingen

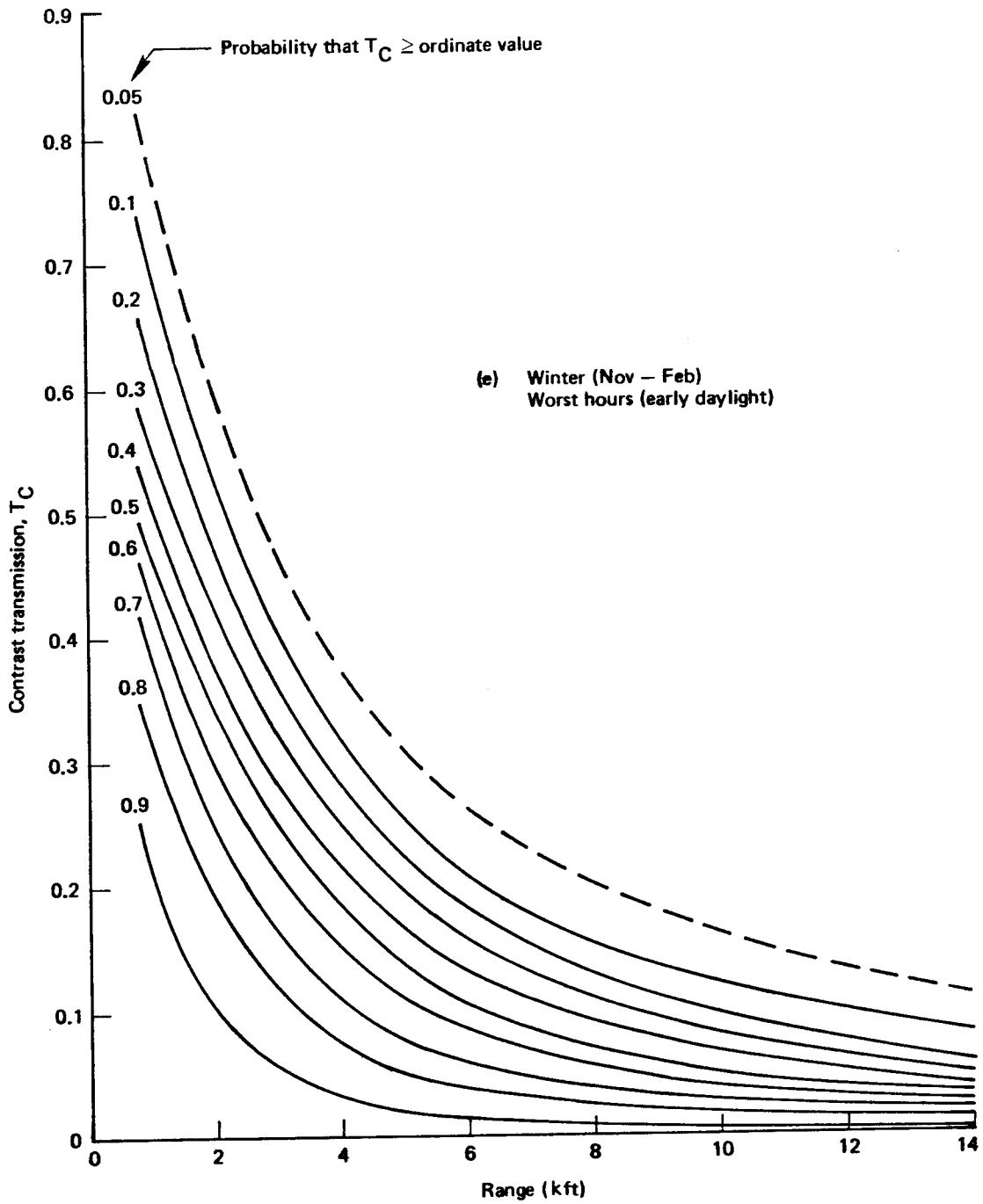


Fig. 45—Curves of Cumulative Contrast Transmission Probability vs. Range at Kitzingen

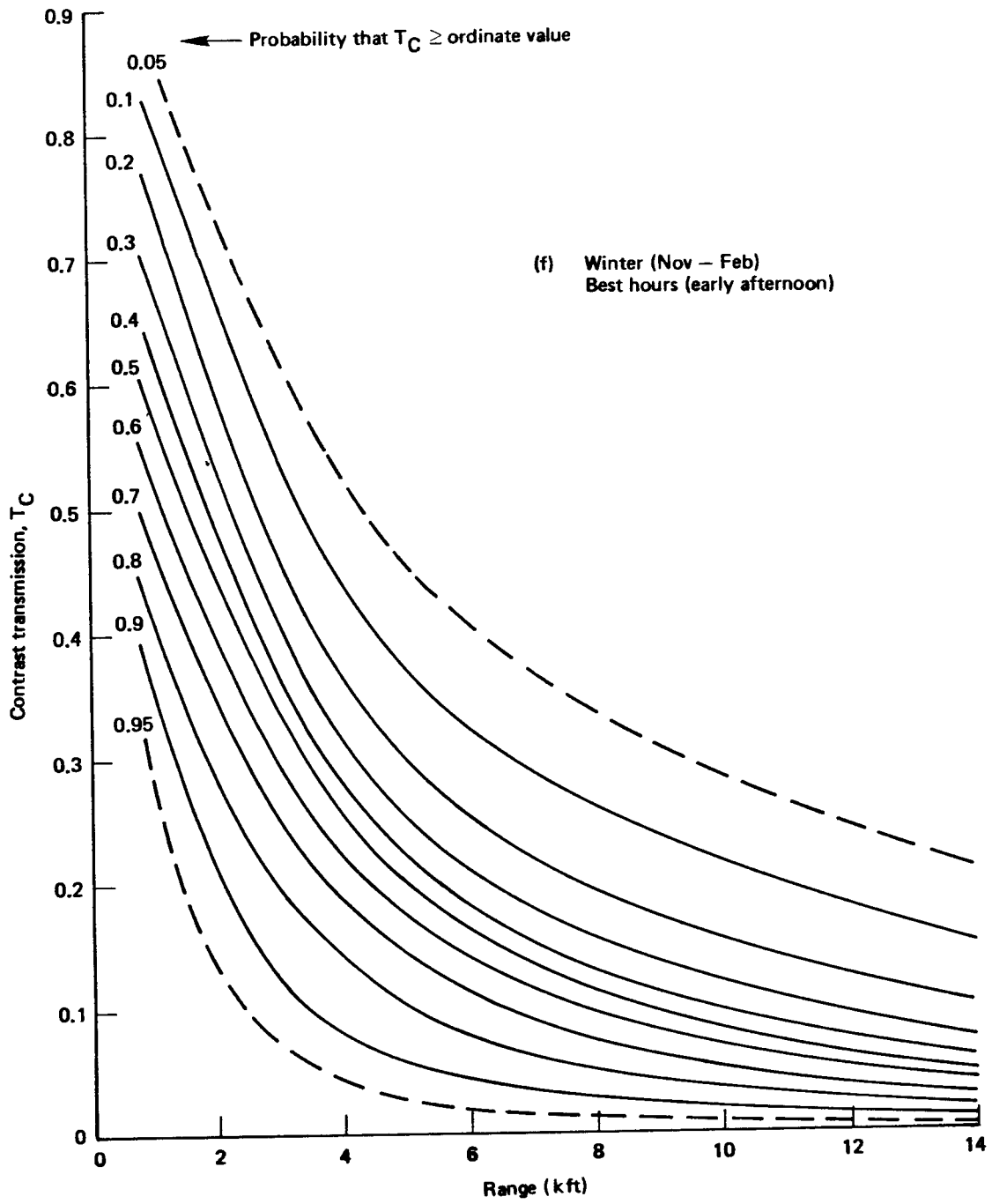


Fig. 45—Curves of Cumulative Contrast Transmission Probability vs. Range at Kitzingen

5. INTRA-ANNUAL 8-12 μm EXTINCTION COEFFICIENT PROBABILITIES FOR THE SURFACE LAYER AT FOUR GERMAN LOCATIONS

Many applications of imaging IR systems will take place on the ground or in the lower atmosphere beneath clouds. The WETTA model calculations summarized here are based on surface weather data, assumed to be representative of the cloud-free (but not necessarily fog-free) portions of the lowest several hundred feet of the atmosphere.

Four locations, spanning Germany from the North Sea to the Czechoslovakian border, were selected for these calculations: Hamburg, Hannover, Kitzingen, and Grafenwöhr. Six years of hourly or three-hourly weather data were used, from 1965 through 1970.

Probabilities, based on individual calendar months and all months combined, were tabulated for 14 class intervals of total 8-12 μm extinction coefficient at each location. These probability distributions are depicted in Figs. 46-49 as cumulative distributions. The annual (all months combined) cumulative probability distributions are shown as solid curves. The extremes among the monthly distributions are shown as dashed curves consisting of segments of individual monthly cumulative probability distributions. The upper dashed curve shows the highest probability that any given value of extinction coefficient will be equaled or exceeded in any month of the year. Each segment of the upper curve, then, represents the "worst month" for a range of extinction values. For example, in Fig. 46, Hamburg, segment A indicates that July and August have the highest probability of extinction coefficient values in excess of about 0.12 to 0.22 km^{-1} ; segment B shows that January has the highest probability of excessive extinction coefficients in the range from 0.22 to 4.0 km^{-1} . Similarly, the lower dashed curve segments represent the "best months": segment E of Fig. 46 shows that March has the lowest probability of excessive extinction coefficients in the range from ≈ 0.125 to 0.2 km^{-1} , etc.

Similarities among the four figures are much more apparent than differences. Grafenwöhr (Fig. 49) seems clearly to have the least favorable weather for 8-12 μm transmission among the four locations. The spread between "best months" and "worst months" is greatest at Hamburg (Fig. 46), especially for extinction coefficients in the range from ≈ 0.2 to 1.5 km^{-1} .

A consistent pattern of monthly extremes runs through these graphs, suggesting a physical explanation of the annual variability of IR extinction. Figure 50 is a schematic illustration of the monthly extreme-value curves of the cumulative distributions. Curve segments 1 and 2, which encompass the extinction coefficient ranges of highest frequency, reflect primarily the annual maxima and minima of absolute humidity. Segments 3 and 4 represent months of most frequently poor and least frequently poor visibility, respectively. Segment 5, when it exists, represents months having high joint frequencies of high relative humidity and very low visibility (heavy fog). Altogether, these WETTA calculations strongly reflect the independent distributions of two atmospheric quantities: absolute humidity, which dominates at low extinction, and aerosol content, which dominates at high extinction.

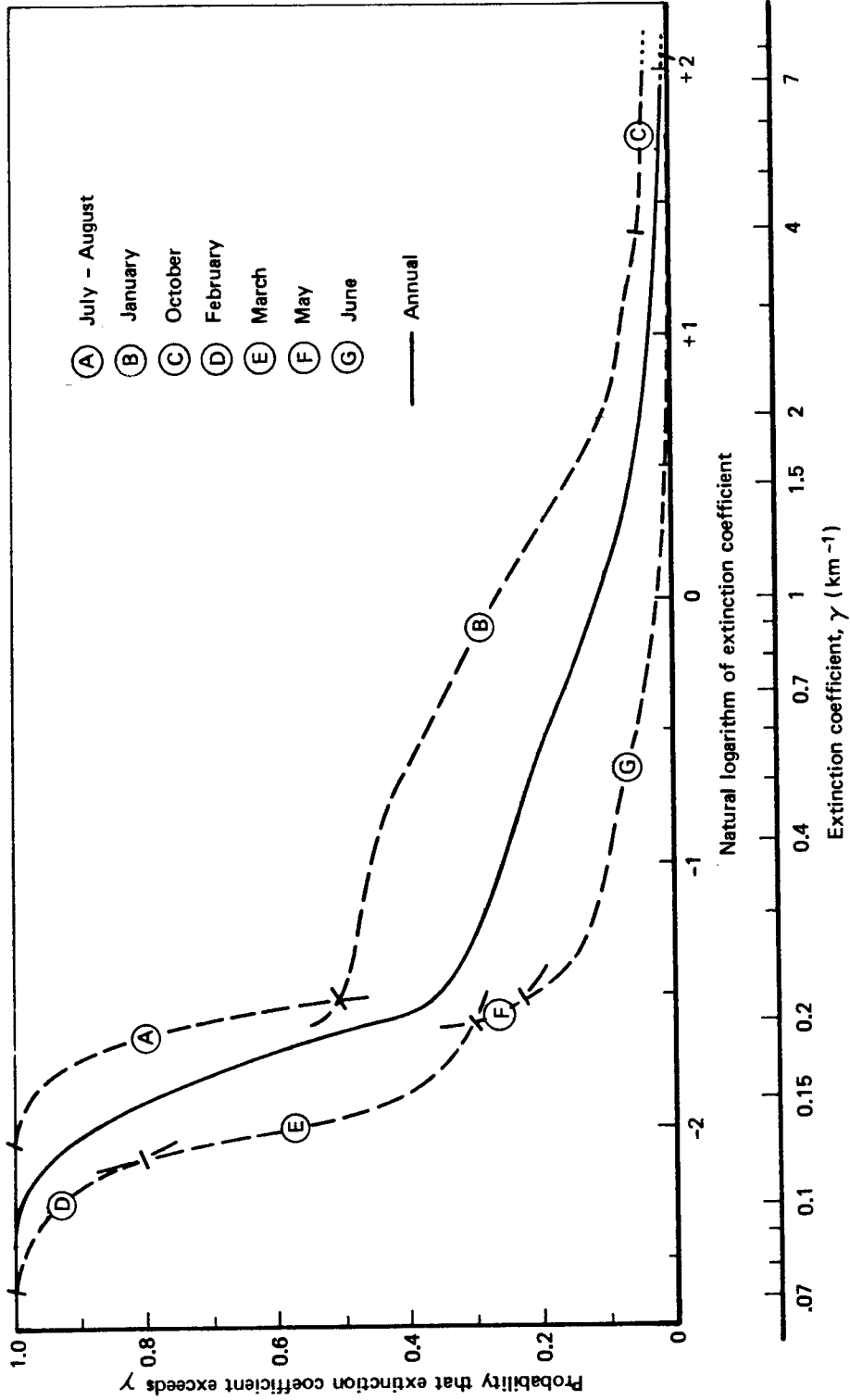


Fig. 46—WETTA Calculations of 8-12 μm Extinction Coefficient Probabilities at Hamburg

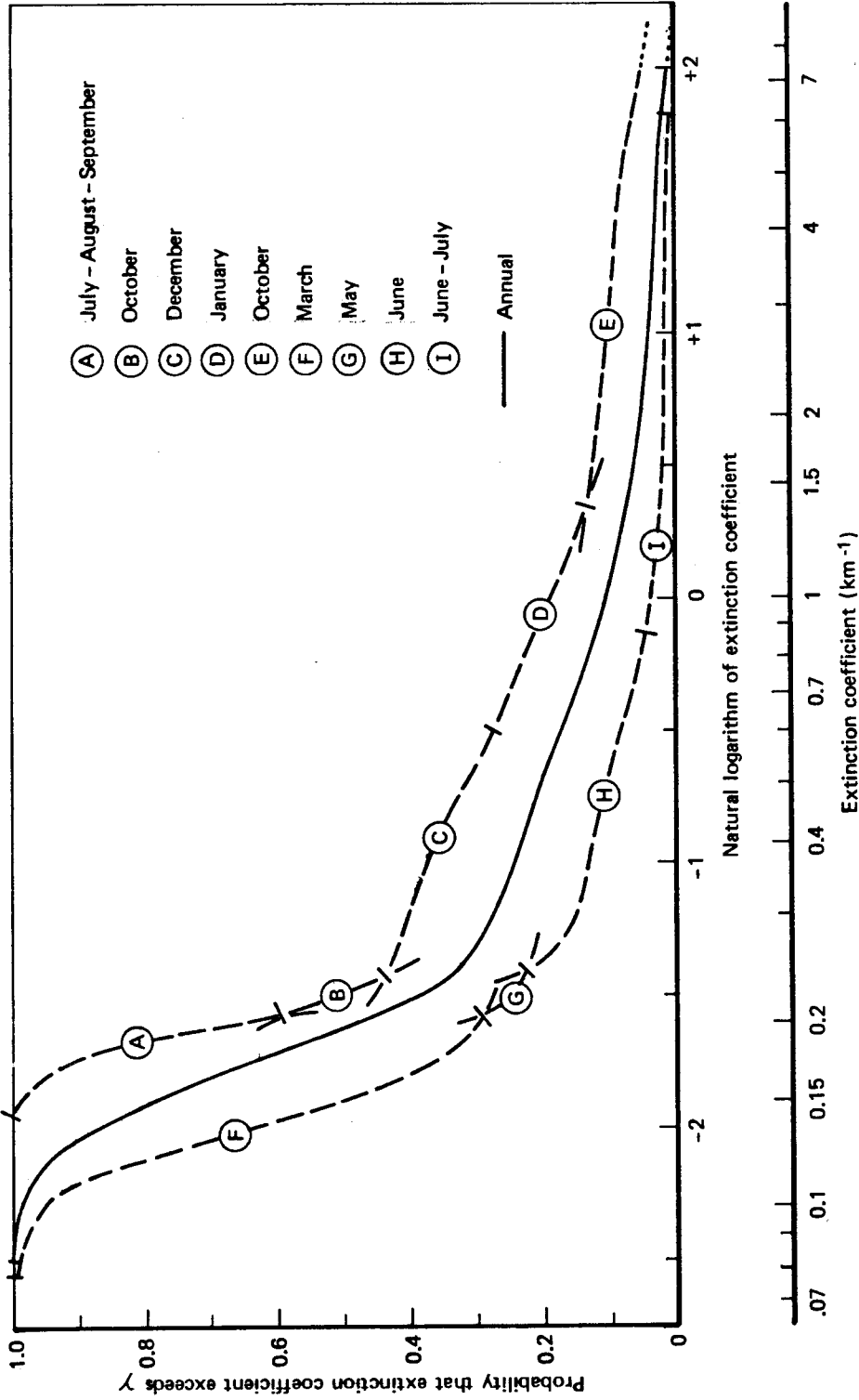


Fig. 47—WETTA Calculations of 8-12 μm Extinction Coefficient Probabilities at Hannover

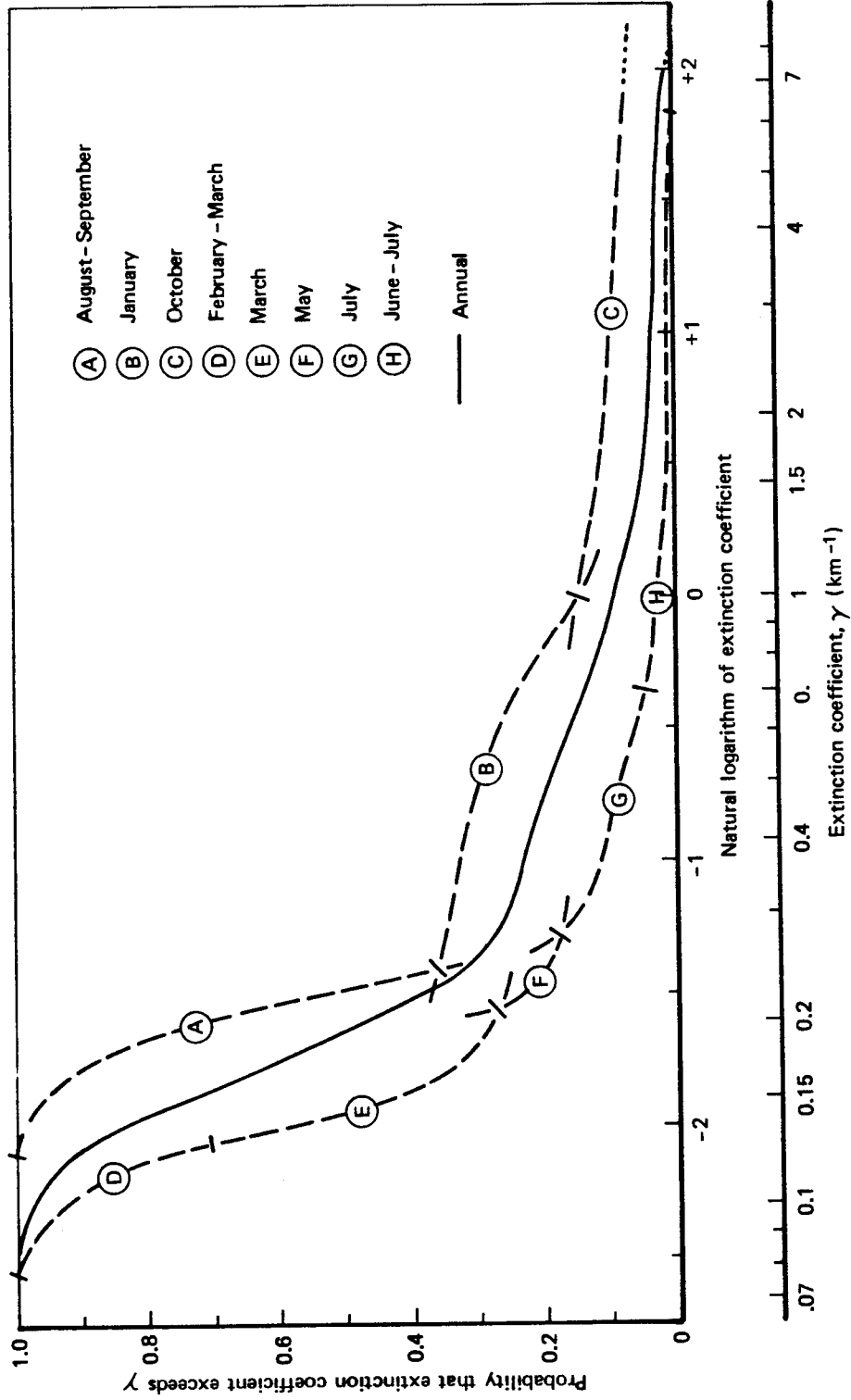


Fig. 48—WETTA Calculations of 8-12 μ m Extinction Coefficient Probabilities at Kitzingen

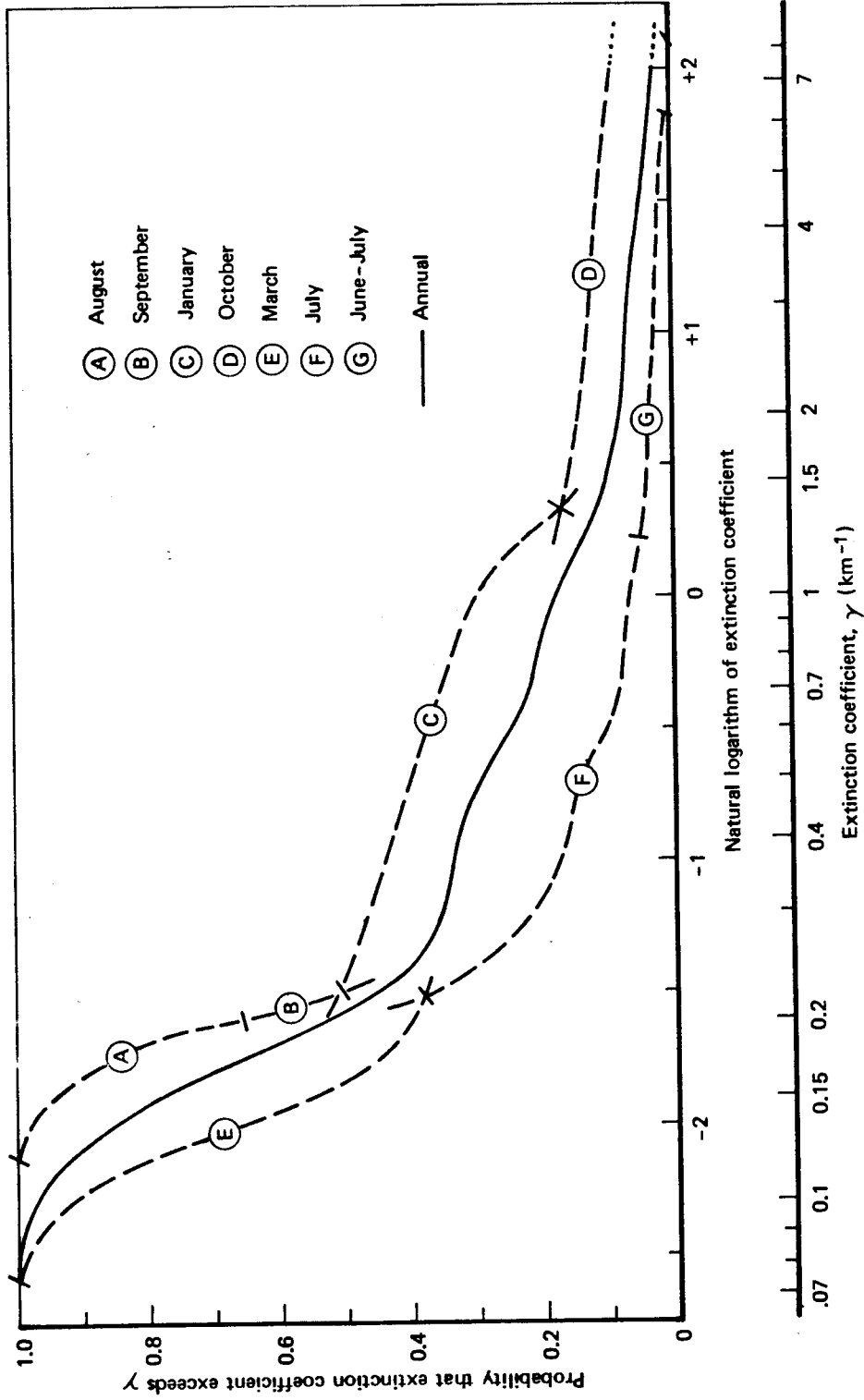


Fig. 49—WETA Calculations of 8-12 μm Extinction Coefficient Probabilities at Grafenwöhr

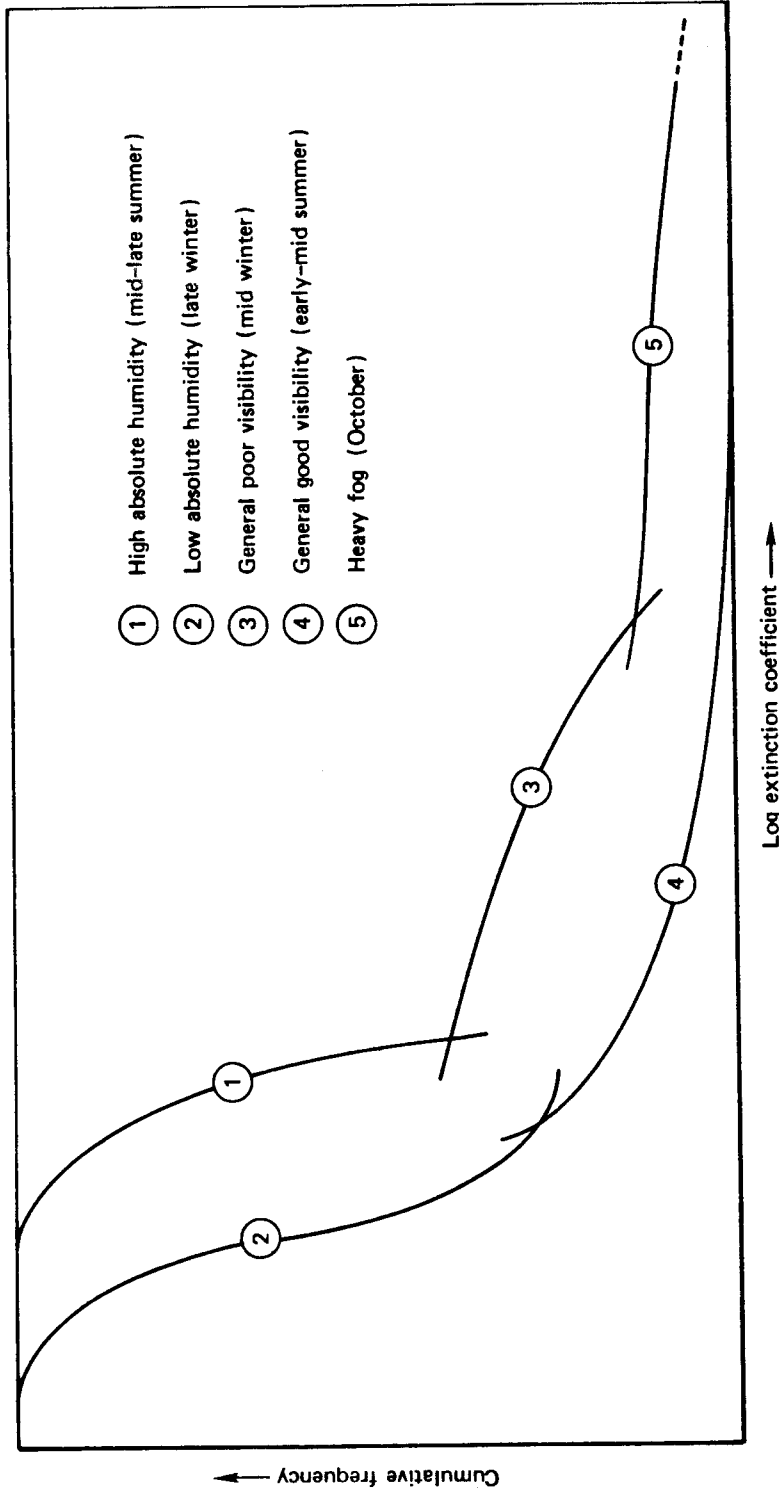


Fig. 50—Schematic of Monthly Extreme Cumulative Frequency Distributions of 8-12 μ m Extinction Coefficient

Appendix A

VISUAL TARGET DETECTION PROBABILITIES AS A FUNCTION OF RANGE, SIZE, CONTRAST, AND TRANSMISSION

The model used in the following calculations is Bailey's visual target acquisition model (Bailey, 1970).

The question addressed is that of simple detection ("I see something that might be an enemy tank"). Assuming that a potential target is in the observer's foveal field of view, the detection probability, P_D , is given by the following approximation:

$$P_D \approx \frac{1}{2} \pm \frac{1}{2} \sqrt{1 - \exp \left[- 4.2 \left(\frac{C_R}{C_T} - 1 \right)^2 \right]}, \quad (\text{A.1})$$

where " \pm " is plus for $C_R/C_T \geq 1$, minus otherwise; C_R is the target-to-background contrast as it appears to the observer, and C_T the threshold contrast of the observer-target-range combination. Equation (A.1) is the Bailey "contrast term," which expresses the probability of detecting an object, given its apparent size and apparent contrast. It is consistent with the Johnson (1958) requirement for detection that one "resolution element" (line pair) be contained within the apparent dimension of the target.

The apparent target-to-background contrast, C_R , is less than the inherent (zero range) contrast, C_o , by the factor T_C , herein called the "contrast transmission." (See discussion of these variables on p. 86.) Hence,

$$C_R = C_o T_C. \quad (\text{A.2})$$

The threshold contrast, C_T , is a function of the angular subtense, α , of the target at the eye.

$$\alpha = 3.44 ML/R, \quad (\text{A.3})$$

where α is expressed in minutes of arc, M is magnification power ($M = 1$ for the unaided eye), L is a characteristic dimension of the target (meters or feet), and R is range (kilometers or kilofeet). For the case of simple detection, the eye effectively integrates the target area for targets whose length:width ratio $< 7:1$ (Overington, 1976); this includes the vast majority of tactical targets. For detection of this class of targets, L is approximated by the diameter of a circle whose area is the same as that of the target. C_T is defined as the received contrast required to yield a 50 percent detection probability, which Bailey has approximated by the hyperbola,

$$\log_{10} C_T \approx \left(\log_{10} \alpha + 0.5 \right)^{-1} - 2. \quad (\text{A.4})$$

Combining Eqs. (A.3) and (A.4),

$$C_T = 10 \left\{ \left[\log_{10} (3.44 \text{ ML/R}) + 0.5 \right]^{-1} \right\}^{-2} \quad (\text{A.5})$$

Equations (A.2) and (A.5) may then be substituted into Eq. (A.1), and the resulting equation solved for appropriate and relevant values of C_o , T_C , and the apparent target size parameter, ML/R . This was done for $C_o = 0.2, 0.4, 0.6, \text{ and } 0.8$; $0.02 \leq T_C \leq 1.0$; and $0.25 \leq \text{ML/R} \leq 25$.

In Fig. A.1 (a through d), curves of P_D are plotted as a function of R/ML and T_C , one graph for each of the four values of C_o .¹ In themselves, these graphs have a variety of uses—for example, to examine the sensitivity of P_D to variations among the five variables.

In conjunction with the curves of Fig. 45 (Sec. III.4) or similar frequency distributions of T_C in the real world, these graphs can be used to estimate the “utility” of visual systems. For example, assume that a target for which $C_o = 0.4$ and $L = 8$ ft (roughly like the end view of a tank) “needs” to be detected by the unaided eye ($M = 1$) with high confidence, say $P_D \geq 0.8$, at a range $R = 4000$ ft (4 kft). We wish to know how often this requirement can be satisfied in Germany. Entering Fig. A.1(b) at the ordinate value $\text{R/ML} = 0.5$, we find that, for $P_D \geq 0.8$, a T_C value of 0.19 or greater is required. The curves of Fig. 45 then tell us the probability that $T_C \geq 0.19$ in daytime at 4000 ft range at the “typical” West German location of Kitzingen. Put differently, the Fig. 45 curves tell us what fraction of time the above job can be done. Answers to this example are as follows:

Season and Time of Day	Fraction of Time Job Can Be Done
Summer	
All daylight hours	0.86
Early daylight	0.65
Early afternoon	> 0.95
Winter	
All daylight hours	0.58
Early daylight	0.50
Early afternoon	0.70

¹ The inverse form, R/ML , of the size parameter was selected for use in the original study (Huschke, 1978), and is retained here.

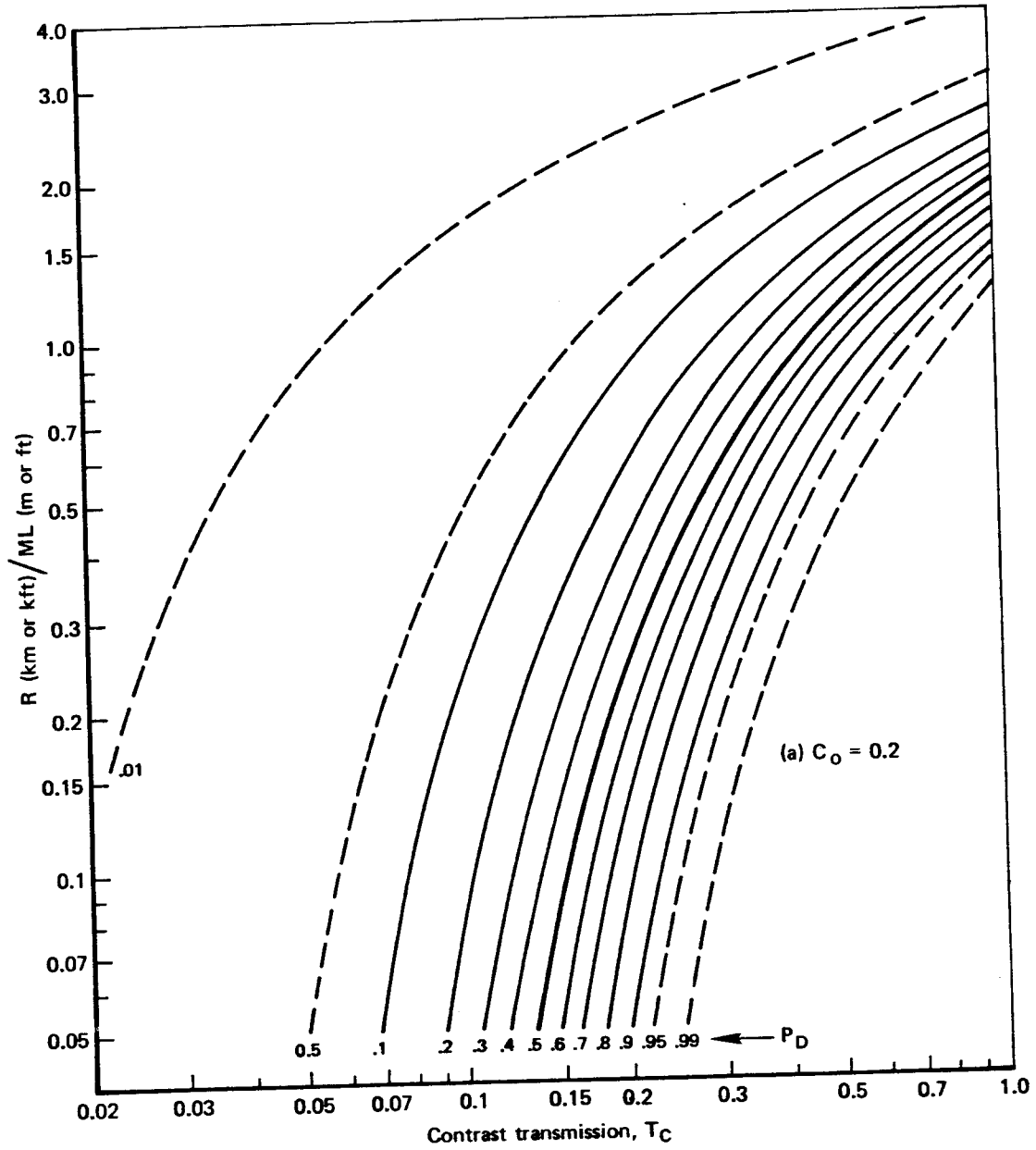


Fig. A.1—Probability of Detecting a Target as a Function of Range, R (km or kft), Magnification Power, M , Characteristic Target Size, L (m or ft), Atmospheric Contrast Transmission, T_C , and Inherent Target-to-Background Contrast, C_0

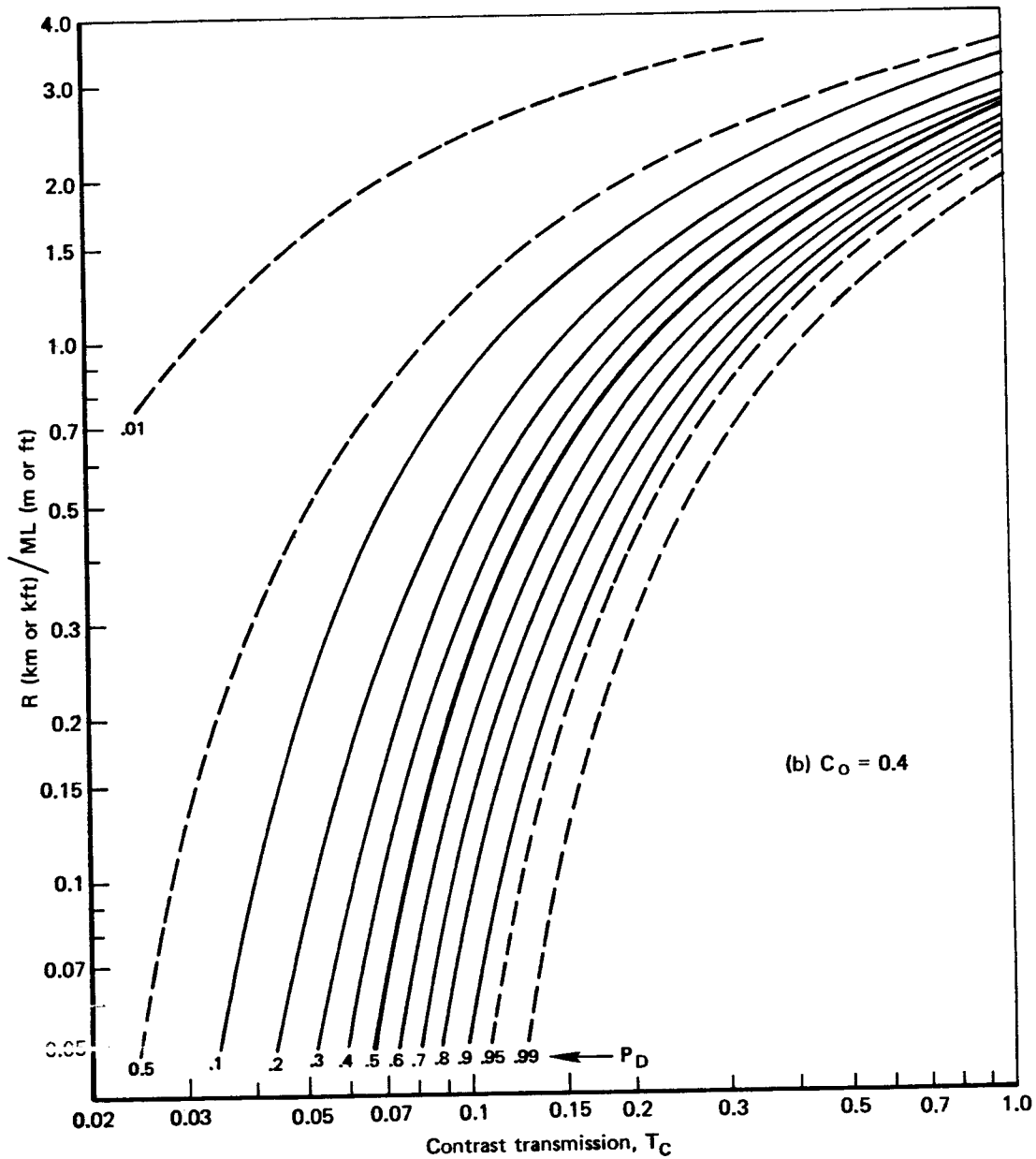


Fig. A.1—Probability of Detecting a Target as a Function of Range, R (km or kft), Magnification Power, M , Characteristic Target Size, L (m or ft), Atmospheric Contrast Transmission, T_C , and Inherent Target-to-Background Contrast, C_0

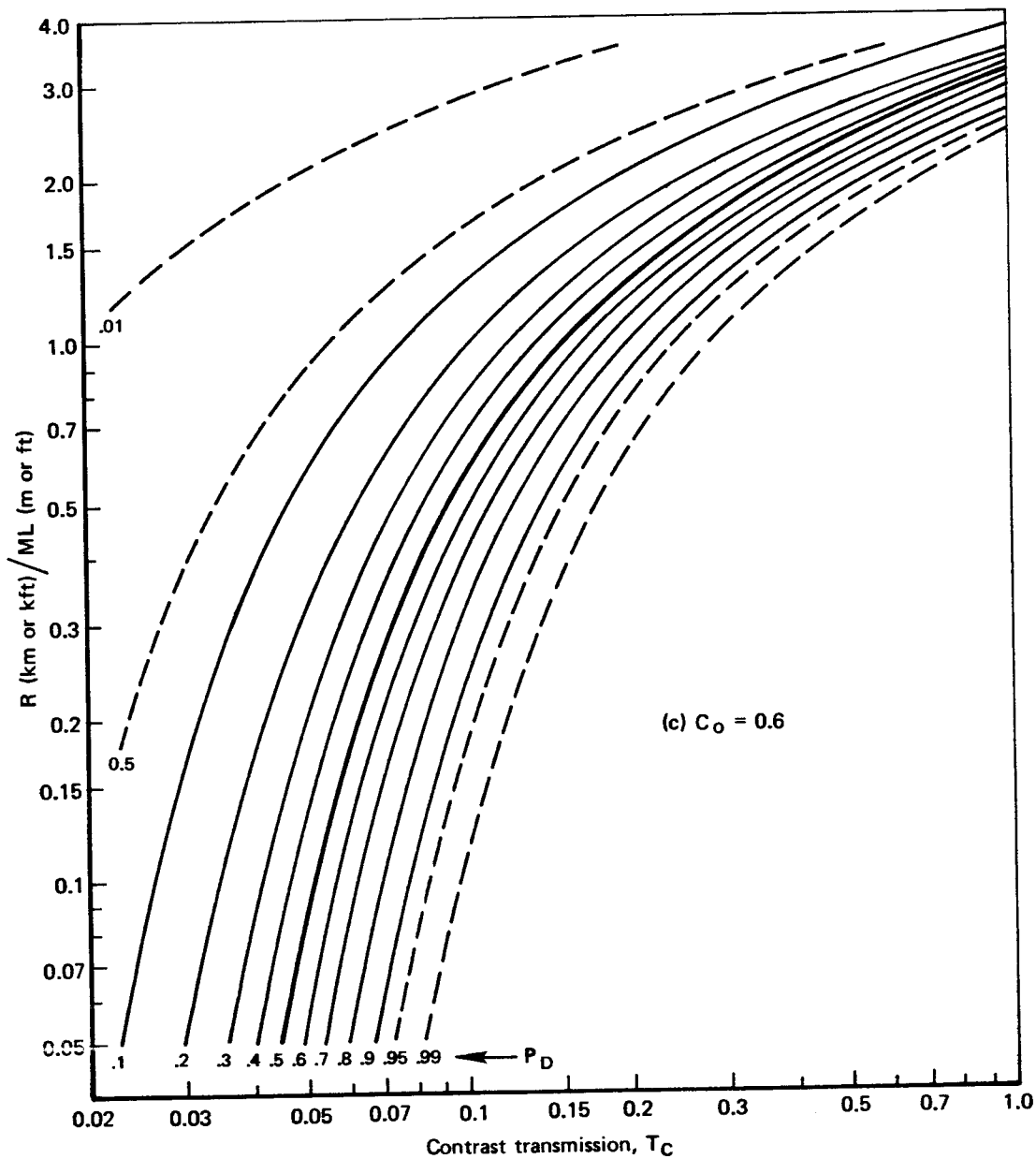


Fig. A.1—Probability of Detecting a Target as a Function of Range, R (km or kft), Magnification Power, M , Characteristic Target Size, L (m or ft), Atmospheric Contrast Transmission, T_C , and Inherent Target-to-Background Contrast, C_0

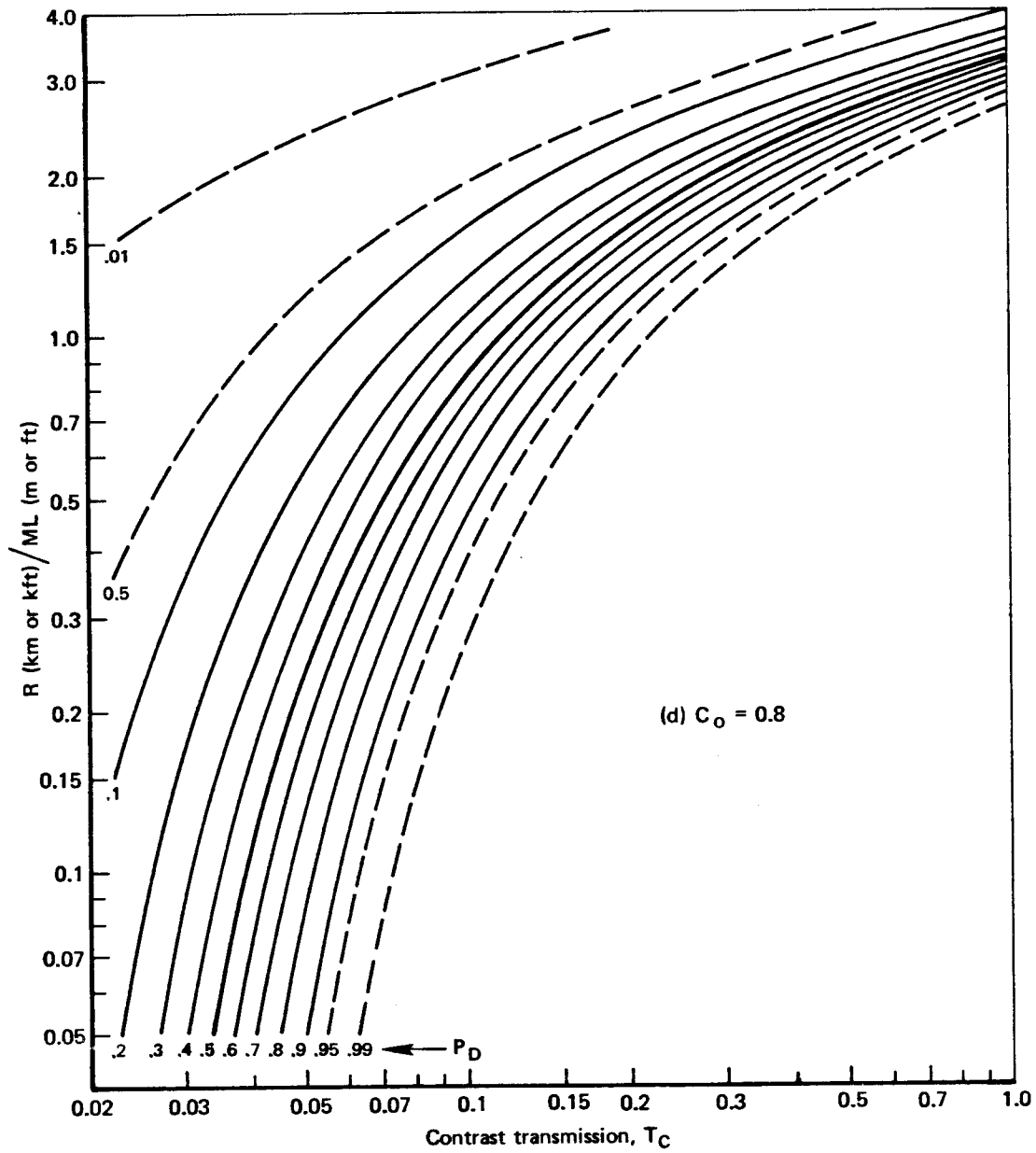


Fig. A.1—Probability of Detecting a Target as a Function of Range, R (km or kft), Magnification Power, M , Characteristic Target Size, L (m or ft), Atmospheric Contrast Transmission, T_C , and Inherent Target-to-Background Contrast, C_0

Appendix B

GLOSSARY

absolute humidity—The ratio of the mass of water vapor present in air to the volume occupied by the mixture of water vapor and air; that is, the density of the water vapor component, commonly expressed in g m^{-3} . (It is a measure of the “water-vapor content” of air, and the latter term is sometimes used to mean absolute humidity.)

The absorption by water vapor of infrared and microwave radiation is a direct function of absolute humidity. Absolute humidity is not a standard weather observable, but the dewpoint (which is) can be used to estimate absolute humidity (see *dewpoint*).

absorptance—The ratio of radiant flux absorbed by a substance to the flux incident on the substance.

absorption—The process by which incident radiant energy is retained by a substance; the absorbed radiation is always converted to some other form of energy within and according to the nature of the absorbing substance. When radiation traverses a medium that contains absorbing substances (for that wavelength of radiation), absorption contributes to the total extinction experienced by that radiation.

Absorption nominally plays an insignificant role in the atmospheric extinction of visible radiation; but it plays a significant role, quite variable with wavelength, in the atmospheric extinction of infrared radiation.

absorption coefficient—A measure of the space rate of diminution by absorption of electromagnetic radiation in transit through a medium containing absorbing substances; absorptance per unit distance. The absorption coefficient is a part (or form) of extinction coefficient. For visible and infrared radiation it is commonly expressed in neper km^{-1} . Absorption coefficients, for any given wavelength of radiation, are normally calculated separately for each absorbing substance (as water vapor, CO_2 , ozone, etc.), and summed to constitute part of the extinction coefficient.

aerosol—A system of solid or liquid particles dispersed in a gas. Atmospheric hazes and fogs, smokes and other particulate air pollutants, and most clouds, are or can be regarded as aerosols. (The strict physico-chemical definition requires an aerosol to be a true colloidal system, i.e., a stable suspension of particles in a gas.)

To be able to calculate with precision the extinction of radiation traversing an aerosol, the aerosol must be described by its particle size distribution, particle number density, and the complex indexes of refraction of all substances constituting the aerosol.

aerosol extinction—Loosely, the atmospheric extinction of radiation because of scattering and absorption by aerosol particles.

airlight—Same as *path luminance*.

albedo—See *reflectance*.

apparent contrast (or **received contrast**)—The target-to-background contrast perceived by an observer (or other sensor) separated from the target scene by a contrast-degrading medium, such as the atmosphere.

$$C_R = T_C C_o,$$

where C_R is apparent contrast, T_C is contrast transmission, and C_o is inherent contrast.

attenuation—See *extinction*.

black body—A hypothetical “body” that absorbs all of the electromagnetic radiation striking it. It neither reflects nor transmits any of the incident radiation, but it emits radiation as a function of its temperature and the wavelength of the radiation.

brightness—See *luminance*.

ceiling—The height of the base of the lowest cloud layer to which a cloud amount (or sky cover) of more than one-half ($> 4/8$ or $> 5/10$, in observing practice) is ascribed. When a ceiling is caused by a surface based obscuring phenomenon (e.g., fog), ceiling height is the vertical visibility into the obscuring phenomenon. U.S. weather observers report ceiling in hundreds of feet above the elevation of the weather station.

cloud amount—See *sky cover*.

cloud cover—See *sky cover*.

contrast (strictly, **target-to-background contrast**)—In visual range and target acquisition theory, a relationship between the apparent luminances of a target and its background; namely,

$$C = \left| \frac{L_t - L_b}{L_b} \right|,$$

where C is contrast, L_t is target luminance, and L_b is background luminance. For target scenes made visible solely by reflected light, target and background reflectances can be substituted for luminances. See also *apparent contrast*, *inherent contrast*, *thermal contrast*.

contrast transmission—The ratio of apparent contrast to inherent contrast. (Strictly, neither “transmission” nor “transmittance” should be applied to the transfer of visible contrast through the atmosphere, because apparent contrast is affected by light scattered into the field of view, “path luminance” or “airlight,” rather than by light removed from the field of view by the extinction processes of scattering and absorption.)

By visual range theory,

$$T_C = \left[1 + \frac{L_s}{L_b} (e^{\sigma R} - 1) \right]^{-1},$$

where T_C is contrast transmission, L_s/L_b is the "sky-ground ratio" (the ratio of the luminances of the horizon sky to the target's background), σ is visible extinction coefficient (neper km^{-1}) and R is range (km).

dewpoint (or **dewpoint temperature**)—The temperature to which air at a given pressure and water-vapor content (absolute humidity) must be cooled for saturation to occur.

The dewpoint, which is measured and reported in standard weather observations, is a useful surrogate for absolute humidity, which is not normally reported. A dewpoint, T_d , approximation for absolute humidity, A , valid near sea level is

$$\log_{10}A \approx 0.016 T_d + 0.16,$$

for T_d in degrees Fahrenheit, or

$$\log_{10}A = .029 T_d + .672,$$

for T_d in degrees Celsius.

emission—The generating and sending out of radiation, to be distinguished from reflection and transmission.

All substances emit radiation, and the distribution of energy across the wavelength spectrum is dependent on the substance's temperature and composition. The sun emits most strongly in the visible spectrum, with peak energy at about $0.5 \mu\text{m}$. The earth, and objects of similar temperature, emit most strongly in the infrared spectrum, peaking near $10 \mu\text{m}$.

emissivity—The ratio of the radiant emittance of a substance to the radiant emittance of an ideal black body at the same temperature.

emittance (or **exitance**)—The flux per unit area of radiation emitted by a substance. The common units of radiant emittance are watt cm^{-2} ; of luminous emittance, lumen cm^{-2} .

exitance—Same as *emittance*.

extinction (or **attenuation**)—The action of a medium in removing energy from a beam of radiation traversing it. The removal processes are scattering and absorption.

extinction coefficient (or **attenuation coefficient**)—A measure of the space rate of diminution (extinction, attenuation) of electromagnetic radiation caused by the medium it is traversing. It is a property of the medium and a function of the wavelength of the radiation. The extinction coefficient, σ , is identified in a form of Bouguer's (or Beer's) law:

$$I = I_0 e^{-\sigma R}$$

where I is transmitted flux density, I_0 is incident (or initial) flux density, and R is distance the radiation is transmitted. For visible and infrared radiation, σ is commonly expressed in neper km^{-1} .

The extinction coefficient is the sum of the scattering and absorption coefficients.

flying conditions—In general, the state of the atmosphere as it affects flight safety and the accomplishment of an airborne mission.

fog—A visible aggregate of minute water particles suspended in the atmosphere at and near ground level; an aqueous aerosol. Given sufficient condensation nuclei (e.g., haze particles, industrial pollutants), fog forms and/or becomes optically more dense (fog particles grow in size) as the relative humidity nears 100 percent. Physically, there are no clear lines of distinction between fog, smog, and haze, just continuous transitions in optical density or chemical composition. According to international weather observing procedures, however, “fog” is reported only when the visibility is less than one kilometer.

The terms “evolving” and “stable” fog are occasionally used to denote fogs of growing particle size and fogs of maximum (approximately equilibrium) particle size, respectively.

haze—The aggregate of very fine particles suspended in the atmosphere, less optically dense than fog but giving the atmosphere an opalescence that subdues colors and reduces visibility and contrast. Haze generally connotes natural aerosols as opposed to combustion products and other artificial pollutants. A loose distinction is sometimes drawn between “dry haze” and “damp haze” based on the difference in optical effects caused by the small dry particles and the larger particles that have accreted water. Similarly, the distinction between damp haze and fog is vague and physically meaningless.

IIR—Abbreviation for *imaging infrared*.

imaging infrared (abbreviated *IIR*)—Pertaining to a class of devices that optically collect infrared radiation within a limited wavelength band (e.g., 3-5 μm or 8-12 μm) and convert the received energy into a “thermal image” of the scene within the optical field of view.

infrared (abbreviated *IR*)—Electromagnetic radiation in the wavelength interval from about 0.8 micrometers (μm) to 1000 μm . It is thus bounded at short wavelengths by visible radiation and at long wavelengths by submillimeter microwave radiation.

inherent contrast—Target-to-background contrast at zero range.

IR—Abbreviation for *infrared*.

luminance (or **brightness**)—A measure of the intrinsic intensity of visible light (as perceived by the human eye) emanating from a source in a given direction. It is the luminous flux received from the source on a unit area oriented normal to the line of sight from the source, divided by the solid angle subtended (at the illuminated area) by the source, and assuming no extinction of light between source and illuminated area. The source can be of reflected light or self-luminous. Typical units of luminance are lumens per square centimeter per steradian.

Note: Light, as perceived by the eye, is studied in terms of “luminous efficiency,” a weighting factor applied to radiation quantities so that they are properly related to the physiological response of the human eye, which varies with wavelength. The lumen is the unit of luminous flux that contains the weighting factor.

meteorological range—A theoretically defined “visual range” that depends only on the extinction coefficient of the atmosphere. Meteorological range, V_m , is defined by the visual range formula (see *visual range*) with the assumptions of a prominent black target ($C_R = 1$) and a standard observer threshold contrast ($\epsilon = 0.02$):

$$V_m = \frac{1}{\sigma} \ln\left(\frac{1}{0.02}\right) = \frac{3.912}{\sigma},$$

where σ is the extinction coefficient.

micrometer (abbreviated μm)—One millionth of a meter; 10^{-6} m. Formerly called “micron” (abbreviated μ).

mixed layer—An atmospheric layer based at the earth’s surface within which the vertical distribution of aerosols and pollutants is quite uniform. The top of the mixed layer is usually a temperature inversion that inhibits the further upward transport of airborne particles.

neper—The natural logarithmic analog of the decibel, measuring the relative values of two radiant fluxes or radiant intensities, I_1 and I_2 :

$$n = \ln\left(\frac{I_2}{I_1}\right).$$

observation—See *weather observation*.

path luminance (or **airlight**)—The apparent luminance of the air caused by light being scattered by aerosol particles into the field of view. Path luminance is added equally to the luminances of both target and background and, therefore, reduces apparent target-to-background contrast.

radiance—A measure of the intrinsic intensity of electromagnetic radiation emanating from a source in a given direction. It is the radiant flux received from the source on a unit area oriented normal to the line of sight from the source, divided by the solid angle subtended (at the irradiated area) by the source, and assuming no extinction of radiation between source and irradiated area. Typical units of radiance are watts per square centimeter per steradian.

received contrast—See *apparent contrast*.

reflectance (or **reflectivity**)—The ratio of the reflected flux of radiation to the incident flux. Reflectance is a property of the reflecting surface, and varies with the wavelength of the radiation.

The often complicated dependence of reflectance upon ray geometry is described by the distribution function of “bidirectional reflectance,” which relates incident and reflected fluxes to all possible combinations of directions of incident and reflected rays.

The broad-spectrum reflectance of a surface type, such as the reflectance of a pine forest in the visible spectrum, is that surface’s “albedo.”

reflection—The action of a surface in turning radiation back into the medium whence it came.

reflectivity—Same as *reflectance*.

relative humidity (abbreviated *RH*)—The ratio of the actual (water) vapor pressure of the air to the vapor pressure that would obtain if the air were saturated with water vapor. Equivalently, it is the ratio of the absolute humidity to the saturation absolute humidity. Loosely, relative humidity is the amount of water vapor in the air relative to the maximum amount that the air could contain at the existing temperature and pressure. It is commonly expressed as percent.

Relative humidity influences the rate at which atmospheric aerosol particles grow or shrink in size because of their assimilation of water or loss of water through evaporation. This influence is strongest with relative humidity very near 100 percent.

scattering—The removal of energy from a beam of radiation traversing a medium by reflection and refraction from particles of matter within the medium. Scattering particles (as within an atmospheric aerosol) have a different index of refraction than that of the medium.

Scattering varies as a function of the ratio of particle diameter to the wavelength of the radiation. In general, the scattered intensity (and the scattering coefficient) increases with that ratio. Scattering is by far the major cause of the extinction of visible radiation and reduction of visible contrast by the atmosphere and an important cause of infrared extinction at least to wavelengths of the order of tens of micrometers.

scattering coefficient—A measure of the space rate of diminution by scattering of electromagnetic radiation in transit through a scattering medium. The scattering coefficient is a part (or form) of extinction coefficient. For visible and infrared radiation it is commonly expressed in neper km^{-1} .

sky cover (or **cloud cover**, **cloud amount**)—As observed from a point on the earth's surface, that fraction of the sky concealed from view by clouds or obscuring phenomena (such as fog or smoke). The vertical dimension of clouds adds to the apparent sky cover seen by the ground observer, especially at low viewing angles. Therefore, sky cover differs from "earth cover" (e.g., a plan view of cloud amount as observed by satellite at nadir point). The amount of sky cover for any given cloud layer is determined according to the "summation principle." In essence, this principle states that the sky cover at any level is equal to the summation of the sky cover of the lowest layer, plus the additional sky cover provided at all successively higher layers up to and including the layer in question. Thus, no layer can be assigned a sky cover less than a lower layer, and no sky cover can be greater than 1.0 (10/10 or 8/8).

"Cloud cover" or "cloud amount," in addition to being used as loose synonyms for sky cover, often connote the coverage of individual cloud layers or of amounts of cloud within specified altitude bands.

sky-ground ratio—In visual range and target detection theory, the ratio of the luminance of the horizon sky to the inherent luminance of the background of a target, with reference to a given viewing geometry. Both of these luminances, and

hence their ratio, vary in a complicated fashion with viewing angle, sun angle, composition of the background, state of the sky, and the atmospheric aerosol.

The sky-ground ratio is a parameter for the light scattered into the field of view of a visual sensor, "path luminance" or "airlight," and airlight is solely responsible for the reduction of apparent target-to-background contrast by the atmosphere.

surface visibility—Same as *visibility*.

surface weather observation—A formalized weather observation made at a point on the earth's surface, as opposed to upper-air (sounding) and aircraft (reconnaissance) observations. Surface weather observations include point measurements of atmospheric state parameters (temperature, pressure, humidity, wind) and measurements and judgments of visibility, state of the sky, and weather phenomena.

target-to-background contrast—See *contrast*.

thermal contrast (or target-to-background temperature difference)—The difference between the apparent temperatures of a target and its immediate background.

thermal radiation—Electromagnetic radiation emitted by a substance as the result of the thermal agitation of its molecules.

threshold contrast—That target-to-background contrast, for a given target angular size, at which 50 percent of observers will detect the target and 50 percent will not.

transmission—The passage of electromagnetic radiation through a medium. It is often loosely used to mean the fractional (or percent) transmission of radiation through a medium—i.e., the same as "transmittance." (See *contrast transmission*.)

transmissivity—Same as *transmittance*.

transmittance (or transmissivity)—The fractional transmission of radiation through a medium; the ratio of the transmitted flux density, I , to the incident flux density, I_0 . Transmittance, τ , is related to the *extinction coefficient*, σ , of a medium by

$$I/I_0 = \tau = e^{-\sigma R}$$

where R is the distance traversed through the medium.

visibility (or surface visibility)—The greatest distance in a given direction in which it is just possible to see and identify with the unaided eye a prominent dark object against the horizon sky in daytime, and an unfocused, moderately intense light source at night. The "prevailing visibility," which is the quantity reported in a surface weather observation, is the greatest directional visibility that is equaled or exceeded over half the horizon circle. U.S. observers report visibility in statute miles; for internationally coded "synoptic observations," visibility is coded according to a table based on metric units.

Although often used interchangeably with "visibility," the terms "visual range" and "meteorological range" are distinctly and differently defined, and the distinctions should be maintained.

visible contrast (or **visual contrast**)—Target-to-background contrast in the visible spectrum.

visible radiation (or **light**)—Electromagnetic radiation in the wavelength range approximately 0.4 to 0.7 micrometers, the wavelengths to which the human eye is sensitive.

visual range—The distance, under daylight conditions, at which a given target can be detected against its background, by the unaided eye, with a probability of 0.5. It is the range at which the apparent target-to-background contrast is equal to the threshold contrast of the observer for that angular size of target.

Visual range will usually be smaller than visibility, because the inherent contrast presented by targets of practical interest will usually be less than the contrast presented by targets used for visibility estimation—namely, “prominent dark objects against the horizon sky.”

The visual range, V , is a function of the atmosphere extinction coefficient, σ , the apparent contrast, C_R , and the threshold contrast, ϵ , as follows:

$$V = \frac{1}{\sigma} \ln \left(\frac{C_R}{\epsilon} \right).$$

water-vapor content—See *absolute humidity*.

weather observable—Loosely, any atmospheric characteristic that is described in a “standard” weather observation and, hence, is found in weather data archives.

weather observation—A formalized set of measurements and judgments of atmospheric quantities and weather phenomena. Content, format, schedule, and geographic distribution of weather observations are subject to available instrumentation and to rules laid down by agencies and governments and by international agreements.

There are several types and subtypes of “standard” weather observations: surface weather observations (aviation, marine, international synoptic, etc.); upper-air observations (radiosonde, rawinsonde, pilot balloon, etc.); and aircraft (weather reconnaissance) observations. Less “standardized” are weather radar and weather satellite observations.

REFERENCES

- Bailey, H. H., *Target Acquisition Through Visual Recognition: A Quantitative Model*, The Rand Corporation, RM-6158-PR, February 1970.
- Breitling, Patrick J., "A Comparison of the AFGL FLASH, DRAPER DART and AWS Haze Models with the RAND WETTA Model for Calculating Atmospheric Contrast Reduction," *Proceedings of the 8th Technical Exchange Conference, Air Force Academy, Colorado, 28 November-1 December 1978*, AWS/TR-79/001, Air Weather Service (MAC), Scott Air Force Base, Illinois, May 1979.
- Crichlow, W. A., et al., *Hourly Probability of World-Wide Thunderstorm Occurrence*, Telecommunications Research Report OT/TS RR 12, U.S. Department of Commerce, Office of Telecommunications, Institute for Telecommunication Sciences, Boulder, Colorado, April 1971.
- Duntley, Seibert Q., R. W. Johnson, and Jacqueline I. Gordon, *Airborne Measurements of Optical Atmospheric Properties in Southern Germany*, Visibility Laboratory, UCSD, San Diego (AFCRL-72-0255) Air Force Cambridge Research Laboratories, Bedford, Massachusetts, July 1972.
- Federal Meteorological Handbook No. 1—Surface Observations*, Second Edition, U.S. Department of Commerce, U.S. Department of Defense, and U.S. Department of Transportation, Effective January 1, 1979.
- Fenn, Robert W., *OPAQUE-A Measurement Program on Optical Atmospheric Quantities in Europe; Volume I—The NATO OPAQUE Program*, AFGL-TR-78-0011, Air Force Geophysics Laboratory, Hanscom Air Force Base, Massachusetts, January 1978.
- Huschke, R. E., *Atmospheric Visual and Infrared Transmission Deduced from Surface Weather Observations: Weather and Warplanes VI*, The Rand Corporation, R-2016-PR, October 1976.
- Johnson, J., "Analysis of Image Forming Systems," *Proceedings of the Image Intensifier Symposium*, U.S. Army Engineers Research and Development Laboratory, Ft. Belvoir, Virginia, October 1958.
- Overington, Ian, *Vision and Acquisition*, Pentech Press, London, 1976.
- Revised Uniform Summary of Surface Weather Observations (RUSSWO)—Part C (Surface Winds)*, Data Processing Branch, U.S. Air Force Environmental Technical Applications Center, Air Weather Service (MAC), Scott Air Force Base, Illinois, 1972.
- Rodriguez, E., and R. E. Huschke, *The Rand Weather Data Bank (RAWDAB): An Evolving Base of Accessible Weather Data*, The Rand Corporation, R-1269-PR, March 1974.
- World Distribution of Thunderstorm Days—Part 2: Tables of Marine Data and World Maps*, WMO/OMM No. 21.TP. 21, World Meteorological Organization, Secretariat of the World Meteorological Organization, Geneva, Switzerland, 1956.